

**Studies towards the Total Synthesis of DEM30355/A and
Related Polyketides**

A thesis submitted in partial fulfilment of the requirements for the degree of

Doctor of Philosophy

by

Abrar Ahmad Bayazeed



School of Chemistry

March 2016

Acknowledgment

In the Name of Allah, the Most Gracious, the Most Merciful

First and foremost, I would like to thank Allah for giving me the strength and perseverance to fulfil my goals and ultimately making my success possible.

I would like to express my gratitude and appreciation to my supervisor, Dr. Michael Hall, for his constant advice and support throughout my Ph.D. research.

I would also like to thank all members of Dr. Michael Hall's research group, past and present, who have made the research lab such an enjoyable place to work. Additionally, special thanks to my friends, Enas Filimban and Rua Al-Noman for their encouragements and making every day more entertaining.

I would like to extend my sincerest thanks and appreciation to my sponsor Umm Al-Qura University for giving me the opportunity to complete my postgraduate studies and also for their generous financial support. I also would like to thank the Saudi Arabian Cultural Bureau in London for their kind supervision, encouragement and support.

Finally, I would like to dedicate this work to my family. To my father, Dr. Ahmed Bayazeed, who taught me to always fight for what I believe in. To my mother, Nariman Ghulman, who's unconditional love and guidance sustained me throughout. To my siblings, for their comfort, humor and inspiration. I am sincerely thankful to my husband, Dr. Basim Makhdoum, for his care and patience during my academic career, as his unwavering support has given me the confidence and motivation to achieve my goals. To my children, Anas and Saffanah, for the joy they bring to my life.

Abstract

DEM30355/A **1** is a novel bioactive natural product polyketide isolated from an *Amycolatopsis* bacteria. **1** shows antibacterial activity against several pathogenic Gram positive bacteria, including methicillin-resistant *Staphylococcus aureus*. Thus we have explored the total synthesis of **1** and a number of related polyketide natural products (**Figure 1**).

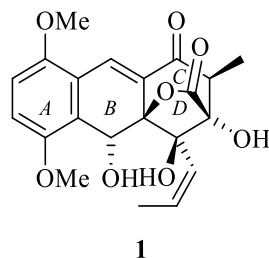
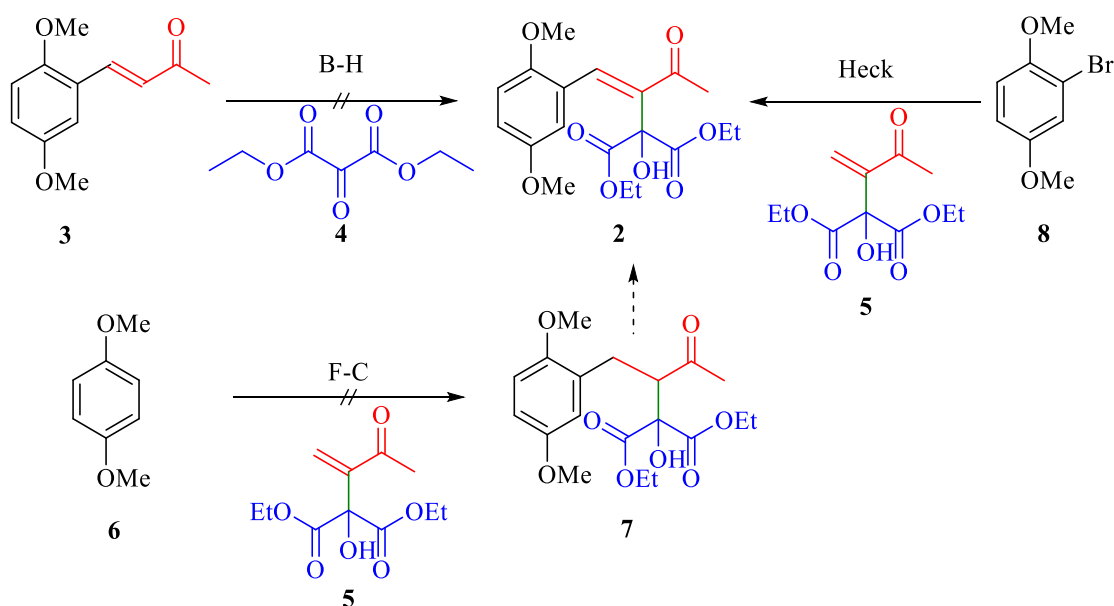


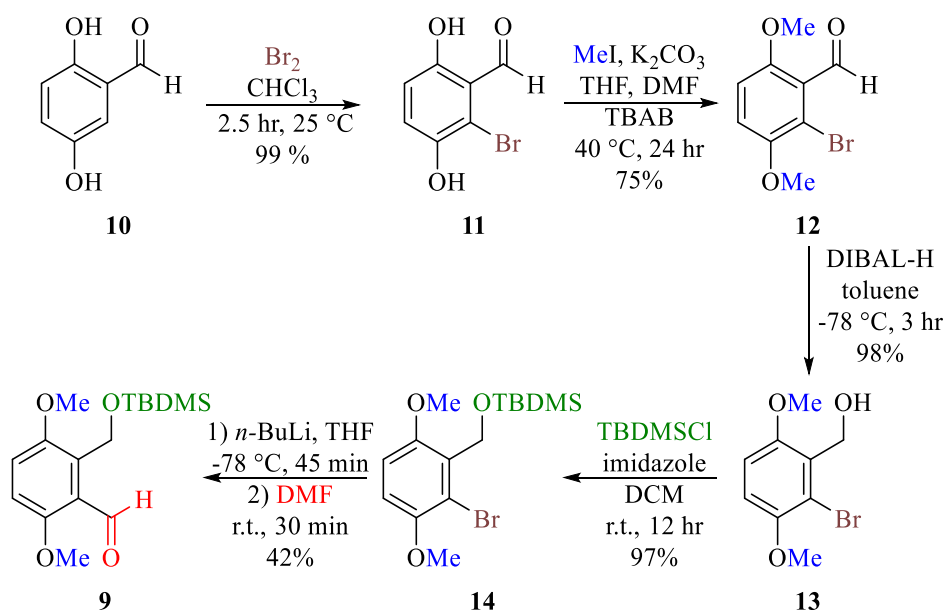
Figure 1: Structure of DEM30355A 1.

In our first attempts towards the synthesis of target molecule **1** we examined several synthetic routes towards a key intermediate **2**. These routes included: (a) the synthesis of Wittig product **3**, followed by an unsuccessful attempt at a sterically challenging Baylis-Hillman reaction with diethyl ketomalonate **4**; (b) following the synthesis of **5**, an attempted Lewis acid catalysed Friedel-Crafts reaction between 1,4-dimethoxybenzene **6** and **5**; and (c) Heck coupling of 2-bromo-1,4-dimethoxybenzene **8** with **5**. The best results were obtained via route (c) although the yields from the Heck coupling were low, prompting us to examine an alternative route (**Scheme 1**).



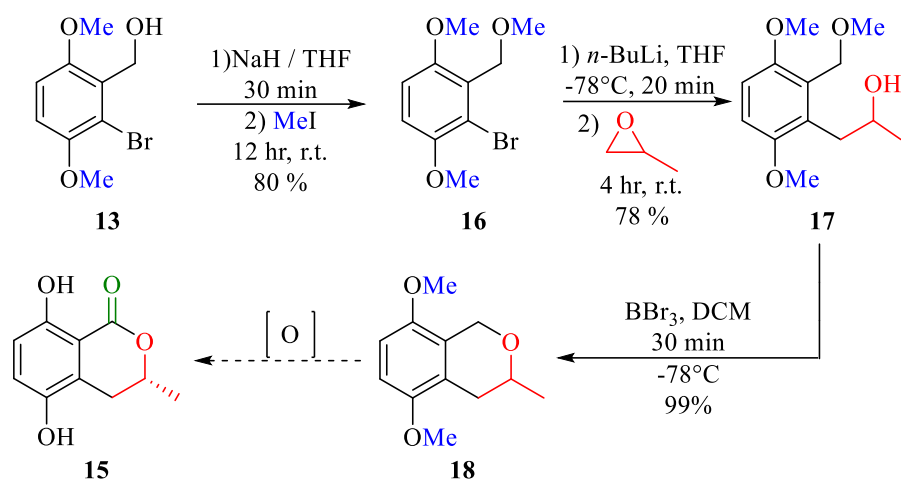
Scheme 1: Examined routes to key synthetic intermediate 2.

We then examined alternative synthetic approaches towards the aromatic ring A of target molecule **1**, based on the formation of the synthetic intermediate **9**. Compound **11**, which contains the core substitution pattern needed to create ring A, was successfully produced via an unusual bromination of 2,5-dihydroxybenzaldehyde **10**. After considerable optimisation we developed a method for the di-methylation of **11**. Reduction of aldehyde **12** into corresponding alcohol **13** and subsequent protection of **13** with TBDMSCl gave **14** in a high yield. The synthesis of **9** was completed via a halogen-metal exchange reaction of **14** followed by trapping with DMF (Scheme 2).



Scheme 2: Synthesis of ring A.

Alongside our work towards the synthesis of **1**, we have examined the total synthesis of the polyketide natural product (-)-(3*R*)-5-hydroxymellein **15**, starting from the previously synthesised common intermediate **13**. We have successfully synthesised **18**, the deoxy-analogue of **15**, via a halogen-metal exchange reaction of **16** followed by ring opening of propylene oxide and followed by deprotection and cyclisation.



Scheme 3: Progress towards the total synthesis of (-)-(3R)-5-hydroxymellein 15.

List of Abbreviations

Å	Angstrom
Ac ₂ O	Acetic acid anhydride
ACP	Acyl carrier protein
AMR	Antimicrobial resistance
Ar	Aromatic
AT	Acyl transferase
B-H	Baylis-Hillman
Bn	Benzyl
Cat.	Catalytic
CDC	Centers for Disease Control and Prevention
CSA	Chondroitin sulfate A sodium salt
D-A	Diels–Alder
DABCO	1,4-Diazabicyclo[2.2.2]octane
DBU	1,8-Diazabicyclo[5.4.0]undec-7-ene
DCM	Dichloromethane
DDQ	2,3-Dichloro-5,6-dicyano-1,4-benzoquinone
DH	Dehydrates
DIB	(Diacetoxyiodo)benzene
DIBAL-H	Diisobutylaluminum hydride
DMAC	Dimethylaluminum chloride
DMDO	Dimethyldioxirane
DMF	Dimethylformamide
DMG	Directed metalation group
DMSO	Dimethyl sulfoxide
E ⁺	Electrophile
ER	Enoyl reductase
Et	Ethyl
EtOH	Ethanol
F-C	Friedel–Crafts
G-n	Gram-negative
G-p	Gram-positive
HGT	Horizontal gene transfer

H-M	Halogen-metal
hr	Hour
<i>i</i> -Pr ₂ NEt	<i>N,N</i> -Diisopropylethylamine
IC ₅₀	Maximal inhibitory concentration
KR	Ketoreductase
KS	Ketosynthase
LDA	Lithium diisopropylamide
Lit.	Literature
<i>m</i> -CPBA	<i>meta</i> -Chloroperoxybenzoic acid
MAT	Malonyl acyl transferase
MDR-TB	Multi-drug resistance tuberculosis
Me	Methyl
Me ₃ OBF ₄	Triethyloxonium tetrafluoroborate
MeI	Methyl iodide
MeOH	Methanol
MIC	Minimum inhibitory concentration
min	Minutes
MOMCl	Methoxymethyl chloride
MRSA	Methicillin-resistant <i>Staphylococcus aureus</i>
NaOMe	Sodium methoxide
NBS	<i>N</i> -bromosuccinimide
NCS	<i>N</i> -chlorosuccinimide
NIS	<i>N</i> -iodosuccinimide
NMR	Nuclear magnetic resonance
NRR	National Risk Register of Civil Emergencies
°C	Centigrade
<i>p</i>	Para
<i>p</i> -TSA	<i>p</i> -toluenesulfonic acid
PHE	Public Health England
PMB	Para-methoxybenzyl
Sat.	Saturated
S _N 2	Bimolecular nucleophilic substitution
TAS-F	trimethylsilyl difluoride

TB	Tuberculosis
TBAB	Tetrabutylammonium bromide
TBDMSCl	<i>tert</i> -butyldimethylsilyl chloride
TEA	Triethylamine
Temp.	Temperature
TFA	Trifluoroacetic acid
THF	Tetrahydrofuran
TIPSCl	Triisopropylsilyl chloride
TLC	Thin layer chromatography
TM	Tris(dimethylamino)sulfur
TMSI	Trimethylsilyl iodide
UV	Ultra-violet
VGT	Vertical gene transfer
WHO	World Health Organisation
XDR-TB	Extensively multidrug resistance tuberculosis

Table of Contents

Acknowledgement	i
Abstract	ii
List of Abbreviations	v
Table of contents	viii

Chapter 1- Introduction

1.1.	Bacterial Diseases and Resistance	1
1.2.	Antibiotics.....	1
1.2.1.	Nature as a Source of Antibiotics	2
1.2.2.	Natural Products and Antibiotics Drug Discovery	2
1.2.3.	Antibiotics Isolated from Natural Sources	3
1.2.4.	Timeline of Antibiotic Discovery and New classes of antibiotics.....	4
1.3.	Antibiotic Resistance	6
1.3.1.	Origin of Antimicrobial and Antibiotic Resistance	6
1.3.2.	Genetic Mechanisms of Antibiotic Resistance	7
1.3.3.	Biological Mechanisms of Antibiotic Resistance	8
1.3.4.	Superbugs and Multidrug Resistance.....	10
1.3.5.	Antibiotic Resistant <i>Mycobacterium tuberculosis</i> (MDR-TB and XDR-TB)	10
1.3.6.	Methicillin-resistant <i>Staphylococcus aureus</i> (MRSA)	12
1.4.	Conclusions.....	12
1.5.	Polyketides.....	13
1.5.1.	The Biosynthesis of Natural Product Polyketide	13
1.6.	Conclusions.....	15
1.7.	Project Background.....	15
1.8.	Rishirilides	17
1.8.1.	The Biosynthesis of Rishirilides A and B.....	17
1.8.2.	The Total Synthesis of Rishirilides B	19

Chapter 2- Studies towards the Total Synthesis of DEM30355/A 1.14 via a Friedel-Crafts Approach

2.1.	Project Aims.....	22
2.2.	Retrosynthesis of DEM30355/A 1.14.....	22
2.2.1.	Friedel-Crafts Acylation Approach.....	22
2.2.2.	Aldol Condensation Approach.....	23

2.3.	Retrosynthetic Analysis of DEM30355/A 1.14 Based on an Intramolecular Friedel-Crafts Acylation Approach	24
2.4.	Synthesis of Ring A and B: Synthesis of 2.16 via an Intramolecular Friedel-Crafts Acylation.....	26
2.4.1.	Baylis-Hillman Reaction.....	26
2.4.2.	Synthesis of Diethyl 2-hydroxy-2-(3-oxobut-1-en-2-yl)malonate 2.18 via a Baylis-Hillman Reaction	27
2.4.3.	Heck Coupling of Baylis-Hillman Adduct 2.18 and 2-Bromo-1,4-dimethoxybenzene 2.3	28
2.4.4.	Attempt to Optimise Heck Reaction Condition.....	30
2.4.5.	Examination of the Iodination of 1,4-Dimethoxybenzene 2.29.....	31
2.4.6.	Heck Coupling of Baylis-Hillman Adduct 2.9 and 2.28.....	34
2.5.	Synthesis of Ring A and B: Alternative Route for the Synthesis of 2.17	34
2.5.1.	Synthesis of Ylide 2.31 and α,β -Unsaturated Ketone	35
2.5.2.	Synthesis of the Key Synthetic Intermediate 2.10 via Baylis-Hillman Approach.	36
2.6.	Synthesis of Ring A and B: Synthesis of 2.17 via a Friedel-Crafts Reaction.....	37
2.7.	Conclusion	39

Chapter 3- Examination of Synthetic Routes to 1,2,3,4-substituted Aromatic Rings as Precursors in the Total Synthesis of DEM30355/A 1.14

3.1.	Introduction.....	40
3.1.1.	Classic Methods for the Formation of 1,2,3,4-Substitued Aromatics.....	40
3.1.2.	Directed <i>Ortho</i> -Lithiation Approach	42
3.2.	Synthesis of Ring A of DEM30355/A 1.14 via an <i>Ortho</i> -Lithiation Approach....	42
3.2.1.	Planned Route for the Synthesis of Ring A via a Key <i>Ortho</i> -Lithiation Step.....	42
3.2.2.	Protection of 1,4-Dimethoxybenzaldehyde 2.32	43
3.2.3.	<i>Ortho</i> -Deprotonation Reaction of 3.12	44
3.3.	Synthesis of Ring A of DEM30355/A 1.14 via Thiele-Winter Like Bromination Approach.....	45
3.3.1.	Planned Route for the Synthesis of Ring A via a Key Bromination Step.....	45
3.3.2.	Thiele-Winter Reaction.....	46
3.3.3.	Porco Bromination	47
3.3.4.	Synthesis of 2-Bromo-3,6-dihydroxybenzaldehyde 3.20	48
3.3.5.	Methylation of 2-Bromo-3,6-dihydroxybenzaldehyde 3.19	50

3.3.6. Synthesis of (<i>E</i>)-4-(2-Bromo-3,6-dimethoxyphenyl)but-3-en-2-one 3.36	55
3.3.7. Protection of (<i>E</i>)-4-(2-Bromo-3,6-dimethoxyphenyl)but-3-en-2-one 3.37	55
3.3.8. Biological Assay of the Synthetic Intermediates 2.30 and 3.36	56
3.4. Conclusion	57
3.5. Future Work	57
Chapter 4- Studies towards the Total Synthesis of DEM30355/A 1.14 via an Intramolecular Aldol Condensation	
4.1. Retrosynthetic Analysis of DEM30355/A 1.14 Based on an Intramolecular Aldol Condensation Approach.....	59
4.2. Synthesis of Ring C and D of DEM30355/A 1.14 an via Intramolecular Aldol Condensation Approach.....	61
4.2.1. Synthesis of 2,2-Dimethyl-1,3-dioxolane-4-carbaldehyde 4.13	61
4.2.2. Grignard Addition of 1-Propynylmagnesium Bromide to (<i>R</i>)-4.13.....	64
4.2.3. Swern Oxidation of 4.12	65
4.2.4. Investigation of the Aldol Reaction of 4.18 and 4.17	66
4.3. Synthesis of the Synthetic Intermediate 4.5 of DEM30355/A 1.14 via an Intramolecular Aldol Condensation Approach	67
4.3.1. Reduction of Aldehyde 3.19 Using DIBAL-H	68
4.3.2. Silyl Ether Protection of 4.24.....	69
4.3.3. Halogen-Metal Exchange Reaction of 4.23	69
4.4. Conclusion	70
4.5. Future Work	70
Chapter 5- Towards the Total Synthesis of (-)-(3<i>R</i>)-5-Hydroxymellein	
5.1. Introduction.....	72
5.2. Retrosynthesis of (-)-(3 <i>R</i>)-5-hydroxymellein 5.1	72
5.3. Examination of Routes towards of (-)-(3 <i>R</i>)-5-Hydroxymellein 5.1	73
5.3.1. The Halogen-Metal Exchange and Trapping Reactions of 4.23.....	73
5.3.2. Protection of Alcohol 4.24 with TIPSCl.....	76
5.3.3. Halogen-Metal Exchange Reaction of 5.17	77
5.3.4. Protection of Aldehyde 3.19 as a Cyclic Acetal	78
5.3.5. Halogen-Metal Exchange Reaction of Cyclic Acetal 5.21	78
5.3.6. Protection of Aldehyde 3.19 as an Acyclic Acetal	79
5.3.7. Halogen-Metal Exchange Reaction of Acyclic Acetal 5.23	79

Table of Contents

5.3.8. Deprotection of Acetal 5.24	81
5.3.9. Protection of Alcohol 4.24 with Methyl Iodide	85
5.3.10. Halogen-Metal Exchange Reaction of Methyl Ether 5.28.....	86
5.3.11. Deprotection of Methyl Ether 5.29	86
5.3.12. Oxidation of the Benzyl Ether 5.31	89
5.4. Conclusion	90
5.5. Future Work.....	91

Chapter 6- Experimental Section

6.1. Experimental Information.....	94
References	132
Appendix	137

Chapter 1

1. Introduction

1.1. Bacterial Diseases and Resistance

Despite the availability of antibiotics, bacterial infections are still the second leading-cause of death, causing 17 million fatalities every year worldwide.¹ In recent years, there has been a growing concern in society towards the increasing levels of resistance in bacteria and other microorganisms to antimicrobial agents. Infection caused by resistant pathogenic bacteria increases the mortality rate of infected patients as there are no effective treatments.^{2,3} Public Health England (PHE) agency reported in 2014 that antimicrobial resistance (AMR) is “*one of the greatest threats we face today*”⁴, whilst the World Health Organisation (WHO) warned in a report published on 2014 that the world is moving towards “post-antibiotic era” when minor injuries and ordinary infections can be fatal.⁵ The Centres for Disease Control and Prevention (CDC) have listed antibiotic resistance as a “*worldwide problem that pose a catastrophic threat to people in every country in the world*”³, and the World Economic Forum in 2014 classified bacterial resistance to antibiotic as a major global risk.⁶

The emerging threat of resistant pathogenic microbes is already leading to a decrease in positive patient outcomes. For instance, at least 2 million people in USA are infected with antibiotic resistant bacteria leading to 23,000 deaths per year, whilst the additional healthcare cost have been estimated at around \$20 billion.³ In Europe, 400,000 people suffer from infections caused by resistant bacteria, resulting in 25,000 deaths each year costing the healthcare systems in the European Union over €1.5 billion.⁷

In 2015, following PHE warnings, the National Risk Register of Civil Emergencies (NRR) in the UK classified AMR infections as a serious long-term risk, as the rate of resistant infections are expected to increase in the next 20 years. NRR claimed that if an outbreak of an antimicrobial resistant infections were to occur, nearly 200,000 people would be likely to be affected by bacterial blood infections (sepsis) that do not respond effectively to existing antibiotics and around 80,000 people could die.⁸ Currently, sepsis due to antimicrobial resistance affects 100,000 people in the UK, causing 36,800 deaths each year.⁹

Before proceeding to identify the origin and the mechanisms of antibiotic resistance, we will review the sources of existing antibiotic classes, with a focus on antibiotics from nature, and their mode of action.

1.2. Antibiotics

1.2.1. Nature as a Source of Antibiotics

It has been postulated that antibiotic producing microorganisms (bacteria and fungi) employ a form of chemical warfare to compete with neighbours for nutrition and space.^{10,11} Many microorganisms have the ability to produce molecules which either kill (bactericidal) or slow the growth (bacteriostatic) of other bacteria. This gives a Darwinistic advantage to the producing microorganism allowing them to consuming nutrients from the defeated neighbor. Antibiotic producing bacteria can also regulate the production of secondary metabolites in response to environmental pressure (such as a decrease in available nutrients), turning on antibiotic producing pathways only when necessary.^{12,13}

1.2.2. Natural Products and Antibiotics Drug Discovery

Natural products have played an essential role in the discovery of antibiotics and are likely to remain a key source of new antibiotic lead molecules for the future.^{1,14} The majority of natural product-derived antibiotics are produced by bacteria and fungi. Of the antibiotic producing bacteria, most are actinomyces and streptomyces a genera of actinobacteria that exist in soil and marine environments. Of these naturally derived antibiotics, actinobacteria, Gram-positive (G-p) bacteria with high percentage of guanine and cytosine bases in their DNA, are a major source.¹⁵ Figure 1.1 illustrates the sources of new antibiotics approved for human use between 1981 and 2010 showing that a large proportion of clinically used antibiotics are derived from natural products.¹⁶

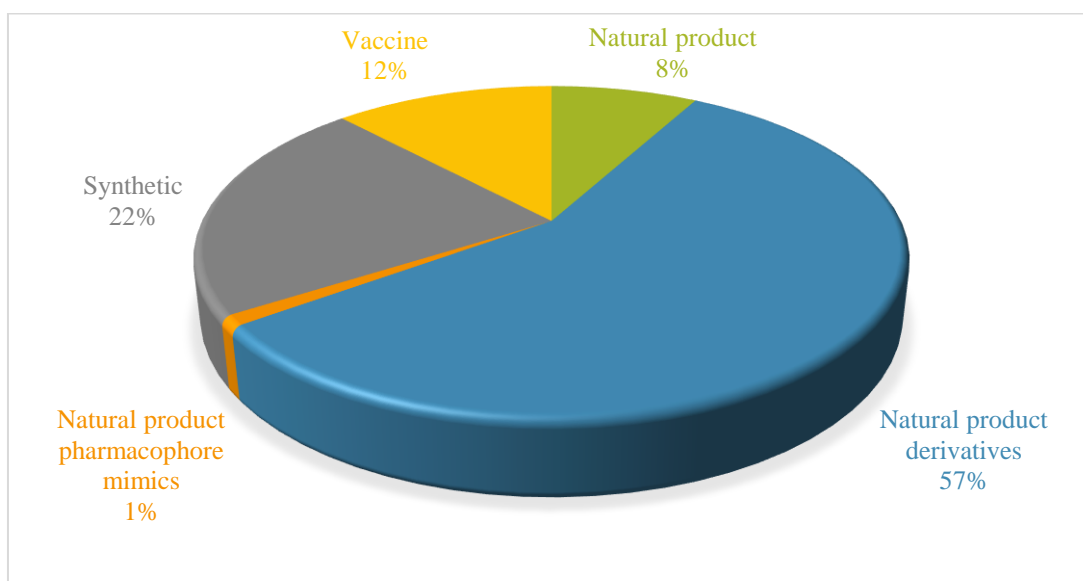


Figure 1.1: New antibacterial agents approved between 1981-2010.

1.2.3. Antibiotics Isolated from Natural Sources

There are five major classes of antibiotics that have been derived from natural sources, the β -lactams, aminoglycosides, tetracyclines, macrolides and streptogramins (Figure 1.2).^{17,18, 19,20}

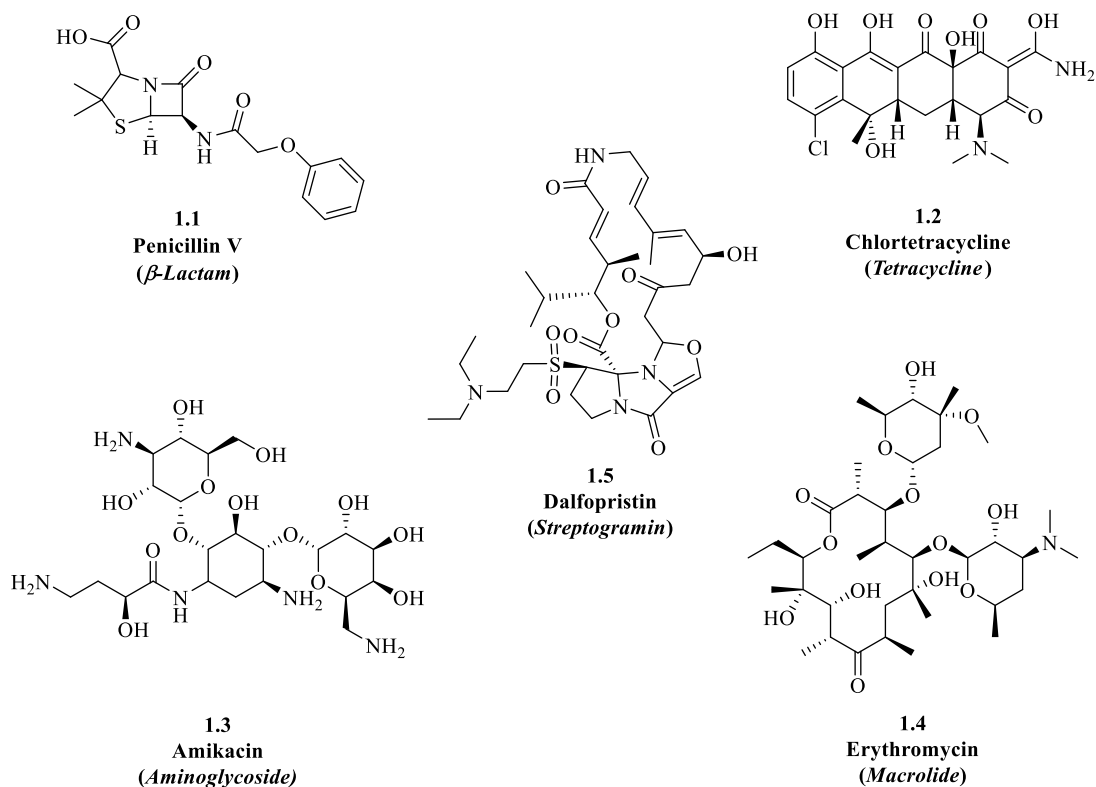


Figure 1.2: Antibiotics isolated from nature.

These antibiotics target five key biological pathways in bacteria by disrupting cell wall biosynthesis, protein biosynthesis, DNA or RNA synthesis, folate biosynthesis or membrane integrity (Table 1.1).^{17,18, 19,20}

Class	Source	Pharmacophore	Mode of Action
β -lactams	<i>Penicillium notatum</i> mould	Four-membered β -lactam ring.	Inhibit cell wall biosynthesis of Gram-positive (G-p).

Aminoglycosides	<i>Streptomyces griseus</i>	Amino sugars linked by glycoside bonds.	Broad-spectrum, first antibiotics that showed activity against Gram-negative (G-n) bacteria, bactericidal, inhibit protein synthesis at a ribosomal level of G-p and G-n bacteria.
Tetracyclines	<i>Streptomyces</i>	Polyketide antibiotics containing four fused six-membered rings.	Inhibit protein synthesis at a ribosomal level of G-p and G-n bacteria.
Macrolides	<i>Streptomyces</i>	Polyketide antibiotics include macrocyclic lactone ring.	Disrupt protein biosynthesis of G-p and G-n bacteria.
Streptogramins	<i>Streptomyces</i>	Include two structurally unrelated molecules: group A (macrolactones) and group B (cyclic hexadepsipeptides)	Inhibit protein synthesis at the ribosomal level. Each molecule is bacteriostatic, however, a combination of the A and B is bactericidal.

Table 1.1: Source, pharmacophore and mode of action of selected natural product antibiotics.

1.2.4. Timeline of Antibiotic Discovery and New classes of antibiotics

However, from 1970 until recently only six new classes of antibacterial agents (mupirocins, oxazolidinones, lipopeptide daptomycin, mutilins, fidaxomicin and bedaquiline) were approved for use in humans.^{1,21,22,23} Therefore there is a need for novel antibiotics with new modes of action to be discovered to combat the current resistance to many of the existing classes of antibiotics. The following Figure 1.3 shows the timeline of the discovery of antibiotics from 1908 to 2012.

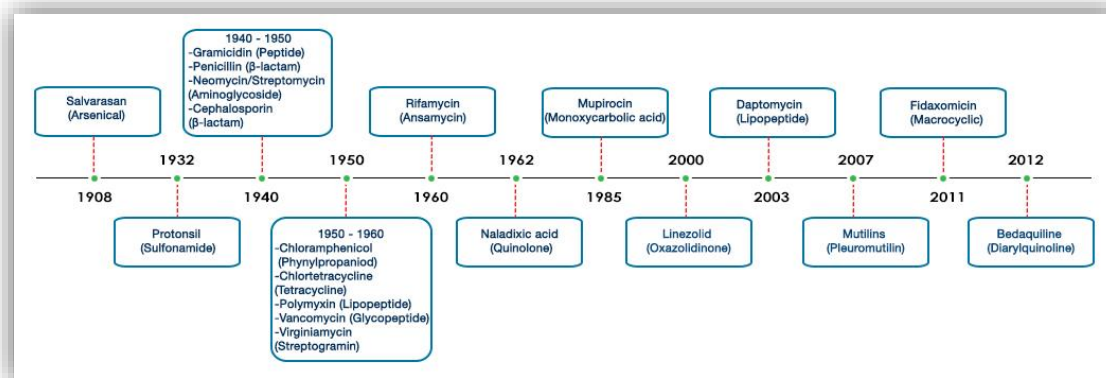


Figure 1.3: Timeline of Antibiotic discovery from 1908 to 2012.

More recently a number of new compounds are being researched as part of the strategy to overcome resistant infections. Thus in 2015, NovoBiotic Pharmaceuticals LLC announced the discovery of teixobactin, a new class of antibiotics which interfere with the lipid II pathway, isolated from a G-n soil bacterium, *Eleftheria terrae*. Teixobactin **1.6** is a depsipeptide made up of a number of modified amino acids, including enduracididine, methylphenylalanine, and four D-amino acids (Figure 1.4).²⁴

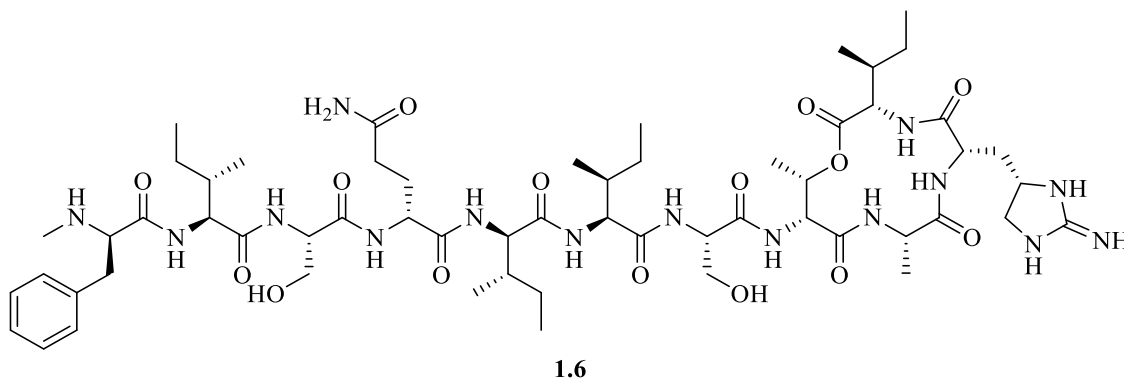


Figure 1.4: Chemical structure of teixobactin **1.6**.

Teixobactin **1.6** shows remarkable antibiotic activity against G-p bacteria, including drug resistant strains such as methicillin-resistant *Staphylococcus aureus* (MRSA) and vancomycin resistant enterococci. Despite the fact that the producer of **1.6** antibiotic is a G-n bacterium, **1.6** shows no activity against most of G-n bacteria since it cannot penetrate the outer membrane. This was demonstrated by testing **1.6** on a strain of *E. coli asmB1* with an impaired “leaky” outer membrane, against which teixobactin was active (Table 1.2).²⁴

Species	Teixobactin MIC µg/ml
<i>Clostridium difficile</i>	0.005
<i>Staphylococcus aureus</i> (MRSA)	0.25
<i>Enterococcus faecium</i> (VRE)	0.5
<i>Escherichia coli</i>	25
<i>Escherichia coli</i> (asmB1)	2.5

Table 1.2: The activity of teixobactin 1.6 antibiotic against pathogenic bacteria.

The mode of action of teixobactin involves in the inhibition of bacterial cell wall biosynthesis by binding to two cell wall components: lipid II (peptidoglycan) and lipid III (teichoic acid). No resistance has yet been observed from *Staphylococcus aureus* or *Mycobacterium tuberculosis* against teixobactin, thus this antibiotic shows promise for the future treatment of MDR G-p infections.²⁴

1.3. Antibiotic Resistance

1.3.1. Origin of Antimicrobial and Antibiotic Resistance

Antimicrobial resistance refers to the ability of a pathogenic microbe (bacteria, fungi, virus or parasite) to survive in the presence of a drug used to kill or stop their growth.^{4,5} Antimicrobial resistance is a natural phenomenon caused by the application of Darwinistic selection pressure via an antibiotic on the microbe. Thus exposure of any microbial population to an antibiotic will, over time, lead to the generation of resistance. Antibiotic resistance increases as a consequence of antibiotic usage. Bacterial resistance to antibiotics has been observed in the clinic from as quickly as a few months to many years after the first use of an antibiotic (**Table 1.3**).²³

Antibiotics	Year of Clinical Use	Resistance Observed
Sulfonamides	1930s	1940s
Penicillin	1943	1946
Streptomycin	1943	1959
Chloramphenicol	1947	1959
Tetracycline	1948	1953
Erythromycin	1952	1988
Vancomycin	1956	1988
Methicillin	1960	1961
Cephalosporins	1960s	late 1960s
Ampicillin	1961	1973

Nalidixic acid	1962	1962
Fluoroquinolones	1980s	1980s
Linezolid	1999	1999
Daptomycin	2003	2003
Retapamulin	2007	2007
Fidaxomicin	2011	2011
Bedaquiline	late 2012	?

Table 1.3: Appearance of resistance to clinically used antibiotics.

1.3.2. Genetic Mechanisms of Antibiotic Resistance

Bacterial resistance to antibiotics at the genetic level can be intrinsic or acquired and resistant traits can be transmitted by both vertically or horizontally. Vertical transmission involves offspring bacteria inheriting resistant genes from their parents, whilst horizontal transmission happens by directly transferring resistant genes from one bacterium to another within a population.²⁵

1.3.2.1 Intrinsic Resistance

Some pathogenic bacteria are naturally resistant to specific classes of antibiotic due to poor penetration of the antibiotic into cellular bacteria or lack of reliance on an antibiotic target enzyme. For instance, vancomycin is a glycopeptide antibiotic that binds to D-Ala-D-Ala peptides and inhibits peptidoglycan crosslinking in the cell wall of most G-p bacteria. Whereas, G-n bacteria are intrinsically resistant to Vancomycin since the molecule cannot penetrate the outer membrane.^{26,27}

1.3.2.2 Acquired Resistance

Much of the antibiotic resistance that occurs in pathogenic bacteria arises when bacteria acquire resistance genes. The increase in resistance genes can occur in several ways:

- After exposure to an antibiotic and a period of bacterial growth, bacteria containing minor genetic variations, which improved their survival, are enriched in the resulting population. Over many iterations this leads to bacteria which have been preferentially selected to be the most resistant. Resistance genes can then be transmitted between bacteria by two means: vertical gene transfer (VGT) or horizontal gene transfer (HGT).^{25,28}

- **Vertical gene transfer (VGT):** offspring bacteria inherit resistance genes from resistant parent bacteria during DNA replication.^{28,29}
- **Horizontal gene transfer (HGT):** receiving antibiotic resistance gene from a neighboring resistant bacteria. HGT occurs via three mechanisms:^{28,30}
 - a) **Transformation:** bacteria absorb “naked” DNA from dead bacteria in their environment and incorporate it into their own DNA. Donor and receiving bacteria are normally close to each other.
 - b) **Conjugation:** transferring a plasmid (small circular part of DNA that carry antibiotic resistance and other genes) via direct contact between the cell walls of the donor and recipient bacteria.
 - c) **Transduction:** transferring resistant DNA from one bacterium to another by a virus called bacteriophage, which can lead to transmission of a resistant gene over a long distance.

Antibiotic resistance genes of this type usually exist in a small piece of DNA called a transposon. Some transposons include a complex DNA fragment known as an “integron” that exist in both G-p and G-n bacteria. Integrons significantly contribute in the evolution of multidrug resistance bacteria since they can carry several antibiotic resistance genes at one time.^{28,30}

1.3.3. Biological Mechanisms of Antibiotic Resistance

After mutation or gene transfer, antibiotic resistance arises when biological modifications in bacterial cell interrupt the activity of the antibiotic. There are several main biological mechanisms of antibiotic resistance (**Figure 1.5**).^{28,31}

- **Efflux:** bacteria develop active or passive transport mechanisms to pump antibiotic molecules outside the cell until the concentration of the antibiotic becomes low enough to be tolerated by the bacteria. Efflux strategies have been used by bacteria against the β -lactams, tetracyclines, macrolides and fluoroquinolones.³²
- **Target modification:** bacteria change the target of an antibiotic to reduce the antibiotic binding affinity. This includes the cell wall biosynthesis, and DNA replication proteins and the ribonucleoprotein complex of the ribosome.³⁰ For example, bacteria become resistant to aminoglycoside through ribosomal alteration.²⁸

- *Inactivating enzymes*: bacteria produce one or more enzymes that modify, destroy or chemically degrade the antibiotic. A well-known example are the β -lactamase enzymes that are produced to hydrolyze β -lactam antibiotics.²⁶
- *Bypass*: by-passing the metabolic pathway targeted by antibiotics.³¹
- *Immunity*: antibiotic or its target binds to a second protein to interrupt antibiotic-target binding process.^{31,33}
- *Cell membrane/wall*: decreasing the permeability of the cell wall towards the antibiotic.³⁴
- *Overproduction*: producing more of the enzyme targeted by antibiotic. For example the chromosomal AmpC enzyme can be overproduced by mutant *Pseudomonas G-n* bacteria, increasing the resistance to most β -lactam antibiotics.³⁵

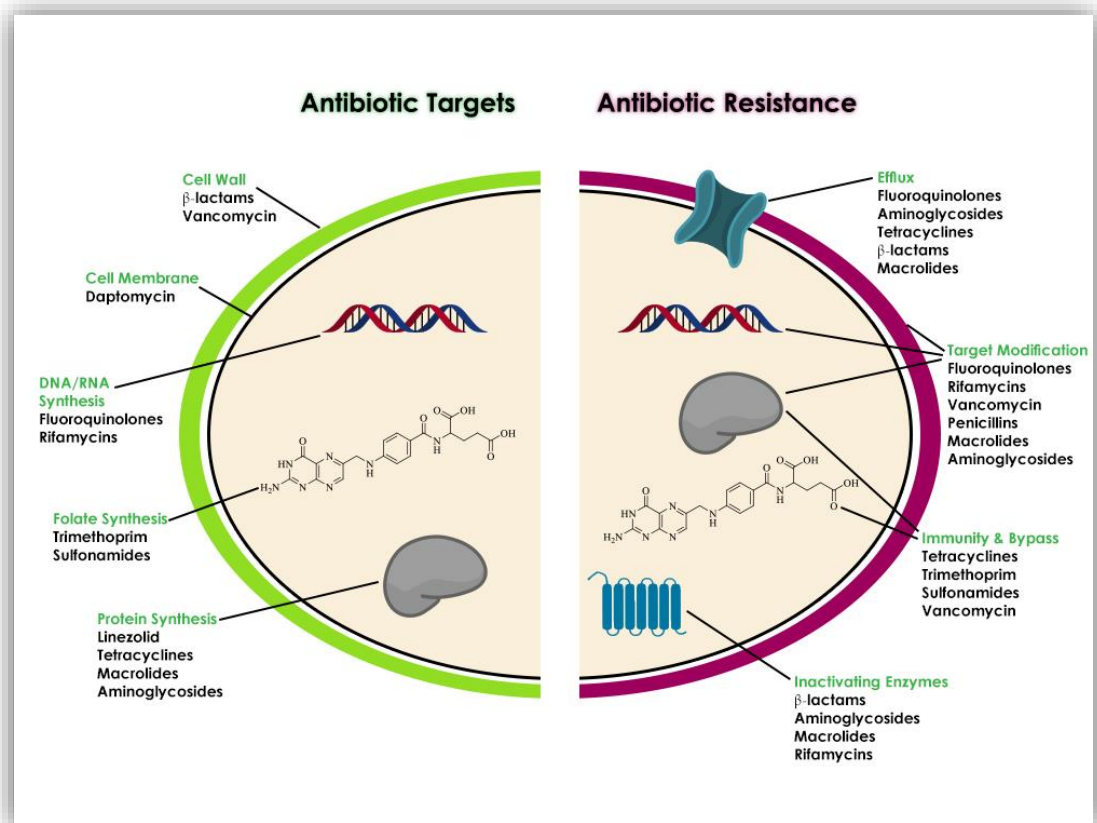


Figure 1.5: Antibiotics mode of action and antibiotic resistance pathways in bacterial cell.

1.3.4. Superbugs and Multidrug Resistance

Superbugs are strains of infectious bacteria demonstrating extreme resistance to multiple antibiotics due to multiple mutations, ultimately leading to poor patient outcomes. Multidrug resistant bacteria display resistance to most available antibiotic classes, particularly those antibiotics used frequently in the clinic.³⁶ Multidrug resistant infectious G-p and G-n bacteria can cause life-threatening infections, both community and hospital acquired, in developed and developing countries. This group includes *Enterococcus faecium*, *Staphylococcus aureus*, *Klebsiella pneumoniae*, *Acinetobacter baumannii*, *Pseudomonas aeruginosa*, and *Enterobacter* species, the ESKAPE pathogens.³⁷

Pathogenic multi-drug resistant bacteria also include *Mycobacterium tuberculosis* that causes multi-drug resistance tuberculosis (MDR-TB) and methicillin-resistant *Staphylococcus aureus* (MRSA). The following case studies highlight recent data about MDR-TB and MRSA morbidity, mortality and available treatments.

1.3.5. Antibiotic Resistant *Mycobacterium tuberculosis* (MDR-TB and XDR-TB)

Tuberculosis (TB) is a very commonly occurring infectious disease caused by Gram-positive bacteria *Mycobacterium tuberculosis*. TB is contagious and air transmitted and mostly affects the lungs. According to WHO, one-third of the world's population is infected with TB.³⁸ It is estimated that 49 people become ill and nearly 7 patients die every hour in Europe because of TB.³⁹ Globally, TB affects around 9 million people, causing 1.4 million deaths in 2013. Despite this, drug susceptible TB is a curable disease.³⁸ Standard treatment for TB consists of a combination of four oral antibiotics (isoniazid **1.7**, rifampicin **1.8**, pyrazinamide **1.9** and ethambutol **1.10**) for 6 months divided into two stages. The first stage of treatment is called “intensive phase” as it includes all four antibiotics for the first two months. The second stage includes rifampicin and isoniazid for the following four months. If the treatment procedure is supervised directly by a healthcare provider, the cure rate from TB is above 95% (**Figure 1.6**).⁴⁰

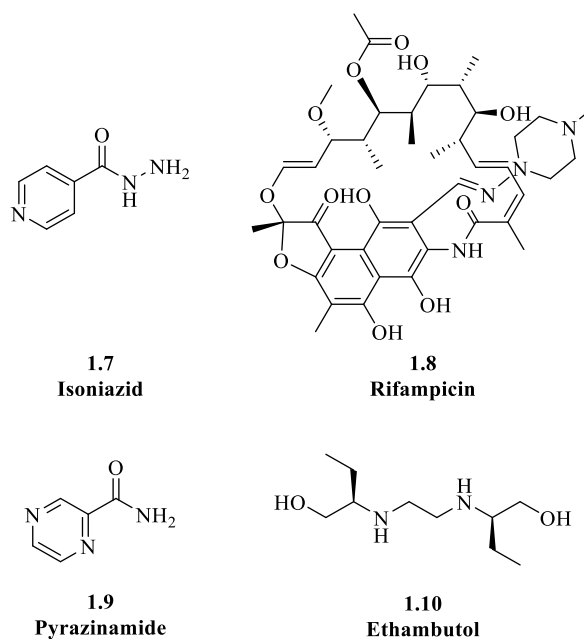


Figure 1.6: Chemical structures of antibiotics used as a first line treatment for TB.

If the TB infection has not been treated properly, *Mycobacterium tuberculosis* can develop a mechanism to resist rifampicin and isoniazid to produce a severe form of TB called Multidrug-resistant TB (MDR-TB).⁴⁰ In 2013, there were around 480,000 new cases of multidrug resistant TB (MDR-TB) and around 210,000 patients died worldwide.⁴¹ Second-line treatment is recommended to fight MDR-TB infection for at least 20 months, the therapy consist of three main groups of oral and injectable antibiotics:⁴⁰

Group 1) IV aminoglycosides: streptomycin, kanamycin, amikacin and **IV polypeptides:** capreomycin, viomycin.

Group 2) Oral and IV fluoroquinolones: ciprofloxacin, levofloxacin, moxifloxacin, ofloxacin, gatifloxacin.

Group 3) Oral: *para*-aminosalicylic acid, cycloserine, terizidone, ethionamide, prothionamide, thioacetazone, linezolid.

Although second line treatment proves effective for many patients, *Mycobacterium tuberculosis* strains have since developed with resistance to first and second line treatments. In 2006 extensively multidrug resistance TB (XDR-TB) was first reported, involving the discovery of TB strains that displays resistance to rifampicin, isoniazid, fluoroquinolones and at least one of the three injectable second-line drugs: amikacin, kanamycin and capreomycin.⁴⁰ Therefore, there is a critical need for new antibiotics capable of overcoming the MDR-TB and XDR-TB Infections.

1.3.6. Methicillin-resistant *Staphylococcus aureus* (MRSA)

S. aureus can cause serious problems in hospitals particularly in patients with surgical wounds.¹² MRSA infects around 50 million individuals worldwide every year.⁴² According to CDC, around 80,461 patients suffered from severe MRSA infections and an estimated 11,285 deaths in 2011 in the USA.³ Penicillins including methicillin are the first line treatment for *S. aureus* infection. However MRSA is resistant to all the penicillins. Vancomycin and linezolid have been used to treat MRSA infected patients. However MRSA strains have recently been discovered exhibiting multidrug resistance against both vancomycin **1.11** and the linezolid **1.12** antibiotics (**Figure 1.7**).^{43,44}

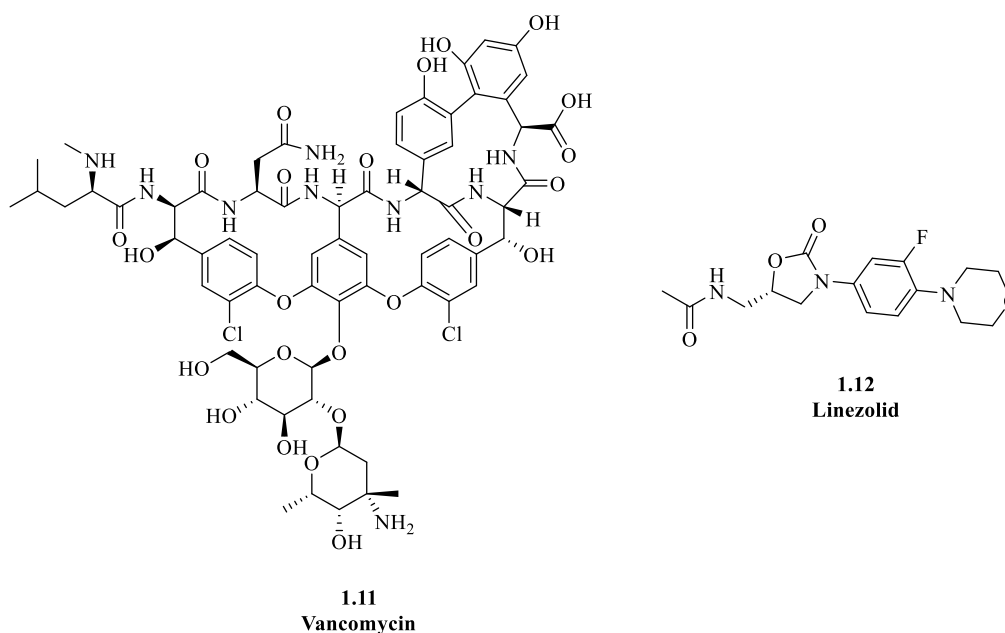


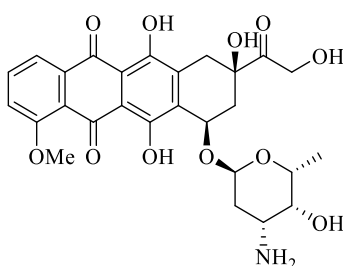
Figure 1.7: Chemical structures of most common antibiotics used to treat MRSA infection.

1.4. Conclusions

Thus antimicrobial agents that in the past might have been effective against bacterial infection become far less effective against increasingly resistant strains. Not only does resistance evolve slowly through classical evolutionary selection, horizontal gene transfer can lead to the appearance of a resistant infectious agent very rapidly. As existing antibiotics therefore became ineffective, along with improved management of antibiotic use, there is a significant need for research to focus on new mode of action antibiotics that can overcome resistant pathogens. If the antimicrobial resistance remains uncontrolled it has been estimated by 2050 there will be an additional 10 million deaths worldwide.⁴⁵

1.5. Polyketides

Polyketides are a class of secondary metabolites that are produced by microorganisms (bacteria and fungi) and plants. Several polyketide natural products are therapeutically useful as antibiotics and anticancer agents. Doxorubicin **1.13** is an anthracycline antibiotic, and is used widely as a cancer chemotherapy treatment, whilst tetracyclines are a well-known family of broad spectrum antibiotics that are effective in the treatment of a wide range of bacterial infections.^{46,47,48} Although the total chemical synthesis of natural product polyketides is highly challenging, gaining an understanding of both their structure and their therapeutic effect are the motivation for researchers to explore the synthesis and biosynthesis of natural product polyketides (**Figure 1.8**).⁴⁹



1.3
Doxorubicin

Figure 1.8: Chemical structure of doxorubicin 1.13.

1.5.1. The Biosynthesis of Natural Product Polyketide

The biosynthesis of polyketides has many similarities to fatty acid biosynthesis, involving two carbon chain elongation steps, oxidation changes and common building blocks (e.g. acetyl coenzyme A and malonyl coenzyme A).

In the biosynthesis of both fatty acids and polyketides, the starter unit is attached to a cysteine thiol of a ketosynthase enzyme (KS). The extender unit is then loaded on to a cysteine thiol of an acyl carrier protein (ACP), by an acyl transferase (AT) or malonyl acyl transferase (MAT).

In fatty acid biosynthesis, acetyl-CoA is the starter unit for chain initiation followed by malonyl-CoA as the extender unit for chain elongation. In contrast, a range of acyl groups can be involved in polyketide biosynthesis including acetyl-, malonyl-, malonamyl-, propionyl-, butyryl-, cyclohexyl-, benzoyl- and 3-hydroxy-5-amino benzoyl-CoA as starter units while, malonyl-CoA and methylmalonyl-CoA are employed as the extender units (**Figure 1.9**).^{47,48,12}

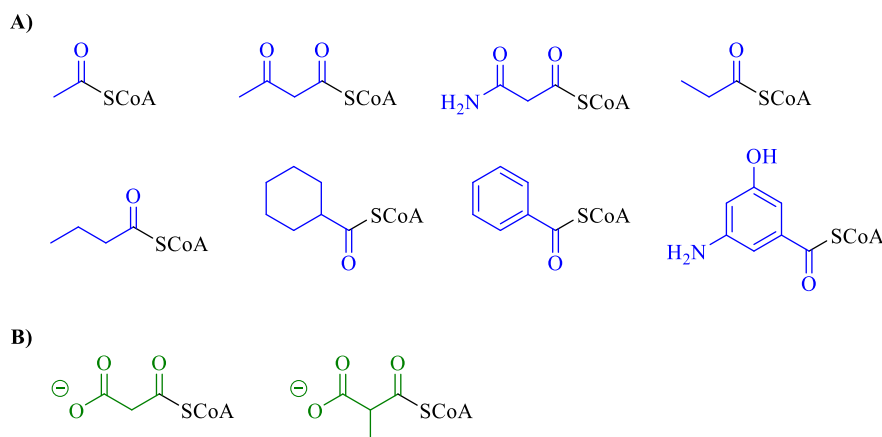
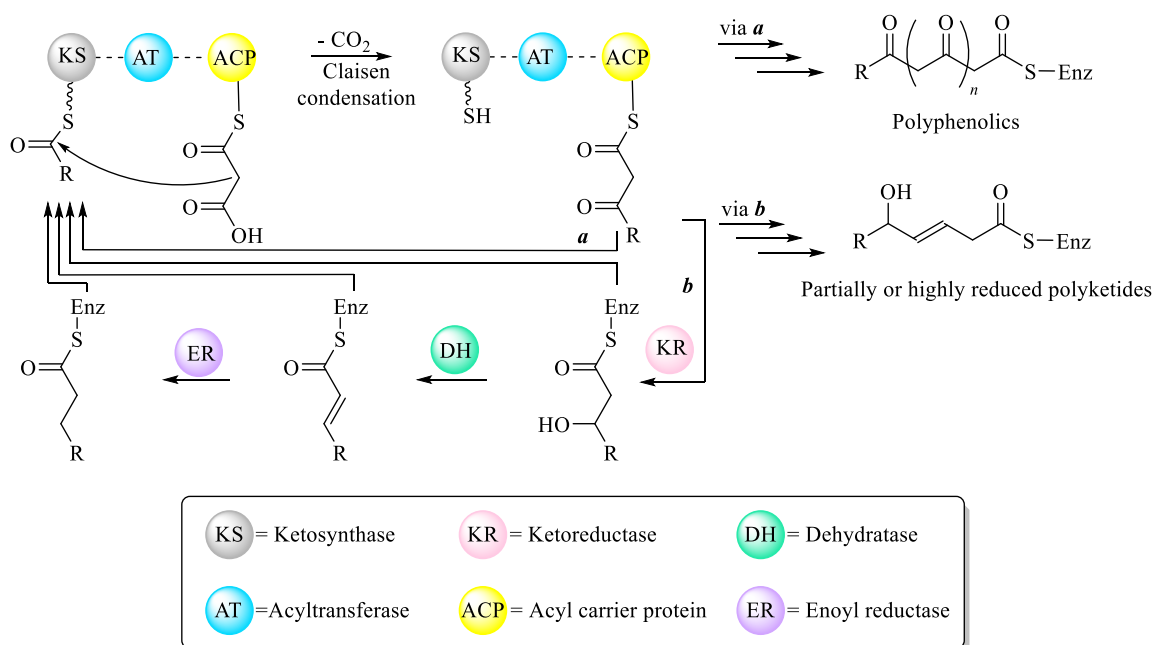


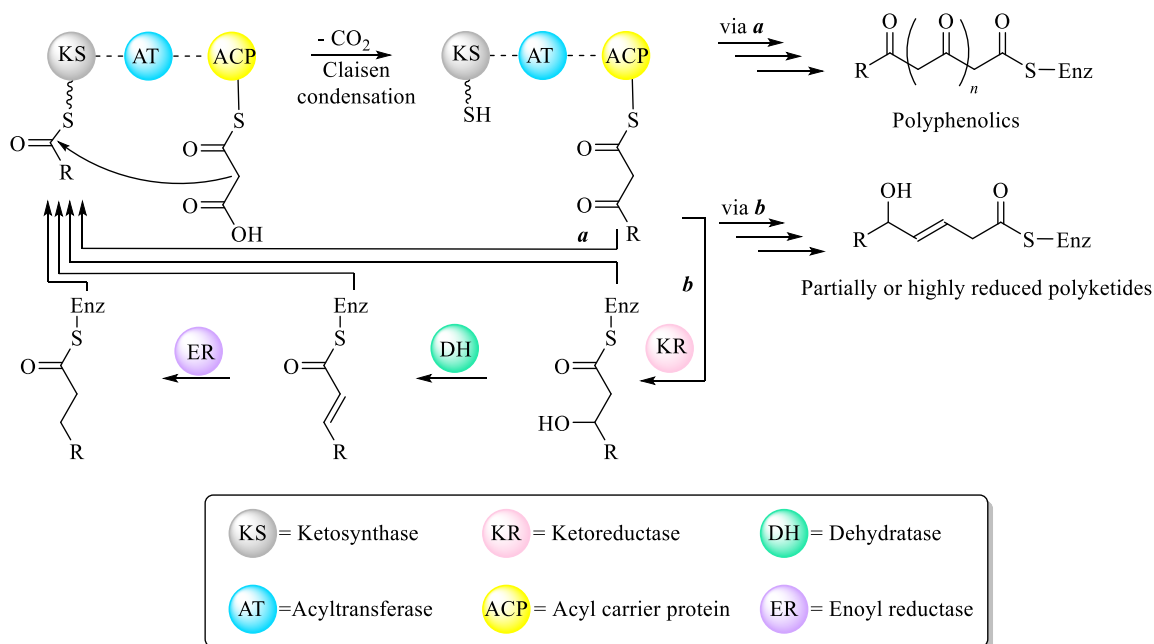
Figure 1.9: Building blocks for (A) initiation and (B) elongation cycles by PKS assembly lines.¹²

Fatty acids are formed by repetitive decarboxylative Claisen thioester condensation of an activated starter unit with an extender unit. After the chain elongation step several other enzymes are involved, ketoreductase (KR) introduces the β -oxo functional group, dehydrates (DH) and enoyl reductase (ER) to produce a saturated acyl backbone (**Scheme 1.1**).^{47,48,12}



Scheme 1.1: General mechanism for fatty acid biosynthesis.^{12,49}

In contrast, in the polyketide biosynthesis more complex molecules can be produced as the chain elongation steps can be followed by many different combinations of enzymatically catalysed reactions (KR, DH, ER and others) as well as non-enzymatic reactions (**Scheme 1.2**).^{47,48,12}



Scheme 1.2: General mechanism for polyketides biosynthesis.^{12,49}

1.6. Conclusions

Due to the potential for variation in the biosynthetic pathways for polyketide biosynthesis, a high variety of different complex molecular structures can be generated. These natural product polyketides from bacteria and other microorganisms are thus a valuable resource for the discovery of new antibiotics.

1.7. Project Background

The aim of this thesis was to explore the total synthesis of DEM30355/A **1.14** and a number of related polyketides. DEM30355/A **1.14** is a novel bioactive compound discovered in Newcastle which displays G-p antibiotic activity, with a mode of action which whilst unknown appears to be different compared to existing clinically used antibiotics. DEM30355/A **1.14** was isolated from an *Amycolatopsis* strain by Demuris Ltd., a Newcastle University spin out company focused on the discovery of novel antibiotics. DEM30355/A **1.14** is a fluorescent polyketide natural product with a high content of oxygen atoms. The complexity of **1.14** arises from its chemical structure which includes five contiguous stereocenters with one distinct five membered lactone ring and three different six membered rings: one aromatic ring, saturated and partially saturated rings. The structure of **1.14** was confirmed by NMR and single crystal X-ray analysis (**Figure 1.10**).

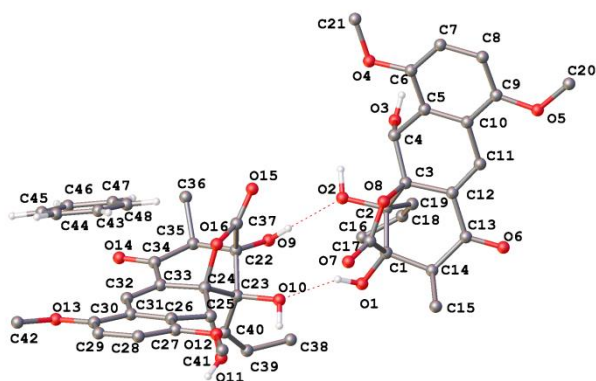


Figure 1.10: X-ray crystal structure of DEM30355/A 1.14.

The antibiotic activity of DEM30355/A **1.14** was examined against different pathogenic G-p and G-n bacteria, and it shows remarkable activity only against a range of G-p bacteria, in particular methicillin-resistant *Staphylococcus aureus* (Table 1.4).

Species	DEM30355/A
<i>S. aureus</i>	8
<i>S. pneumoniae</i>	8
<i>E. faecium</i>	16
<i>E. coli</i>	>128

Table 1.4: MIC of DEM30355/A 1.1 against different pathogenic bacteria.

DEM30355/A **1.14** has some structural similarities to the rishirilides, in particular rishirilide A **1.15** (Figure 1.11).

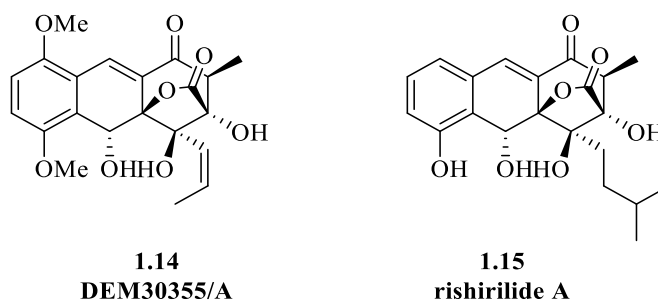


Figure 1.11: Structures of DEM30355/A 1.14 and rishirilide A 1.15.

1.8. Rishirilides

(+)-Rishirilide A **1.15** and (+)-rishirilide B **1.16** were isolated by Iwaki and co-workers from *Streptomyces rishiriensis* OFR-1056 in 1984, they act as α_2 -macroglobulin inhibitors but neither have been reported as having any significant antibiotic activity.⁵⁰ Rishirilide B **1.16** shows higher activity in inhibiting α_2 -macroglobulin with an $IC_{50} = 35 \mu\text{g/ml}$, while rishirilide A **1.15** shows weaker inhibition with $IC_{50} = 100 \mu\text{g/ml}$.⁵¹ The biological activity of rishirilide B **1.16** was further examined and it was classified as a glutathione *S* transferase inhibitor with an $IC_{50} = 26.9 \mu\text{M}$.⁵² Thus **1.16** could be useful in treating cancer since glutathione *S* transferase increases resistance against anticancer drugs. In 2012, the first cloning of the type II PKS biosynthetic gene cluster (*rsl*.) from *Streptomyces bottropensis* was carried out by A. Yan, K. Probst, A. Linnenbrink, M. Arnold, T. Paululat, A. Zeeck and A. Bechthold to produce **1.15** and **1.16** and to study the biosynthesis(**Figure 1.12**).⁵¹

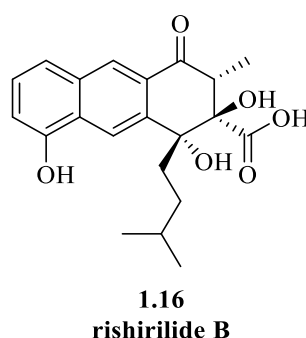


Figure 1.12: Structures of (+) rishirilide B **1.16**.

1.8.1. The Biosynthesis of Rishirilides A and B

The biosynthesis of rishirilides A **1.15** and B **1.16** includes the formation of rishirilide B **1.16** first, which is hypothesized to be the precursor for rishirilide A **1.15** (**Scheme 1.3**).⁵³

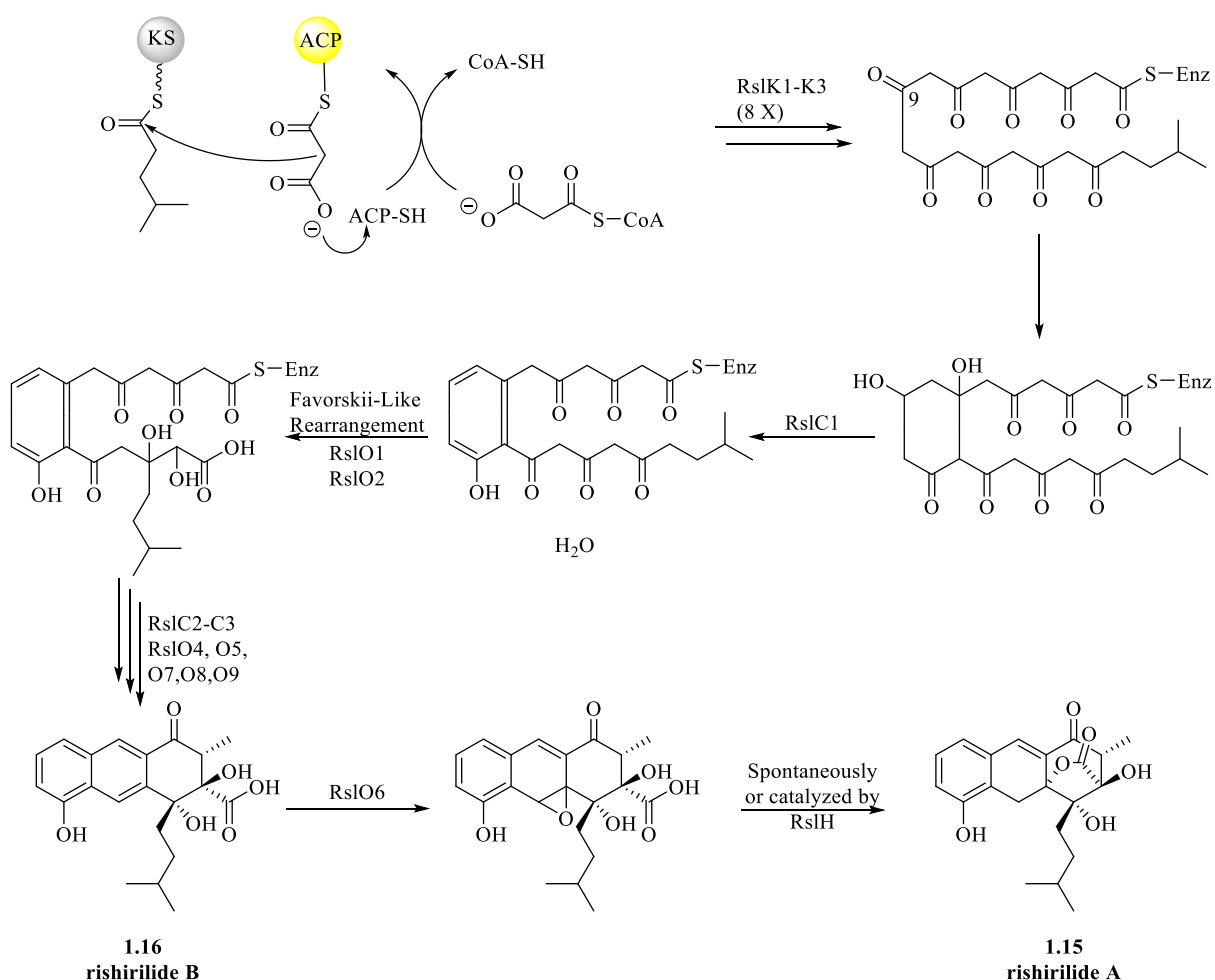
The biosynthesis of rishirilide B **1.16** involves:

- 1) Iterative condensation reactions (8 elongation cycles) between a branched starter unit and several malonyl-CoA or malonyl-ACP extender unit catalysed by RslK1, RslK3 and related PKS enzymes to yield the full length polyketide backbone.
- 2) RslO10 catalysed the reduction reaction of ketone at C-9 to introduce a hydroxyl group followed by ring closure at C-7 and C12.
- 3) The resulting ring aromatises under the control of RslC1 to form the first aromatic ring.

- 4) A Favorskii rearrangement, catalysed by luciferase-like monooxygenase enzymes (RslO1) and (RslO2), introduces an oxygen atom at C-16 to form a reactive intermediate followed by the migration of the isopentyl group from C-18 to C-15. Then hydroxyl and carboxyl groups were formed at C-16 at C-17 respectively.
- 5) The anthracene skeleton of the rishirilides is formed after cyclisation of the second and third rings catalysed by RslC2 and RslC3 respectively. Next, rishirilide B **1.16** is formed after tailoring reactions mediated by several oxidoreductases reactions such as RslO4, RslO7, RslO8 and RslO9.

The biosynthesis of rishirilide A **1.15** from rishirilide B **1.16** occurs in two steps:

- 1) Epoxidation of rishirilide B **1.16** catalysed by RslO6, a luciferase-like monooxygenase enzyme.
- 2) Lactone ring is then formed spontaneously (or possibly assisted by RslH), to generate rishirilide A **1.15**.



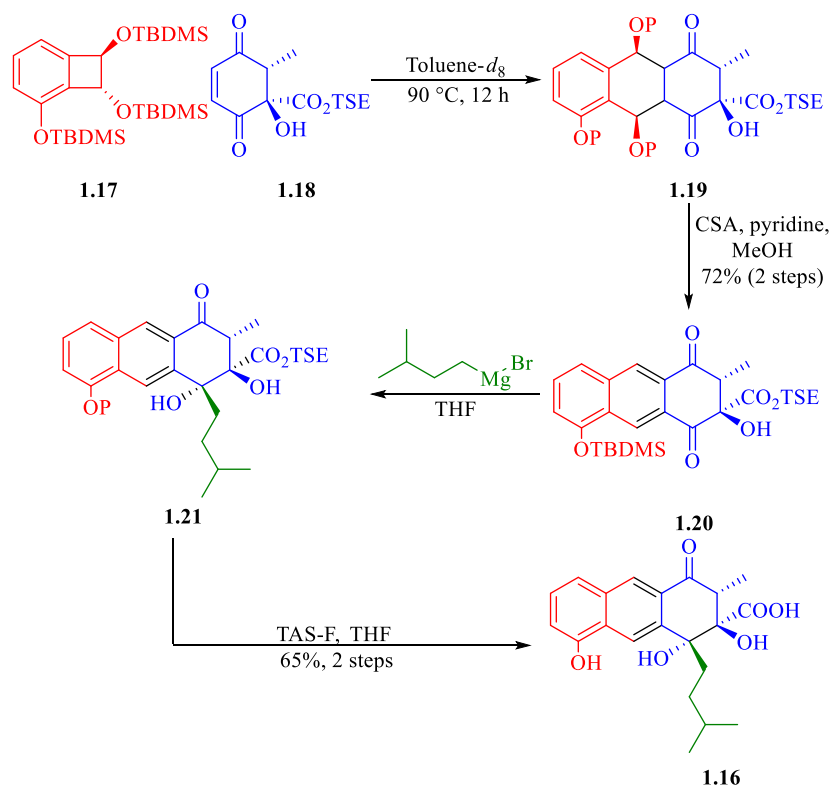
Scheme 1.3: Proposed biosynthetic pathway for rishirilides A **1.15 and B **1.16**.**

1.8.2. The Total Synthesis of Rishirilide B

Due to the interesting biological activity of rishirilide B **1.16** as a small molecule anticlotting factor and anticancer agent, and in order to solve the absolute stereochemistry, several total syntheses have been published.

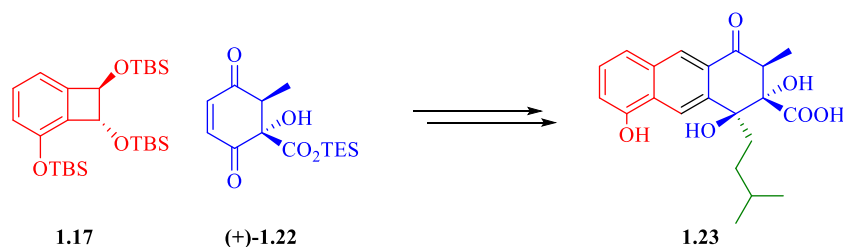
1.8.2.1. Danishefsky Approach

The first total synthesis of racemic rishirilide B **1.16** was achieved by S. Danishefsky and J. Allen in 2001. The key step includes regioselective Diels–Alder reaction of quinodimethide **1.17** and enedione **1.18** to form **1.19** which represents the core structure of rishirilide B **1.16**. Next, a series of chemical modification reactions such as deprotections, dehydration, aromatisation and a Grignard addition were performed to give (±) rishirilide B **1.16** as a racemic mixture in a 47% yield from the dienophile **1.18** (Scheme 1.4).⁵⁴



Scheme 1.4: Synthesis of racemic (±) rishirilide B by Danishefsky.

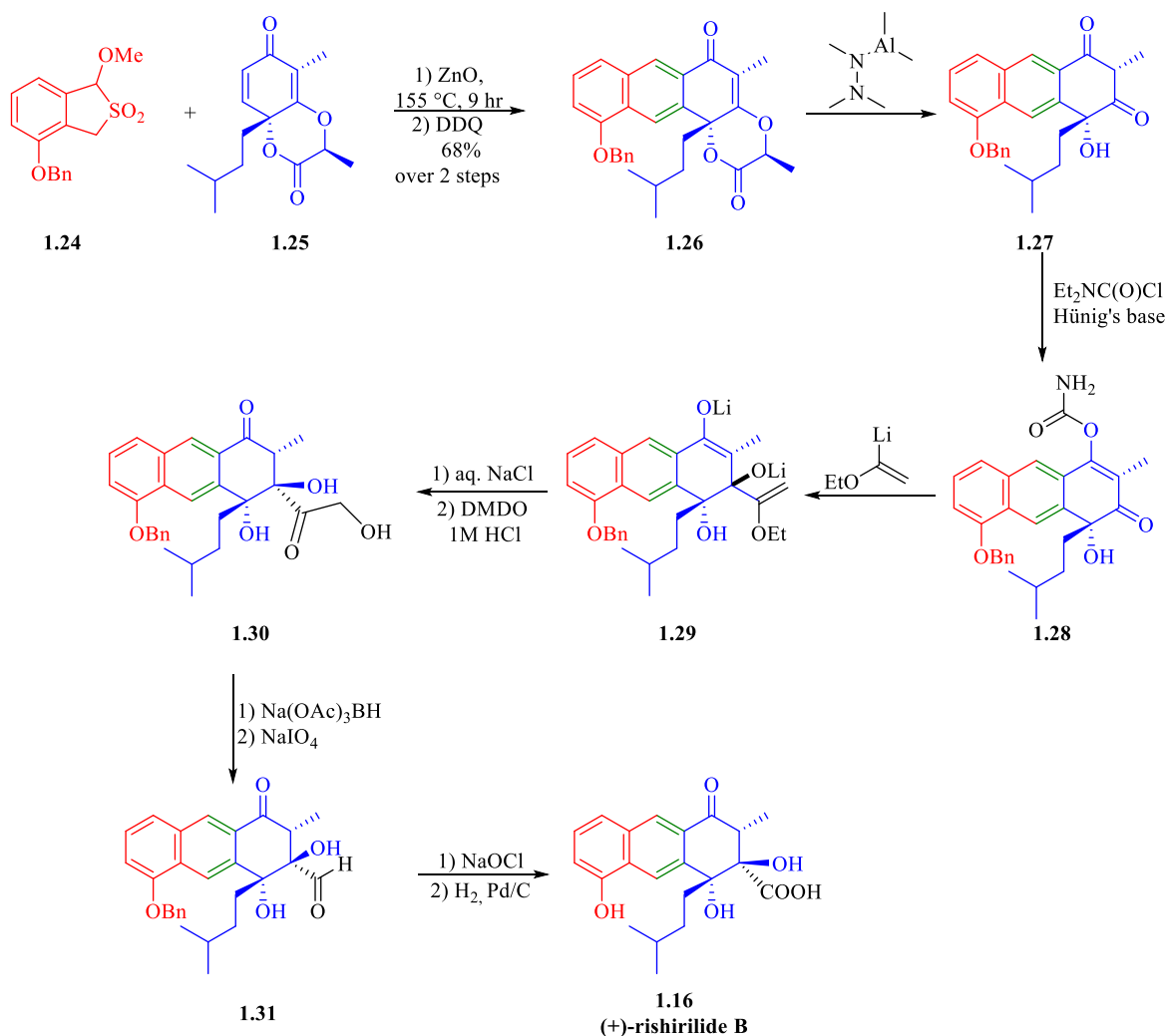
Danishefsky and co-workers revisited the synthesis of rishirilide B, using enantiomerically pure dienophile **1.22** in order to access an enantiopure sample of the natural product for comparison. Completion of the synthesis following the original racemic procedure, gave rishirilide B as a single enantiomer. However, the resulting enantiomer turned out to be the unnatural (-) rishirilide B **1.23** (Scheme 1.5).⁵⁵



Scheme 1.5: Synthesis of unnatural (-) rishirilide B 1.23.

1.8.2.2. Pettus Approach

The total synthesis of (+)-rishirilide B **1.16** as it is found in nature was successfully achieved by T. Pettus and L. Mejorado in 2006. They have developed a synthetic route to **1.16** based on producing anthracene (-)-**1.26**, the skeleton of (+)-rishirilide B **1.16**, via a Diels-Alder cycloaddition reaction of the enantiopure dienophile **1.25** to the diene derived from a cyclic sulfone **1.24** in the presence of DDQ.



Scheme 1.6: Total synthesis of (+) rishirilide B 1.16 by Pettus.

The cleavage of lactone ring from the resulting anthracene **1.26** yielded **1.27**. Next, selective *O*-acylation of the dione **1.27** with diethylcarbonyl chloride in the presence of Hünig's base produced **1.28**. The excess addition of lithiated ethyl vinyl ether to the ketone **1.28** lead to the formation of the enolate **1.29**. Work-up of **1.29** with saturated solution of NaCl followed by an epoxidation with DMDO gave α -hydroxy ketone (-)-**1.30** in a high yield. The aldehyde **1.31** was afforded after reducing α,α' -dihydroxy ketone **1.30** by sodium triacetoxyborohydride followed by oxidizing the resulting tetrol with NaIO₄. The aldehyde **1.31** was converted into desired carboxylic acid **1.32** via NaOCl. At the final step the cleavage of the benzyl protecting group using palladium over carbon catalyst under hydrogen atmosphere gave (+)-rishirilide B **1.16** in 20% (**Scheme 1.6**).⁵⁶

Chapter 2

2. Results and Discussions

2.1. Project Aims

Due to the interest in developing new antibiotic molecules the aim of this project was to examine synthetic approaches to DEM30355/A **1.14** and related polyketides.

2.2. Retrosynthesis of DEM30355/A 1.14

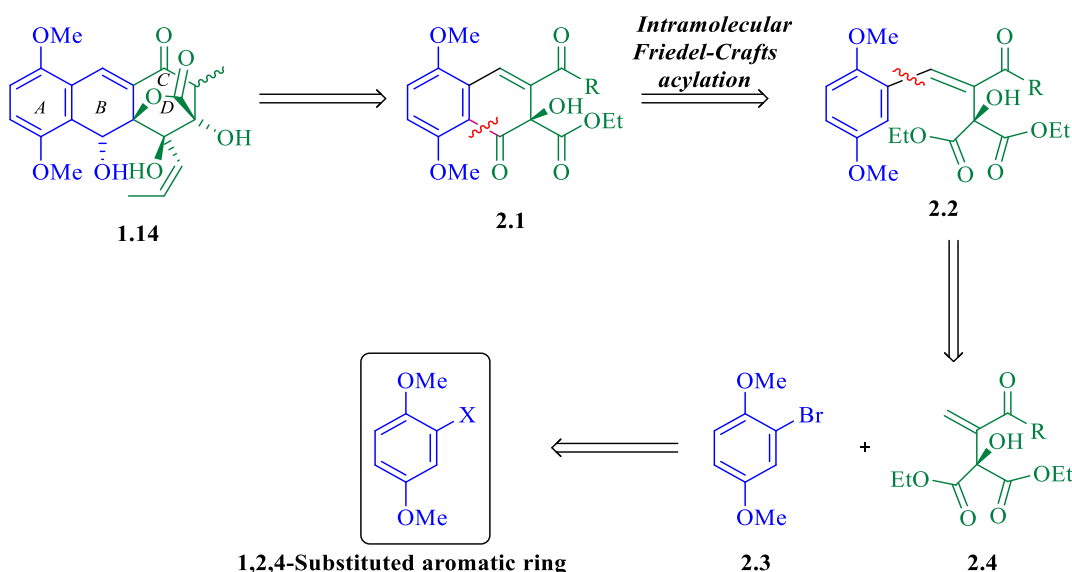
We have considered two different approaches towards the total synthesis of DEM30355A **1.14**. These approaches focus on constructing the carbon skeleton of both rings A and B through an intramolecular cyclisation reaction of ring B. We envisioned that an intramolecular cyclisation to give ring B could be achieved through:

- i. A Friedel-Crafts (F-C) acylation approach.
- ii. An Aldol condensation approach.

Once we can develop a route to allow access to rings A and B we would develop this intermediate to include the synthesis of rings C and D. Therefore the retrosynthetic analysis of DEM30355A **1.14** including the ring C and D will be discussed in detail later.

2.2.1. Friedel-Crafts Acylation Approach

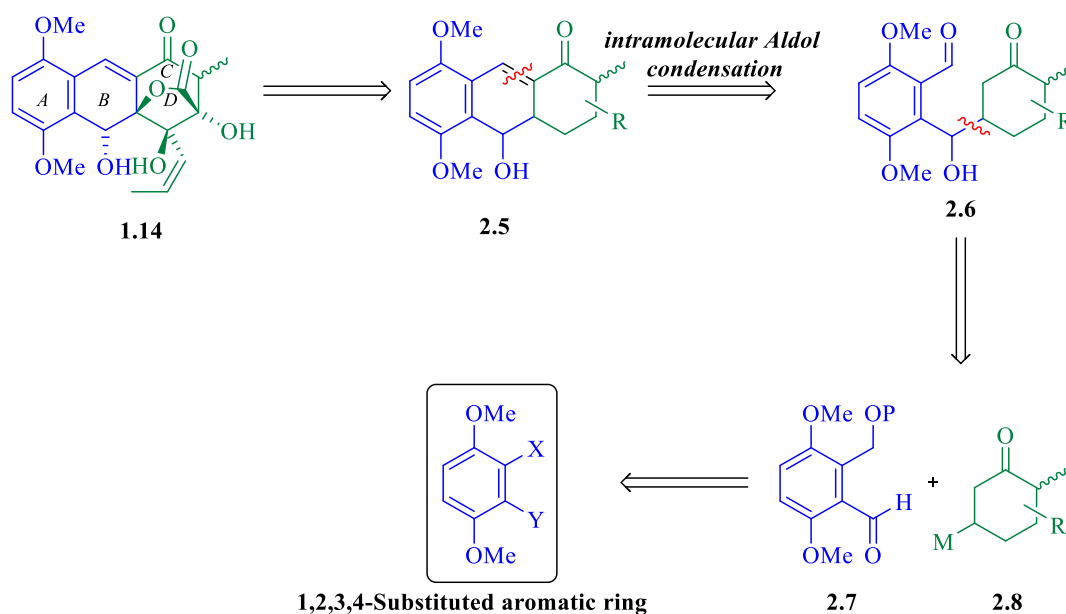
In this strategy we aim to form ring B in compound **2.1** through an intramolecular F-C reaction between the electron rich aromatic ring A and a tethered activated carbonyl group in **2.2**. In turn **2.2** could be produced from a Heck cross coupling reaction between 2-bromo-1,4-dimethoxybenzene **2.3** and Baylis–Hillman adduct **2.4** (Scheme 2.1).



Scheme 2.1: Proposed retrosynthetic approach to **1.14** via an intramolecular F-C reaction.

2.2.2. Aldol Condensation Approach

This approach is based on the formation of two bonds between an aromatic ring A, with a 1,2,3,4-substitution pattern, and a suitably functionalised ring C in order to form ring B. Therefore ring B in compound **2.5** could be formed through an intramolecular Aldol condensation between the aldehyde and ketone in **2.6**. Further disconnection between ring A and C in compound **2.6** gives the aldehyde **2.7** and an organometallic **2.8**. Thus the coupling between ring A and C could be achieved through a nucleophilic addition of an organometallic **2.8** to aldehyde **2.7** via Barbier or Grignard type reaction, with a metal such as magnesium, zinc, indium or barium, to form the secondary alcohol **2.6** followed by cyclization of **2.6** to form **2.5** via an intramolecular aldol condensation (Scheme 2.2).

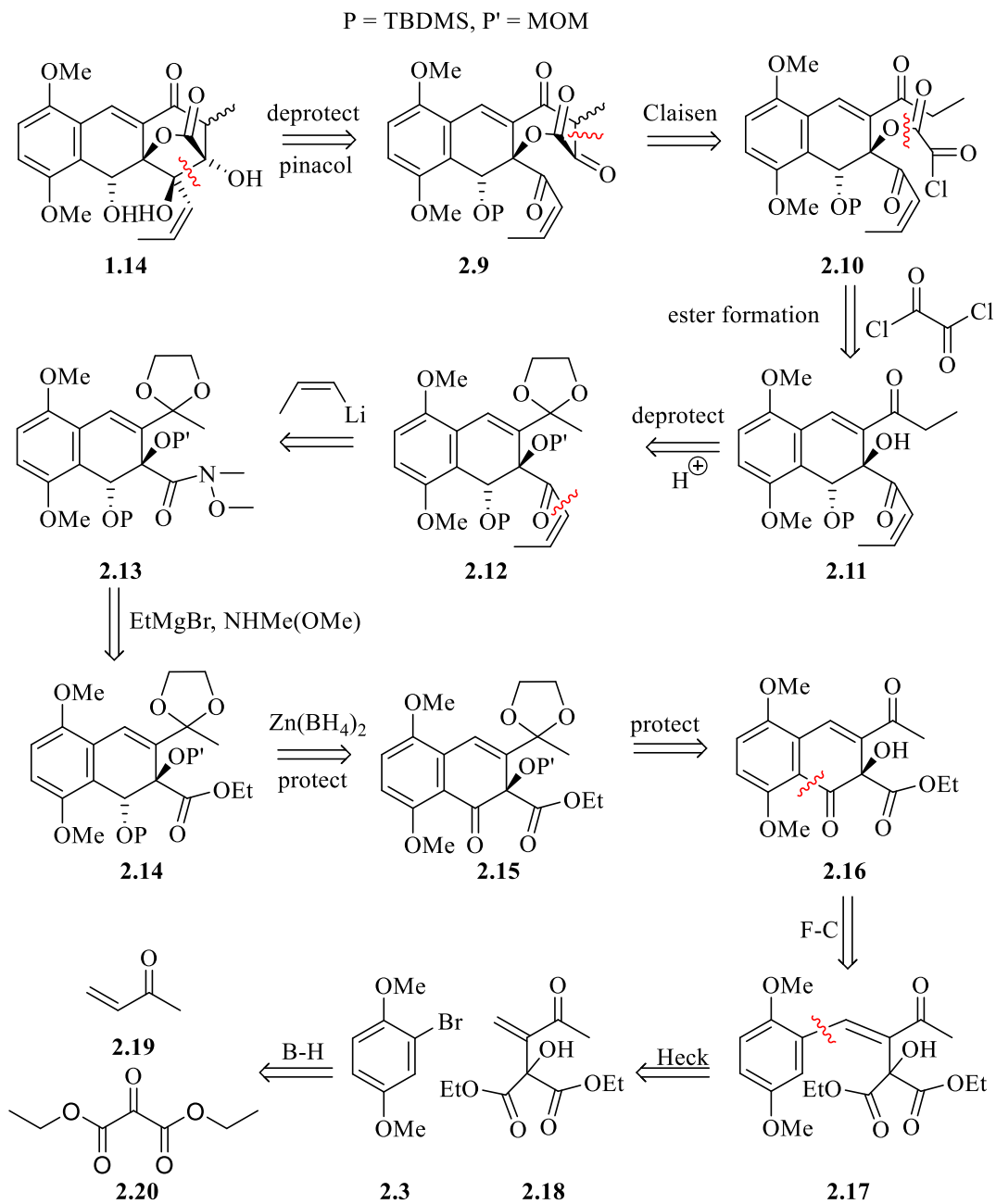


Scheme 2.2: Proposed retrosynthetic approach to 1.14 via an intramolecular Aldol condensation.

In this chapter the retrosynthesis of DEM30355A **1.14** via intramolecular Friedel-Crafts acylation approach will be discussed in detail.

2.3. Retrosynthetic Analysis of DEM30355/A 1.14 Based on an Intramolecular Friedel-Crafts Acylation Approach

We envisioned that our target molecule DEM30355/A **1.14** could be prepared via an intramolecular pinacol coupling of **2.9** followed by alcohol deprotection. Deprotonation of α -hydrogen in **2.10** would produce the corresponding nucleophilic enolate which can undergo an intramolecular Claisen condensation reaction to give the *n* cyclic lactone **2.9**. Compound **2.10** could be obtained through the esterification of alcohol **2.11** with oxalyl chloride. The tertiary alcohol **2.11** could be produced by removing MOM protecting group from compound **2.12**. Next the conversion of ester in compound **2.14** to an *N*-methoxy-*N*-methylamide gives **2.13**, allowing the addition of *cis*-propenyllithium to give **2.12**. Stereoselective reduction of the prochiral ketone **2.15** using $\text{Zn}(\text{BH}_4)_2$ followed by protection of the resulting secondary alcohol with *tert*-butyldimethylsilyl chloride (TBDMSCl) would provide compound **2.14**. The chelation directed reduction with $\text{Zn}(\text{BH}_4)_2$ is used to set the desired relative *anti*-stereochemistry between the resulting two protected alcohol groups. Next, the protection of the keto group in α,β -unsaturated ketone **2.16** as a cyclic acetal is essential to prevent any side reactions during the subsequent ketone reduction. Also due to the reactivity of hydroxyl groups, the protection of tertiary alcohol as a methoxymethyl acetal (MOM) is necessary, thus a double protection to give the compound **2.15** is envisaged. Then compound **2.17** could undergo cyclisation through intramolecular Friedel-Crafts acylation in the presence of a Lewis acid to form the ketone **2.16**. Compound **2.16** includes the skeleton for both rings A and B and introduces the first stereogenic centre, at the tertiary alcohol. Compound **2.17** would be produced through a Heck cross coupling reaction between the commercially available 2-bromo-1,4-dimethoxybenzene **2.3** and the Baylis-Hillman adduct **2.18**. Baylis-Hillman adduct **2.18** could be produced through the Baylis-Hillman reaction of methyl vinyl ketone **2.19** and diethyl ketomalonate **2.20** (Scheme 2.3).



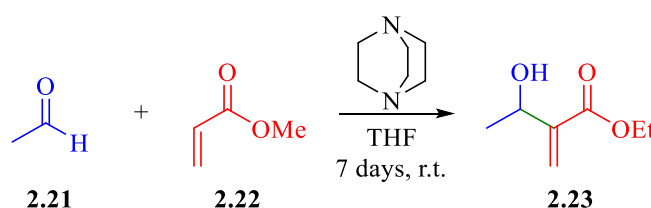
Scheme 2.3: Retrosynthesis of DEM30355/A 1.14 following intramolecular Friedel-Crafts acylation approach.

2.4. Synthesis of Ring A and B: Synthesis of 2.16 via an Intramolecular Friedel-Crafts Acylation

Therefore our first challenge was to investigate a Baylis-Hillman approach to **2.18** as a key starting material in our proposed synthesis.

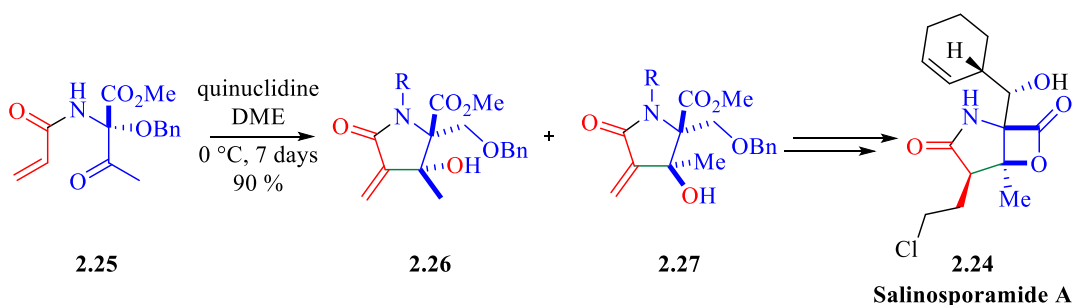
2.4.1. Baylis-Hillman Reaction

Baylis-Hillman reaction is a useful method to form a single C-C bond at the α -position of α,β -unsaturated carbonyl compounds or their derivatives (esters and amides) and aldehydes or ketones, in the presence of a tertiary amine as a nucleophilic catalyst such as DABCO and DBU, to give highly functionalised products.^{57,58} Early example of this type of reaction was reported by K. Mortia in 1968 when methyl acrylate **2.22** reacted with acetaldehyde **2.21** in the presence of tricyclohexylphosphine gave α -hydroxylated product **2.23**.⁵⁹ In 1972, A.B Baylis and M. D. Hillman optimised the Mortia reaction conditions by using DABCO as a catalyst (**Scheme 2.4**).



Scheme 2.4: First reaction reported by A. Baylis and D. Hillman for functionalizing the α -position of an activated alkene **2.22**.

The Baylis-Hillman reaction is widely employed in the total synthesis of many natural products to produce densely functionalized intermediates. For example, Corey and his co-workers developed an efficient stereoselective total synthesis of the anticancer agent Salinosporamide A **2.24** by applying the intramolecular Baylis-Hilman reaction to a ketoamide in the presence of quinuclidine (**Scheme 2.5**).⁶⁰

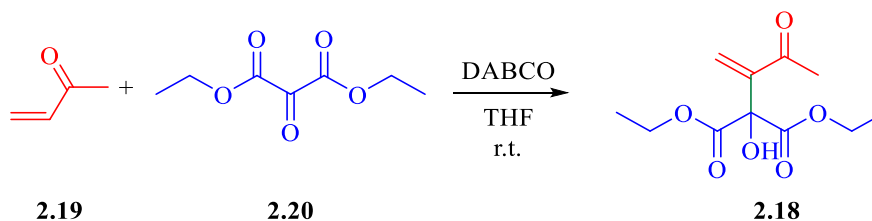


Scheme 2.5: Synthesis of the natural product Salinosporamide A **2.24** via an intramolecular Baylis-Hillman reaction.

However, the major disadvantage of Baylis-Hillman reaction is the slow rate of reaction as it can take several days or weeks.⁵⁸

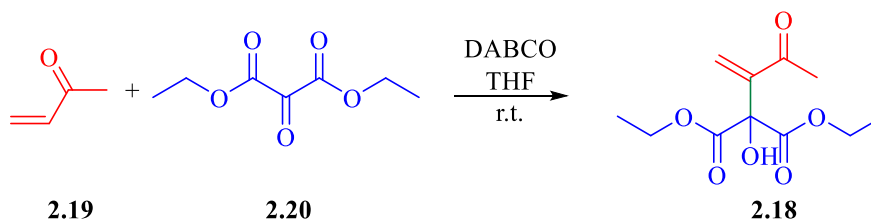
2.4.2. Synthesis of Diethyl 2-hydroxy-2-(3-oxobut-1-en-2-yl)malonate **2.18** via a Baylis-Hillman Reaction

Based on a literature procedure, the preparation of **2.18** was examined by treating methyl vinyl ketone **2.19** solution in THF with diethyl ketomalonate **2.20** in the presence of 10% of DABCO catalyst at room temperature.⁶¹



Scheme 2.6: Synthesis of **2.18** via a Baylis-Hillman reaction.

In our first attempt the reaction was worked up after 45 minutes, no change could be observed by TLC under UV light. However the ¹H NMR of the crude product showed the presence of new signals corresponding to a terminal alkene. Therefore, we subjected the crude product to column chromatography to isolate the desired product **2.18**, unfortunately the isolated yield was low 8%. Therefore, it was decided to increase the reaction time, in addition we investigated staining of the TLC plates with vanillin as this allowed us to observe the formation of the product in this reaction. We therefore repeated the reaction, monitoring by TLC and ¹H NMR. After 24 hours the reaction was worked up and the crude ¹H NMR showed that the yield of the product **2.18** increased significantly, estimated by integration to be approximately 65%. The product **2.18** was purified by column chromatography giving an isolated yield of 40%. We postulated that the low isolated yield was because of the decomposition of **2.18** on the column, therefore we decided to examine increasing the reaction time to increase the yield. Given a sufficiently high yield chromatography would then become unnecessary. Therefore, we repeated the reaction again. After 4 days at room temperature the product **2.18** was successfully formed in an excellent yield 98% with no purification required (Table 2.1 and Figure 2.1).



No.	Reaction Time	%Yield
1	45 min	8*
2	1 day	40*
3	4 days	98

*Isolated yield of the product **2.18** after column purification.

Table 2.1: Yield optimisation in the formation of B-H product **2.18**

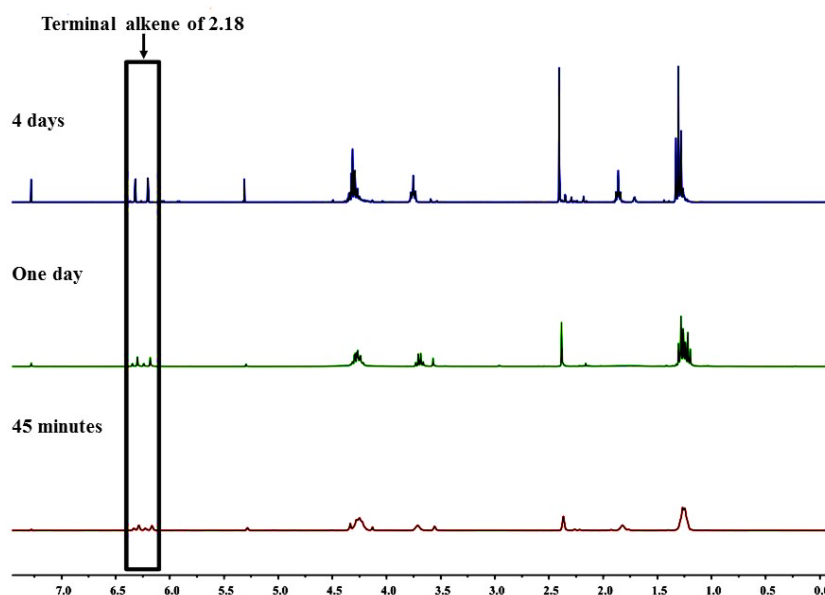
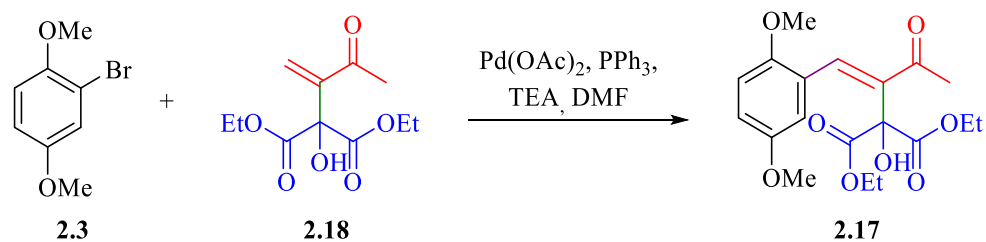


Figure 2.1: The formation of **2.18** against time by ^1H NMR of the crude reaction mixtures. Distinctive terminal alkene signals of **2.18** are highlighted.

2.4.3. Heck Coupling of Baylis-Hillman Adduct **2.18** and 2-Bromo-1,4-dimethoxybenzene **2.3**

The Heck reaction was first reported by Mizoroki and Heck in 1968 and it has proved to be an important coupling reaction between terminal alkenes and aryl and vinyl halides.⁶² The Heck reaction is widely used in constructing complex natural products.⁶³ We decided to examine the use of a Heck reaction in the preparation of compound **2.17** through the reaction with aryl halide **2.3** and our previously synthesised Baylis-Hillman adduct **2.18**.



Scheme 2.7: Proposed Heck reaction of 2.3 and 2.18 to give 2.17.

We therefore examined the synthesis of **2.17** through the coupling of 2-bromo-1,4-dimethoxybenzene **2.3** with **2.18**, catalysed by palladium diacetate in the presence of triphenylphosphine and triethylamine (TEA). After 21 hours at 100 °C, the ¹H NMR and TLC of the reaction mixture showed the presence of a complex mixture of products. The desired product **2.17** appeared to be present in one of the fractions from column chromatography, however **2.17** was isolated along with several other compounds of similar *R_f* values. Analysis of this fraction by mass spectrometry showed the presence of the correct mass for **2.17**, confirming its presence (**Figure 2.2**).

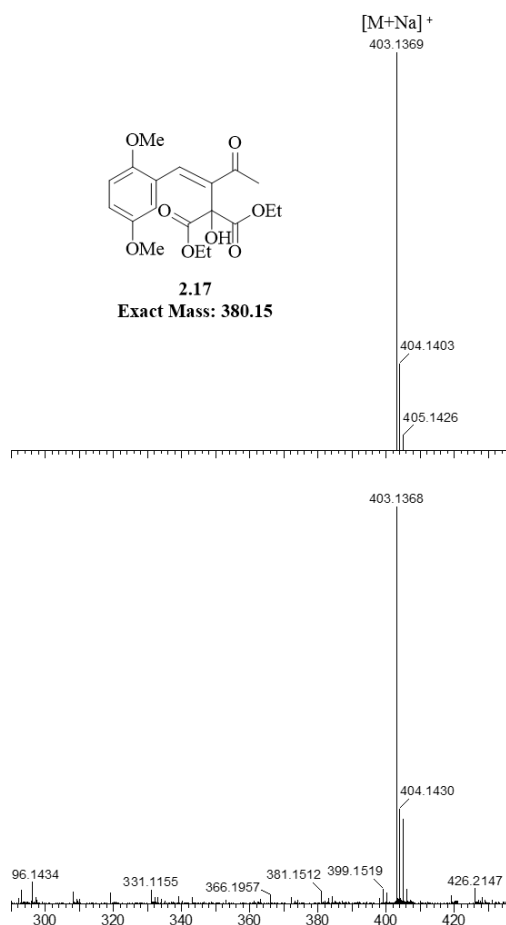
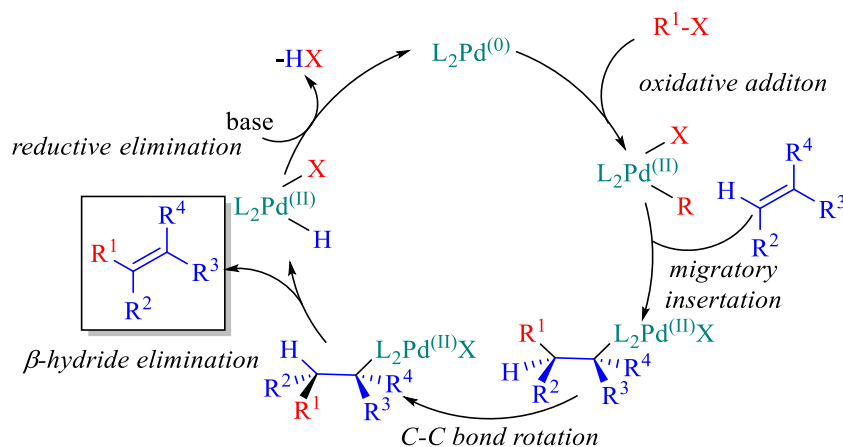


Figure 2.2: Mass spectrum of column fraction containing 2.17. Top: Theoretical mass isotope pattern for 2.17. Bottom: Experimental spectrum.

To understand why these coupling reactions did not succeed, we need to provide a brief overview of the Heck reaction concepts and mechanism. The Heck reaction is a coupling between an electrophilic aryl or vinyl halide (R-X, X= Br or I) and a nucleophilic alkene. The initial step the Heck reaction is the generation of an electron rich palladium (0) which can then readily undergo an oxidative addition into arylhalide or vinylhalide bond to give a $RPdXL_2$ species. The alkene then coordinates to the $RPdXL_2$ species followed by migratory insertion to form a σ bond complex with the palladium. Then β -hydride elimination occurs to produce the desired *trans*-substituted alkene product. The final step in the Heck catalytic cycle is then the reductive elimination of HX from the $HPdXL_2$ intermediate and regenerating the catalyst L_2Pd (Scheme 2.8).^{64,65,66}



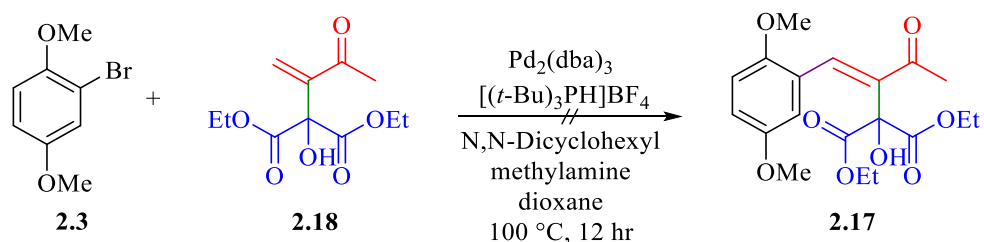
Scheme 2.8: Heck Reaction Mechanism.

Therefore, to improve the outcome of our Heck reaction we decided to examine methods that could speed up the oxidative insertion step to 2-bromo-1,4-dimethoxybenzene 2.3. Thus we wished to investigate the use of σ -donating trialkylphosphine ligands in place of triphenylphosphine to increase the electron density on the palladium and thus facilitate the oxidative addition step.

2.4.4. Attempt to Optimise Heck Reaction Condition

G. Fu and M. Netherton developed a new approach for the coupling of arylbromides and alkenes by employing a trialkylphosphine ligand as an alternative to triphenylphosphine to enhance the rate of the Heck reaction. Because trialkylphosphines are air sensitive, they were converted into their conjugate acids to form the corresponding air-stable phosphonium salts. In the case of Heck reaction, trialkylphosphonium salt [(*t*-Bu)₃PH]BF₄ was used as an *in situ* source of (*t*-Bu)₃P in the presence of a weak base.⁶⁷ We

therefore attempted the Heck coupling reaction of 2-bromo-1,4-dimethoxybenzene **2.3** and alkene **2.18** using tris(dibenzylideneacetone)dipalladium(0), tri-*tert*-butylphosphine tetrafluoroborate and *N,N*-dicyclohexylmethylamine based on Fu and Netherton procedure. However after 12 hours of refluxing in dioxane no product could be detected in the ¹H NMR of the crude product.

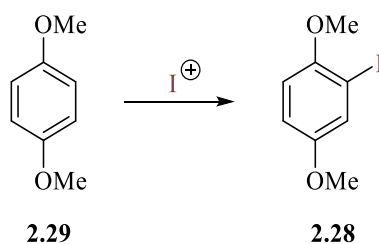


Scheme 2.9: Attempted Heck reaction under Fu conditions

Although low yields of **2.17** could be observed under our first set of conditions, no improvement was obtained by employing σ -donating trialkylphosphine ligands. Next, we decided to optimise the Heck reaction conditions by employing a more reactive arylhalide. In order to find the optimum reaction conditions for the formation of **2.17**, we therefore decided to examine the Heck coupling reaction between 2-iodo-1,4-dimethoxybenzene **2.28** and Baylis-Hillman adduct **2.18**.

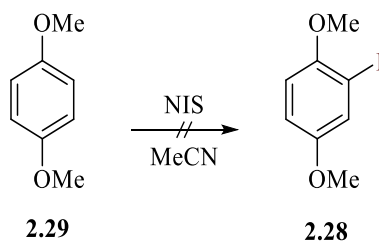
2.4.5. Examination of the Iodination of 1,4-Dimethoxybenzene **2.29**

Therefore, the first step was to examine synthetic routes to aryl iodide **2.28**. We aimed to synthesise aryl iodide **2.28** by an electrophilic aromatic substitution reaction of 1,4-dimethoxybenzene **2.29** with an electrophilic source of iodine (Scheme 2.10).



Scheme 2.10: Proposed route to 2-iodo-1,4-dimethoxybenzene **2.28**.

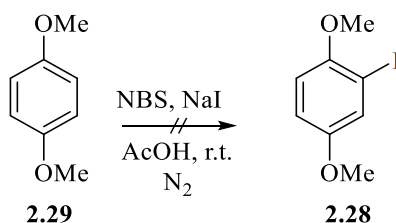
M. C. Carreño reported a method for iodinating methoxybenzenes and naphthalenes using *N*-iodosuccinimide (NIS) as a source of iodine in acetonitrile (Scheme 2.11).⁶⁸



Scheme 2.11: Attempted iodination of **2.29** using NIS in acetonitrile.

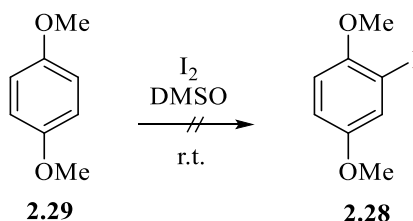
Therefore, we investigated the reaction between 1,4-dimethoxybenzene **2.29** and NIS in acetonitrile. However after 22 hours at room temperature no product was observed. Repeating the reaction at reflux in the dark also failed to provide any of the desired product, with unreacted **2.29** still present.

Due to the poor results in the previous reaction we examined another approach for iodinating 1,4-dimethoxybenzene using iodine monobromide (IBr) as a source of I^+ . IBr can be generated *in situ* from NCS and NaI based on the work of Yamamoto.⁶⁹ Using a modified method we reacted 1,4-dimethoxybenzene with NBS and NaI in AcOH at room temperature however after 20 hours. The 1H NMR of the resulting crude showed only the presence of the starting material **2.29** and the desired product **2.28** was not formed.



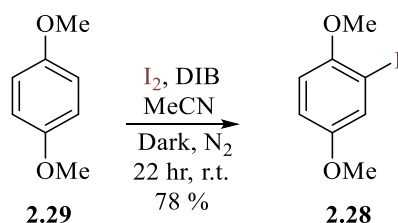
Scheme 2.12: Attempted iodination of **2.29** using NBS and NaI.

Next we turned our attention to the iodination of **2.29** using the molecular iodine I_2 in DMSO based on a literature procedure.⁷⁰ After 21 hours the reaction was quenched using sodium thiosulphate ($Na_2S_2O_3$), however no product could be observed by 1H NMR with only starting material **2.29** present.

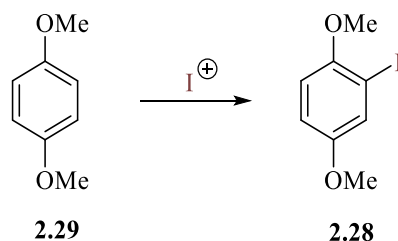


Scheme 2.13: Attempted iodination of **2.29** using I_2 in DMSO.

We continued our research to find an optimum condition for the synthesis of **2.28**. N. Karade and his co-workers have developed an interesting procedure based on using a solvent-free method for halogenating arene substrates using NaCl, NaBr or I₂ in the presence of hypervalent iodine (diacetoxyiodo)benzene (DIB) as an oxidising agent.⁷¹ We therefore examined the reaction between 1,4-dimethoxybenzene **2.29**, iodine and DIB in acetonitrile at room temperature under an inert atmosphere. After 20 hours, the reaction was quenched with Na₂S₂O₃. Gratifyingly, the ¹H NMR of the crude reaction mixture showed the appearance of the three promising peaks in the aromatic region at 7.35 ppm (d, *J* = 3.0 Hz, 1H), 6.87 ppm (dd, *J* = 9.1, 3.0 Hz, 1H) and 6.76 ppm (d, *J* = 9.1 Hz, 1H). This ¹H NMR pattern was indicative of a 1,2,4-substitution pattern in which the two methoxy groups are now inequivalent giving good evidence for a successful reaction. The desired product **2.28** was then isolated by column chromatography in a high yield of 78% (**Scheme 2.14** and **Table 2.2**).



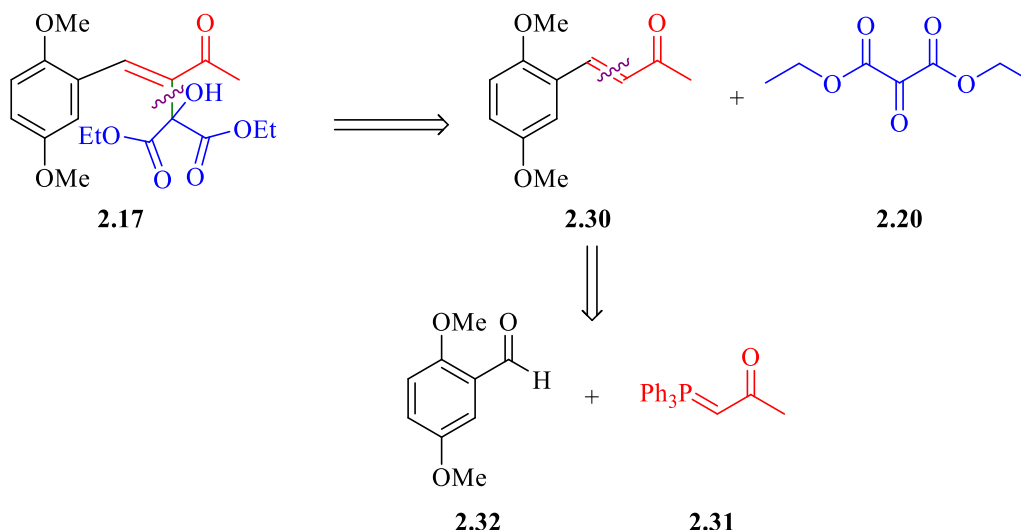
Scheme 2.14: Iodination of **2.29** using DIB and I₂.



No.	Reaction Condition	%Yield
1	NIS, MeCN	Starting material recovered
2	NBS, NaI, AcOH	
3	I ₂ , DMSO	
4	I ₂ , DIB, MeCN, darkness, r.t., 20 hr	78

Table 2.2: Examined reaction conditions towards **2.28**.

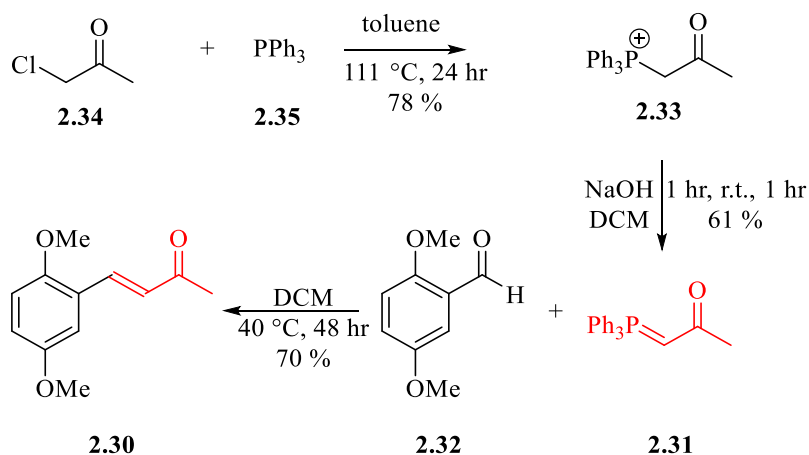
After a successful formation of 2-iodo-1,4-dimethoxybenzene **2.28**, we moved on exploring the Heck coupling reaction using **2.28**.



Scheme 2.16: Proposed plan for the synthesis of 2.17.

2.5.1. Synthesis of Ylide 2.31 and α,β -Unsaturated Ketone 2.30

The initial step in this plan involved in the synthesis of the Wittig reagent 1-(triphenylphosphoranylidene)propan-2-one **2.31**. First, Wittig salt **2.33** was prepared by an S_N2 reaction of α -chloroacetone **2.34** and triphenylphosphine **2.35** in toluene under reflux. After 24 hours the phosphonium salt was isolated by filtration in a good yield of 78%. The phosphonium salt **2.33** was dissolved in DCM and then deprotonated with aqueous sodium hydroxide under phase transfer conditions to give **2.31**. Recrystallization of **2.31** from toluene gave an isolated yield of 61%. Wittig reagent **2.31** was then reacted with 2,5-dimethoxybenzaldehyde **2.32** in refluxing DCM for 48 hours and gave α,β -unsaturated ketone **2.30** as *E*-stereoisomer in a good yield 70% (Scheme 2.17).



Scheme 2.17: Synthesis of 2.31 and 2.30.

The stereochemistry of the alkene **2.30** was confirmed by the ^1H NMR analysis, the alkene protons showing a coupling constant of $J = 16.5$ Hz, consistent with an *E*-alkene. The stereochemistry of **2.30** further confirmed by X-ray crystallography (**Figure 2.3**). Crystals of **2.30** were obtained by slow evaporation from a mixture of petroleum ether and diethyl ether (7:3).

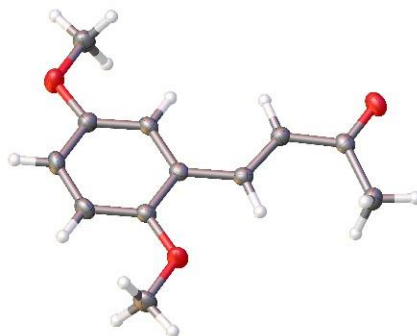
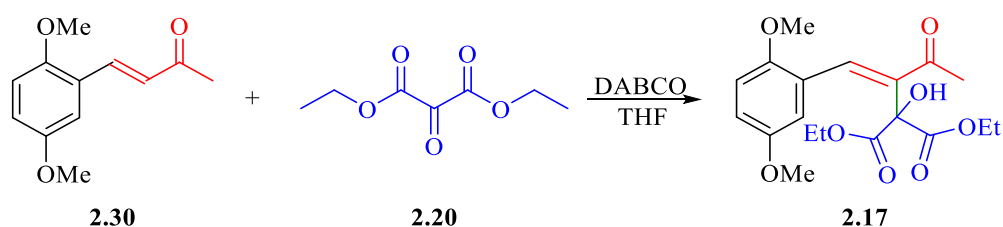


Figure 2.3: Single Crystal X-ray structure of **2.30**.

2.5.2. Synthesis of the Key Synthetic Intermediate **2.10** via Baylis-Hillman Approach

Next, we decided to investigate the use of a Baylis-Hillman reaction to functionalise the α -position of the substituted alkene **2.30** using the diethyl ketomalonate **2.20** in the presence of 10% of DABCO catalyst.



Scheme 2.18: Attempt to produce **2.10** via a B-H reaction.

We therefore reacted **2.30** with diethyl ketomalonate **2.20** in the presence of DABCO. After 7 days at room temperature the ^1H NMR of the crude product showed no reaction had occurred and the starting materials were still present. Increasing the reaction temperature to reflux for 2 days also did not show the production of any product (**Table 2.3**).

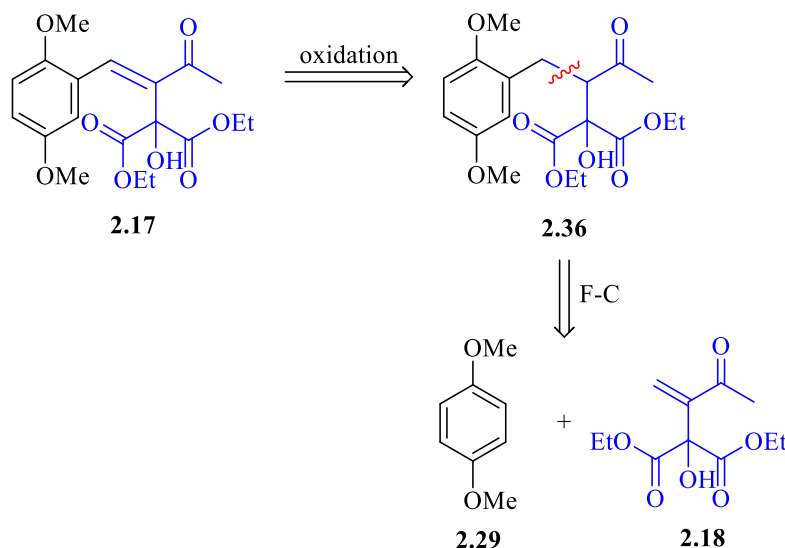
No.	Temperature	Time	%Yield
1	r.t.	7 days	Starting material recovered
2	66 °C	2 days	

Table 2.3: Examination of a B-H reaction conditions towards 2.17.

This attempted Baylis-Hillman reaction has proven to be challenging. A number of studies indicate that a limitation of the Baylis-Hillman reaction is that it works best with terminal alkenes. The Baylis-Hillman reaction of β -substituted alkene often requires harsh reaction conditions such as high pressure.⁵⁸

2.6. Synthesis of Ring A and B: Synthesis of 2.17 via a Friedel-Crafts Reaction

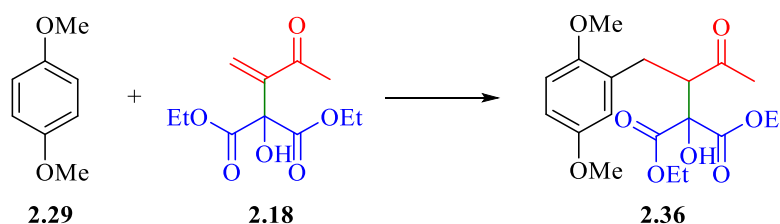
Since the Baylis-Hillman reaction in the previous plan had proved to be unsuccessful, we postulated that compound **2.17** could be produced via a Friedel-Crafts reaction. The newly proposed synthetic route includes the generation of C=C bond in **2.17** via an oxidation reaction of **2.36**. Compound **2.36** could in turn be formed through the Friedel-Crafts reaction of 1,4-dimethoxybenzene **2.29** and the Baylis-Hillman adduct **2.18** (Scheme 2.19).



Scheme 2.19: Proposed route for the synthesis of 2.17 via a Friedel-Crafts reaction.

We therefore examined the proposed route to produce **2.17** intermediate through a Friedel-Crafts reaction. We carried out a F-C reaction between Baylis-Hillman adduct **2.18** and 1,4-dimethoxybenzene **2.29** in the presence of different Lewis acids. We screened a

range of Lewis acids (TiCl_4 , $\text{BF}_3 \cdot \text{O}(\text{C}_2\text{H}_5)_2$, DMAC), temperatures and solvents. The crude ^1H NMR of all reactions that involved the use of boron trifluoride diethyl etherate " $\text{BF}_3 \cdot \text{O}(\text{C}_2\text{H}_5)_2$ " and dimethylaluminum chloride (DMAC) showed the presence of the starting material only. In the case of using titanium tetrachloride (TiCl_4), peaks corresponding the terminal alkene of **2.18** were present along with several new peaks suggesting a number of molecules present which contain as ethyl ester group. Attempts to purify the desired product **2.36** from these complex mixtures proved unsuccessful. Due to the time constraint no further optimization reactions were possible (Table 2.4).



No.	Lewis acid	Solvent	Temperature °C		Product
			Time		
1	TiCl_4	DCM	-78 for 20 min, r.t. for 30 min		Complex mixture of by-products
2	TiCl_4	DCM	-78 for 3 hr, r.t. for 1 hr		
3	TiCl_4	THF	-78 for 30 min, r.t. for 15 hr		
4	$\text{BF}_3 \cdot \text{O}(\text{C}_2\text{H}_5)_2$	DCM	-78 for 3 hr, r.t. for 15 hr		Only starting materials observed
5	DMAC	DCM			
6	$\text{BF}_3 \cdot \text{O}(\text{C}_2\text{H}_5)_2$	THF	-78 for 30 min, r.t. for 15 hr		
7	DMAC	THF			

Table 2.4: Examination of Friedel–Crafts reaction conditions towards **2.36**.

2.7. Conclusion

In conclusion, this chapter has examined three alternative synthetic routes towards the synthesis of **2.17** a key intermediate on the synthetic routes to our target natural product antibiotic DEM30355/A **1.14**. In the first synthetic route to form **2.17** after a successful synthesis of Baylis-Hillman adduct **2.18**, we examined Heck coupling of this Baylis-Hillman adduct **2.18** and 2-bromo-1,4-dimethoxybenzene **2.3**, which proved low yielding. Alongside the screening of alternative ligands for this reaction, we also attempted to optimise the Heck reaction through the use of 2-iodo-1,4-dimethoxybenzene **2.29** as a more reactive alternative coupling partner. However this reaction still did not give a significant yield of the desired product **2.17** to allow progress in the synthesis. Therefore, we developed a second route to produce **2.17** through a Baylis-Hillman reaction between our synthesised β -substituted- α,β -unsaturated ketone **2.30** and diethyl ketomalonate **2.20**. Unfortunately no reaction was observed, potentially due to the low reactivity of β -substituted- α,β -unsaturated ketones in Baylis-Hillman reactions despite the reactivity of the electrophile. In our final synthetic plan of this chapter we examined the production of **2.36** via a Friedel-Crafts reaction of 1,4-dimethoxybenzene **2.29** and Baylis-Hillman adduct **2.18**. Although some promising results we obtained due to time constraints we did not pursue this reaction any further, the next chapter will look at an alternative approach to this synthesis.

Chapter 3

3. Examination of Synthetic Routes to 1,2,3,4-substituted Aromatics Rings as Precursors in the Total Synthesis of DEM30355/A 1.14

3.1. Introduction

The ring A of our target natural product antibiotic DEM30355/A **1.14** is a 1,2,3,4-substituted aromatic ring, based on a hydroquinone structure. Therefore in this chapter we will examine synthetic routes to make the unusual 1,2,3,4-substitution pattern required.

If we consider a classical electrophilic aromatic substitution of a hydroquinone containing either an electron-donating or an electron-withdrawing group, the *ortho*-directing effect of the electron donating group produces a product with a 1,2,4,5-substitution pattern. Whereas the *meta*-directing effect of the electron withdrawing group gives a product with a 1,2,3,5-substitution pattern (**Figure 3.1**).

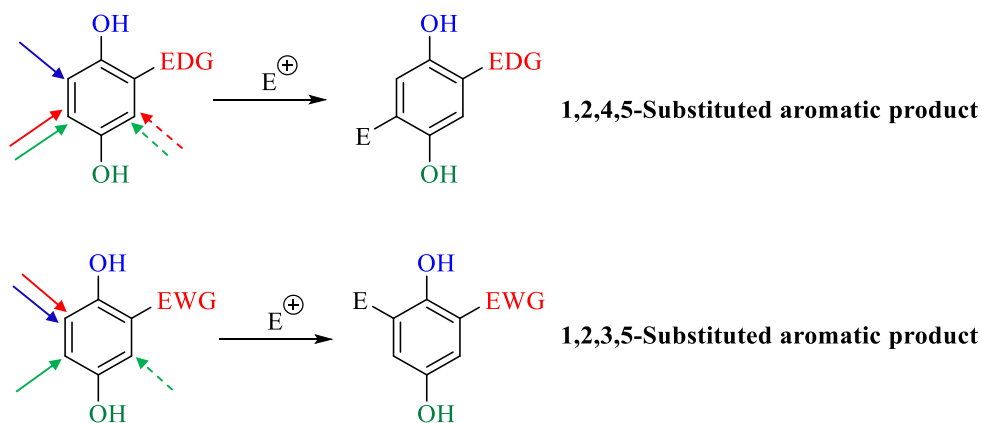


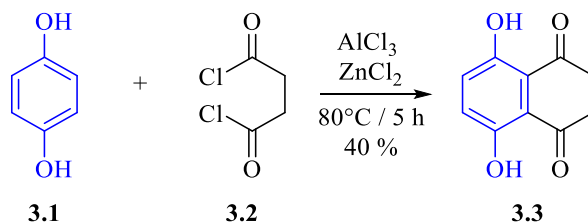
Figure 3.1: Likely outcome of a classical electrophilic aromatic substitution of substituted hydroquinones (Coloured arrows show the directing effects of the different groups, Dashed arrows indicate sterically hindered positions).

Therefore, classical methods cannot generate the 1,2,3,4-substitution pattern that we require for the synthesis of DEM30355/A **1.14**, thus we will explore a number of unusual synthetic approaches towards our target molecules.

3.1.1. Classic Methods for The Formation of 1,2,3,4-Substituted Aromatics

3.1.1.1. Intramolecular Electrophilic Aromatic Substitution

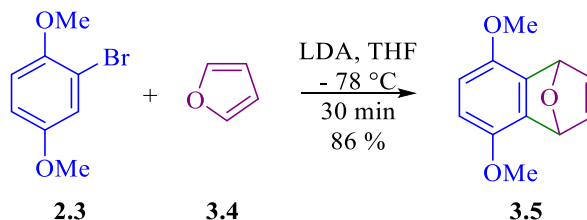
Friedel–Crafts acylation reaction can be employed to generate hydroquinones with a 1,2,3,4-aromatic substitution pattern. The Friedel–Crafts acylation reaction of the hydroquinone **3.1** and succinyl dichloride **3.2** provides compound **3.3** with desired substitution pattern, as the second F-C acylation is intramolecular and thus is under steric control (**Scheme 3.1**).⁷²



Scheme 3.1: Synthesis of the hydroquinone 3.3 via a F-C acylation.

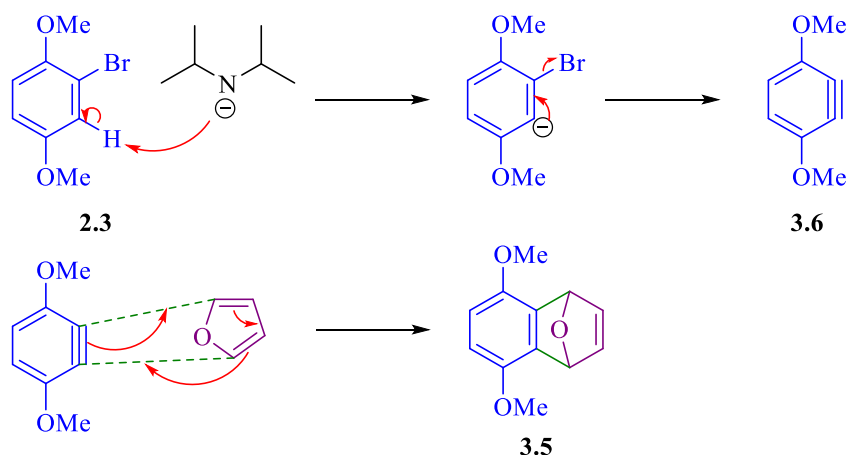
3.1.1.2. Diels-Alder Cycloaddition Reaction

Diels-Alder cycloaddition reaction (D-A) can also be used to generate hydroquinones with 1,2,3,4-aromatic substitution pattern. For example the cycloaddition reaction between the benzyne, formed by the deprotonation of 2-bromo-1,4-dimethoxybenzene **2.3** with lithium diisopropylamide (LDA), and furan **3.4** to give product **3.5** (Scheme 3.2).⁷³



Scheme 3.2: Synthesis of the hydroquinone 3.5 with via a D-A cycloaddition reaction.

The reaction mechanism involves in generating a benzyne intermediate **3.6** by removing a proton *ortho* to the bromine. The resulting benzyne **3.6** then can then undergo a cycloaddition reaction with furan **3.4** to form **3.5** (Scheme 3.3).^{73,74}



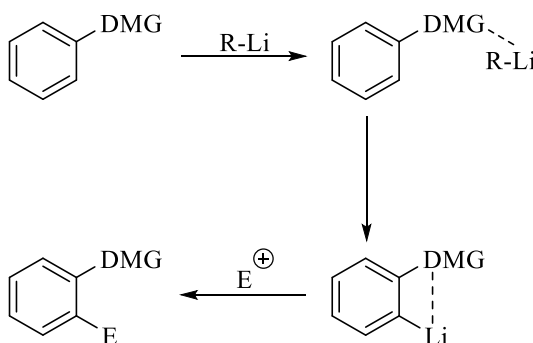
Scheme 3.3: Proposed mechanism for the synthesis of 3.5 with via a D-A cycloaddition reaction.

However both of these reactions have limitations, namely that they both give predominately symmetrical products and they require either strong Lewis acids or strong

Brønsted bases to generate the required reactive benzyne intermediate. An alternative approach to the 1,2,3,4-substitution pattern could be the use of an *ortho*-lithiation chemistry.

3.1.2. Directed *Ortho*-Lithiation Approach

Directed *ortho*-lithiation is a deprotonation on a site *ortho* to a directing group by an alkyllithium base, the subsequent addition of an electrophile gives a 1,2-disubstituted product. These directing groups contain a heteroatom that can coordinate to the lithium species directing the deprotonation. Examples include fluorine, amide and methoxy groups. Directed *ortho*-lithiation allows substitution at a sterically unfavourable position, thus we decided to examine this strategy in our synthesis (**Scheme 3.4**).⁷⁵



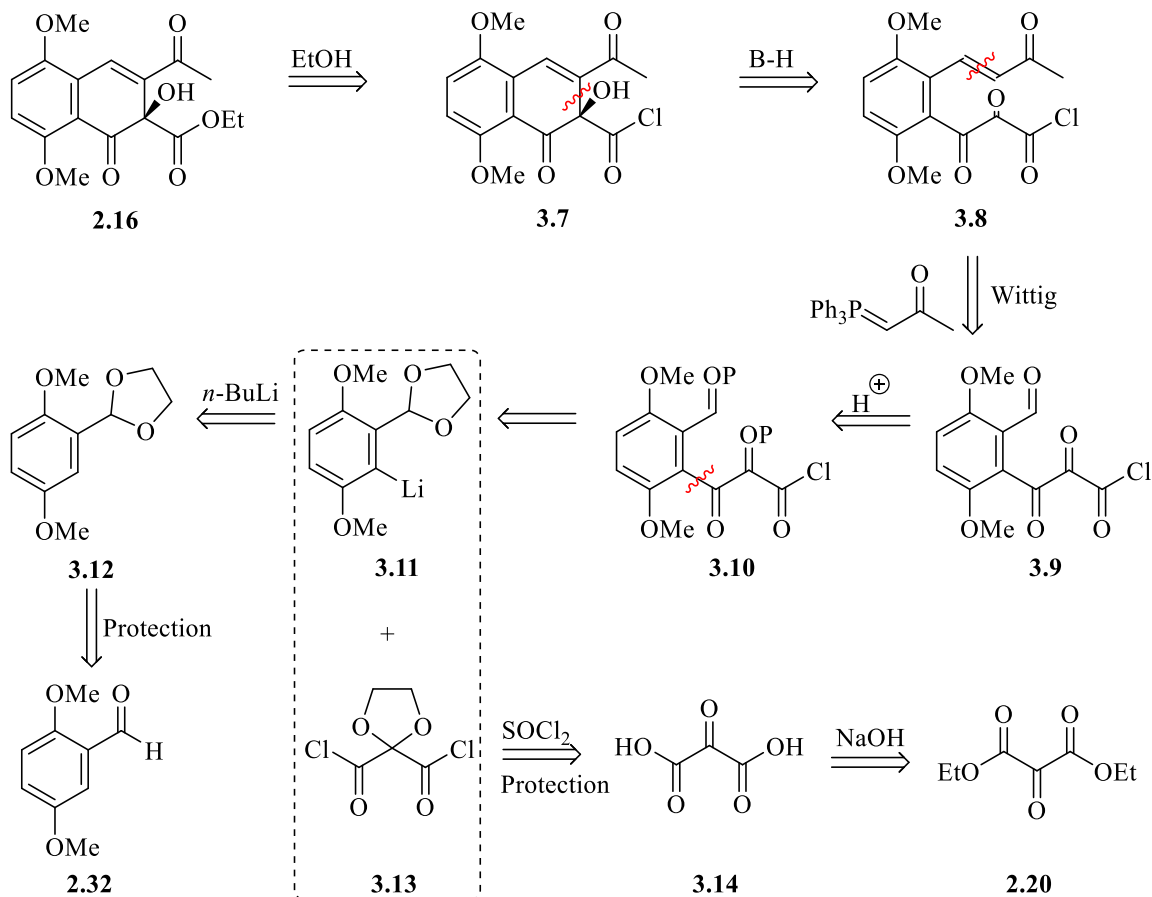
Scheme 3.4: Directed *ortho*-lithiation reaction of an aromatic ring.

3.2. Synthesis of Ring A of DEM30355/A 1.14 via an *Ortho*-Lithiation Approach

3.2.1. Planned Route for the Synthesis of Ring A via a Key *Ortho*-Lithiation Step

Based on this approach we devised a new synthetic plan, focused on building synthetic intermediate **2.16** that includes an aromatic ring with a 1,2,3,4-substitution pattern. We envisioned that the ester moiety in compound **2.16** would be obtained from the acid chloride **3.7**. The partially saturated six membered ring B in compound **3.7** could be formed via an intramolecular Baylis-Hillman reaction between the enolate and the ketone in **3.8**. The formation of α,β -unsaturated ketone **3.8** could be achieved through Wittig reaction of **3.9**. The ketone and the aldehyde in **3.9** would be obtained by removing acetals protecting groups in **3.10**. Trapping the organolithium **3.11** with electrophile **3.13** would produce **3.10**. The organolithium **3.11** could be generated by *ortho*-lithiation reaction of **3.12** with *n*-butyllithium. The acetal **3.12** could be produced from the commercially available 2,5-dimethoxybenzaldehyde **2.32**. Acid chloride **3.13** could be prepared from ketomalonic acid **3.14** and thionyl chloride, followed by acetal

protection. Ketomalonic acid **3.14** could be produced from the hydrolysis of **2.20** (Scheme 3.5).

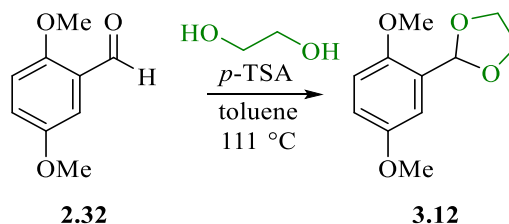


Scheme 3.5: New proposed synthetic route toward DEM30355/A 1.14 via a key *ortho*-lithiation reaction.

3.2.2. Protection of 1,4-Dimethoxybenzaldehyde 2.32

The first step in this plan involves protecting aldehyde **2.32** as a cyclic acetal to prevent the unwanted nucleophilic addition of $n\text{-BuLi}$ to the aldehyde during our planned *ortho*-lithiation step. We have examined the formation of acetal **3.12** through the reaction of 2,5-dimethoxybenzaldehyde **2.32** with 10 equivalents of ethylene glycol in the presence of catalytic amount of acid, *p*-toluenesulfonic acid (*p*-TSA). After 2 hours the crude reaction mixture was purified by column to give 31% of the target product **3.12** and 63% of starting material was recovered. As the acetal formation is reversible, therefore we proposed that using both an excess of ethylene glycol and a Dean-Stark apparatus to remove the water formed would push the equilibrium in favour of the desired product **3.12**. Following a number of optimisation attempts (Table 3.1), the best results were achieved after refluxing the reaction for 4 hours in a Dean-Stark apparatus, the resulting crude

material was purified by column chromatography to give the desired product **3.12** in a good yield 86%.

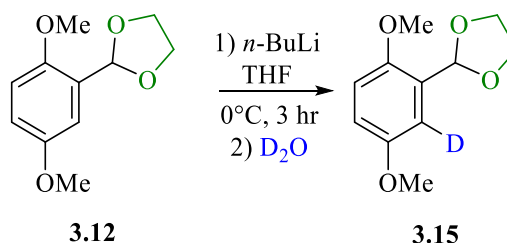


No.	Ethylene glycol equivalents	Time (hr)	%Yield
1	10	2	31
2	30	2	61
3	30	4	86

Table 3.1: Examined reaction conditions for protecting aldehyde **2.32** as a cyclic acetal.

3.2.3. *Ortho*-Deprotonation Reaction of **3.12**

As the first step in the investigation of our planned *ortho*-lithiation, we decided to test the *ortho*-lithiation reaction by trapping **3.12** with D₂O to allow us to easily optimise the deprotonation step. Therefore, we examined the *ortho*-lithiation approach through the reaction of the acetal **3.12** with *n*-BuLi at 0 °C. After 3 hours, the reaction was quenched with deuterated water (D₂O) to confirm the deprotonation site on the aromatic ring.



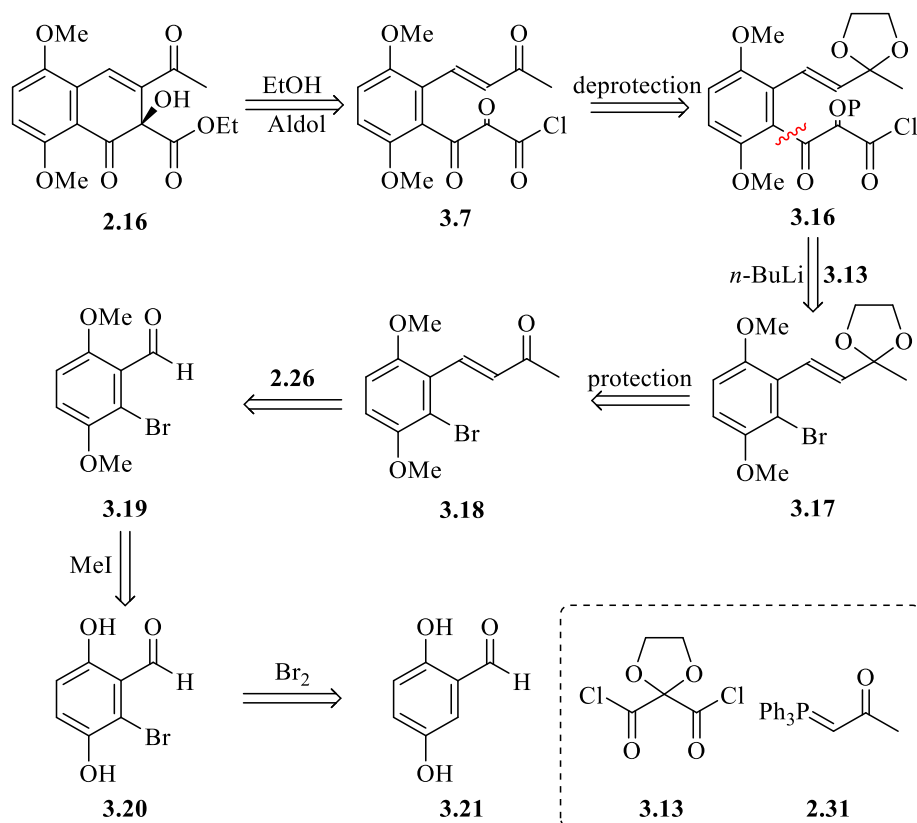
Scheme 3.6: Examination of the deprotonation of **3.12**.

Despite attempting the deprotonation for different lengths of time (0 °C for up to 3 hours) we did not observe the formation of the product **3.15** in the ¹H NMR of the crude product, where we have anticipated that the peak at δ_H 7.12 ppm would decrease in intensity if deuteration had been successful. It has been reported that this type of deprotonation at such a hindered site *ortho*- to the acetal can require up to 10 hours to occur at low temperature.⁷⁶ Due to the poor results for this reaction we decided to focus on alternative approaches. Simultaneous to this work we also investigated an alternative bromination approach to generate the desired substitution pattern discussed below.

3.3. Synthesis of Ring A of DEM30355/A 1.14 via Thiele-Winter Like Bromination Approach

3.3.1. Planned Route for the Synthesis of Ring A via a Key Bromination Step

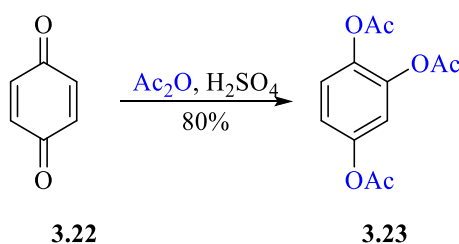
We have thus considered another approach for functionalising position 3 of the ring A of DEM30355/A 1.14 based on Thiele-Winter like bromination of the commercially available 2,5-dihydroxybenzaldehyde **3.21**. The retrosynthesis of the synthetic intermediate **2.16** involved in an intramolecular Baylis-Hillman reaction followed by the esterification of **3.7**. Next, α,β -unsaturated ketone **3.7** would be regenerated by removing the acetal protecting groups from **3.16**. Halogen-metal exchange reaction of **3.17** trapped with **3.13** would produce **3.16**. For a successful halogen-metal exchange reaction, the carbonyl of α,β -unsaturated ketone **3.18** should be converted to acetal **3.17**. Wittig olefination of aldehyde **3.19** would generate α,β -unsaturated ketone **3.18**. Compound **3.19** could be produced through the methylation reaction of **3.20**. The desired 1,2,3,4-aromatic substitution pattern could be achieved through a regioselective Thiele-Winter like bromination of the commercially available aldehyde **3.21** to give **3.20** (Scheme 3.7).



Scheme 3.7: Proposed synthetic route toward DEM30355/A 1.14 via a key bromination reaction.

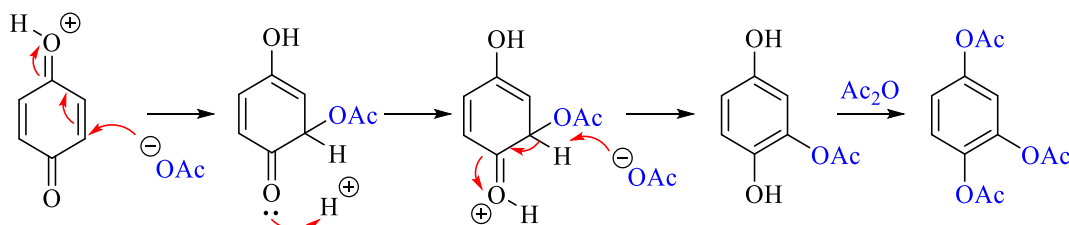
3.3.2. Thiele-Winter Reaction

The reaction of *p*-benzoquinone with acetic anhydride in the presence of a catalytic amount of sulfuric acid to yield 1,2,4-triacetoxybenzene was studied by J. Thiele in 1898. Further investigation was carried out by Thiele and his student E. Winter to study the reaction of other quinones such as 1,2-benzoquinone and naphthoquinones with acetic anhydride catalysed by $ZnCl_2$. They found that the acid catalysed reactions of quinones with acetic anhydride give triacetoxy aromatic compounds (**Scheme 3.8**).⁷⁷



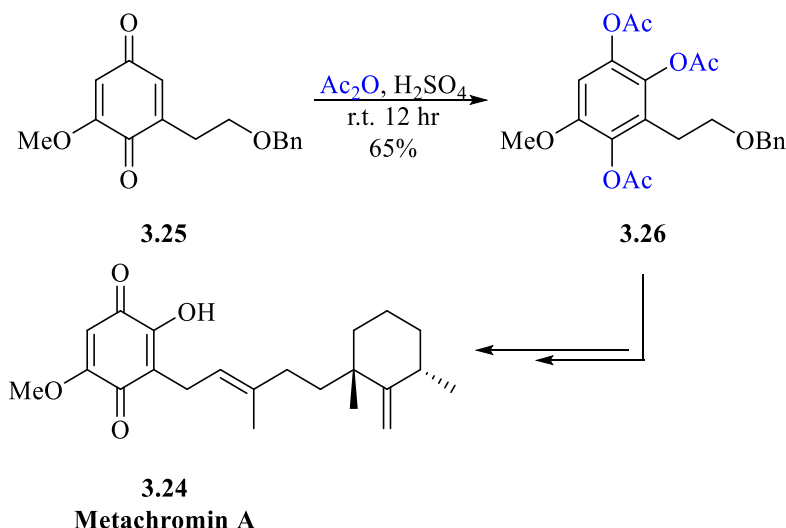
Scheme 3.8: First reaction reported by J. Thiele.

The mechanism of Thiele-Winter acetoxylation reaction involves 1,4-addition of the acetate ion to an activated quinone to generate the corresponding mono-acetoxy hydroquinone, the resulting hydroquinone then further reacts with acetic anhydride to give 1,2,4-triacetoxybenzene (**Scheme 3.9**)



Scheme 3.9: Thiele-Winter acetoxylation reaction mechanism.

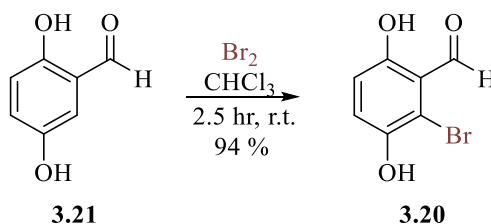
In 1999, C. Correia and W. Almeida reported that the total synthesis of metachromin A **3.24** was achieved by Thiele-Winter acetoxylation as a key step reaction. Thiele-Winter reaction involved in the regioselective 1,4-addition of acetic anhydride to quinone **3.25** in the presence of sulfuric acid gave compound **3.26** that matches our desired aromatic substitution pattern. (**Scheme 3.10**).⁷⁸



Scheme 3.10: The total synthesis of metachromin A 3.24 mediated by Thiele-Winter reaction.

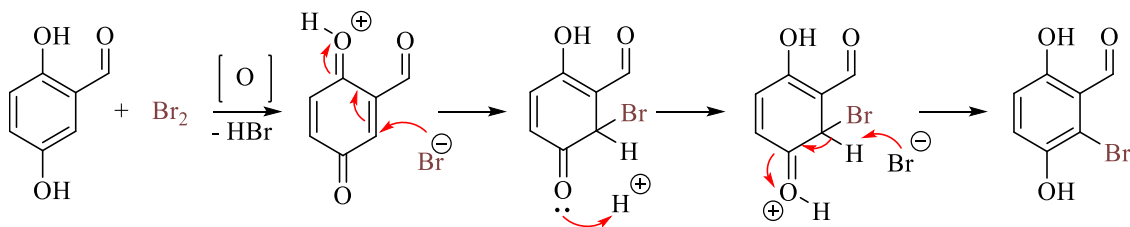
3.3.3. Porco Bromination

J. Porco *et al.* reported unusual bromination reaction of 2,5-dihydroxybenzaldehyde 3.20 to generate hydroquinone compound 3.19 with 1,2,3,4-aromatic substitution pattern (Scheme 3.11).⁷⁹



Scheme 3.11: Bromination of 3.21 reported by Porco.

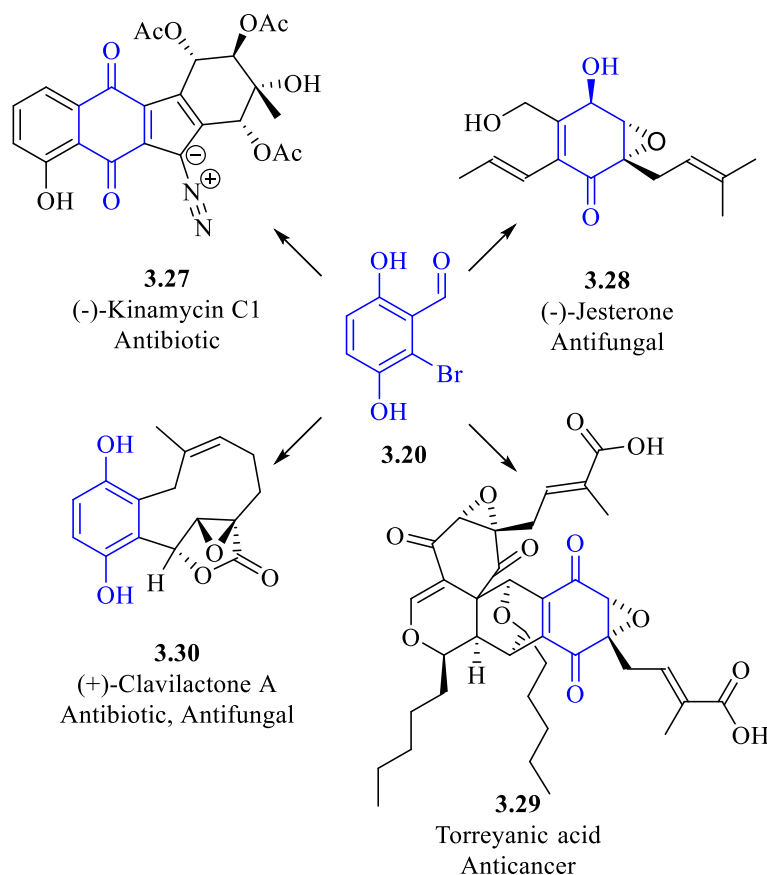
We proposed that the mechanism of the bromination of 2,5-dihydroxybenzaldehyde 3.21 reaction includes the oxidation of hydroquinone 3.21 into a *p*-benzoquinone type compound. Similar to Thiele-Winter acetoxylation reaction, the next step involved in 1,4-addition of the bromine anion to the α,β -unsaturated ketone (Scheme 3.12).



Scheme 3.12: Proposed mechanism for the synthesis of 3.20.

Subsequently, as 2-bromo-3,6-dihydroxybenzaldehyde 3.20 represents a hydroquinone with 1,2,3,4- aromatic substitution pattern, it has been widely used as a

building block for the total synthesis of many natural products and bioactive compounds including (-)-kinamycin C1⁸⁰ **3.27**, (-)-jesterone⁸¹ **3.28**, torreyanic acid⁷⁹ **3.29** and (+)-clavilactone A⁸² **3.30**, and it could also be utilized as a building block for the synthesis of DEM30355/A **1.14** (Scheme 3.13).



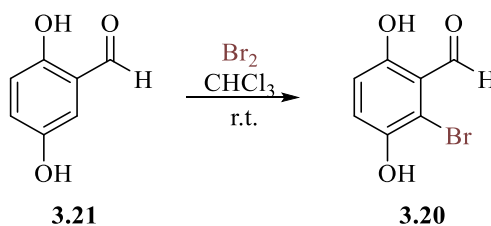
Scheme 3.13: The total synthesis of many natural products using **3.20** as a starting material.

Therefore, we planned to investigate the synthesis of DEM30355/A **1.14** using 2-bromo-3,6-dihydroxybenzaldehyde **3.20** as a key building block.

3.3.4. Synthesis of 2-Bromo-3,6-dihydroxybenzaldehyde **3.20**

Based on the Porco procedure, we examined the synthesis of **3.20** through the regioselective bromination of 2,5-dihydroxybenzaldehyde **3.21**.⁷⁹ We started our reaction by a dropwise addition of molecular bromine to **3.21** in chloroform over 30 minutes. After 1.5 hours the reaction was quenched and washed several times with Na₂S₂O₃, extracted organic layer was dried over MgSO₄. The resulting crude reaction mixture was purified by column to give product **3.20** in 93%. In the second attempt we examined the effect of changing the drying agent from MgSO₄ to Na₂SO₄ since in the first attempt MgSO₄ remained yellow even after using a large amount of wash solvent, potentially due to the

chelation between magnesium and the oxygens of **3.20**. We found that increasing the reaction time to 2.5 hours after bromine addition, along with drying the organic layer over Na_2SO_4 enhanced the yield of the desired product **3.20** to be 99% (**Table 3.2**).



No.	Drying agent	Time (hr)	% Yield
1	MgSO_4	1.5	93
2	Na_2SO_4	2.5	99

Table 3.2: Examination on the bromination reaction of **3.21**.

In the first attempt the dimer **3.31** was isolated as a minor component in a low yield 5% (**Figure 3.2**).

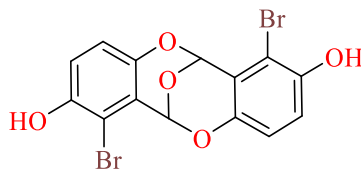


Figure 3.2: The structure of dimer **3.31**.

Crystals of dimer **3.31** were obtained by slow evaporation from a mixture of petroleum ether and diethyl ether (1:1). The crystal structure of **3.31** was obtained through single crystal X-ray crystallography (**Figure 3.3**).

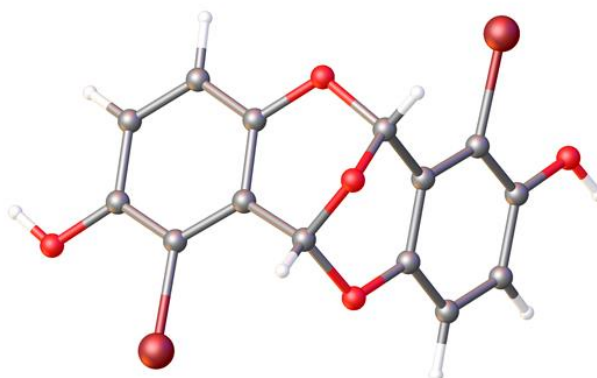


Figure 3.3: Crystal structure of the dimer **3.31**.

Comparing to *ortho*-lithiation approach, the formation of desired substitution pattern was achieved via bromination approach to give **3.20** in an excellent yield 99% in shorter reaction time. Moreover, the deprotonation reaction required strictly anhydrous conditions whereas the bromination reaction is water tolerant. Furthermore *ortho*-lithiation reactions are difficult to perform on a large scale, due to the low temperatures and the reactivity of BuLi, whereas the bromination approach is easier to perform in the lab, as exemplified in the total synthesis of (+)-torreyanic acid **3.29**.⁷⁹

3.3.5. Methylation of 2-Bromo-3,6-dihydroxybenzaldehyde **3.19**

After a successful formation of **3.20**, we turned our attention to producing **3.19** via a double methylation reaction of **3.20**. The problem in the di-methylation of **3.20** is that the two phenolic oxygens do not have the same reactivity. We expected that the phenolic oxygen *ortho* to the aldehyde are less reactive than the other phenolic oxygen due the hydrogen bonding (**Figure 3.4**).

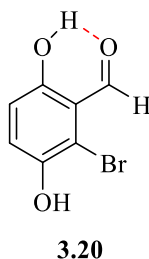
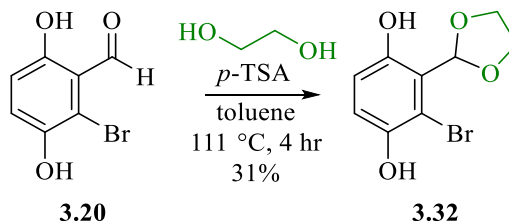


Figure 3.4: The hydrogen bonding between the aldehyde and adjacent phenolic OH in **3.20**.

Thus, we found that the aldehyde protection could be a reasonable solution to disrupt the effect of hydrogen bonding between the aldehyde and hydroxyl.

3.3.5.1. Aldehyde Protection of 2-Bromo-3,6-dihydroxybenzaldehyde **3.20**

Therefore, we examined converting aldehyde **3.20** into a corresponding acetal **3.32** through the reaction of **3.20** with ethylene glycol catalysed by *p*-TSA in a Dean-Stark apparatus. After refluxing the reaction for 4 hours, the ¹H NMR of the crude material indicated that the reaction did not move to completion (estimated conversion 31%). The conversion could be low because the hydrogen bonding between the aldehyde and the phenolic hydroxyl is strong.

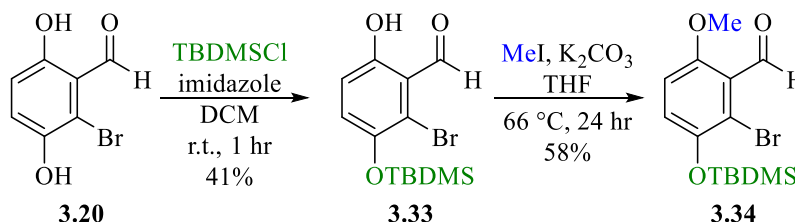


Scheme 3.14: Acetal protection of 3.20.

Due to the low yielding product **3.32** obtained from the acetal protection, we moved to an alternative solution that depends on protecting the most reactive phenolic oxygen.

3.3.5.2. Regioselective Protection of Phenolic Hydroxyl 3.20

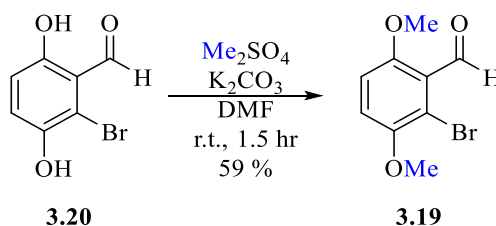
Alternatively, we planned to protect the reactive phenol through the regioselective silylation reaction. Next the methylation of the less reactive phenol will be examined. Based on a literature procedure, we examined the protection of the phenolic oxygen using the silylation agent *tert*-butyldimethylsilylchloride (TBDMSCl) and imidazole in DCM.⁷⁹ The synthesis of **3.33** was successfully achieved after a column purification, however, the isolated yield of **3.33** was relatively low 41%. At the next step, we examined the methylation of protected phenol **3.33** using methyl iodide and potassium carbonate in THF. After refluxing the reaction for 24 hours, the mono-methylated product **3.34** was isolated by column in a moderate yield 58%.



Scheme 3.15: The synthesis of 3.33 and 3.34.

Although the methylation of the more unreactive phenolic oxygen was achieved, the formation of the di-methylated compound **3.19** required silyl deprotection and additional methylation step. The expected overall yield of the di-methylated product **3.19** will be low. Therefore we alternatively decided to methylate both phenolic positions in **3.20** in a single step. A few number of studies demonstrated that the double methylation of hydroquinones and other related phenols can be accomplished under vigorous conditions by refluxing toxic dimethyl sulfate and potassium hydroxide or potassium carbonate for at least 24 hours.^{83,84} In particular, the double methylation of 2-bromo-3,6-

dihydroxybenzaldehyde **3.20** was only reported by Takao and his co-worker using Me_2SO_4 and K_2CO_3 in DMF to provide compound **3.19** in a moderate yield.⁸²

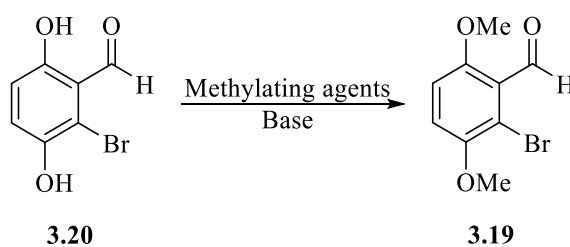


Scheme 3.16: Methylation of 3.20 using dimethyl sulfate.

However, we have not employed dimethyl sulfate as a methylating agent because it is extremely toxic. In the following section we have discussed several conditions that we examined for methylating the two phenolic OH groups of 2,5-dihydroxybenzaldehyde **3.20** in a single step using different methylating agents and various bases.

3.3.5.3. Direct Double *O*-Methylation of 3.20

We have explored the synthesis of di-methylated product **3.19** through the methylation of 2-bromo-3,6-dihydroxybenzaldehyde **3.20** by screening various methylating agents, bases, solvents and temperature. We considered using trimethyloxonium tetrafluoroborate (Meerwein's salt) along with methyl iodide as methylating agents. Meerwein's salts are alkylating agents that refer to any complex consists of trialkyloxonium with a strong Lewis acid, they discovered by Hans Meerwein in 1937.⁸⁵ (**Table 3.3**).



No.	Methyl -ating agents	Base	Solvent	Temp °C	Time <i>hr</i>	Product	%
1	$\text{Me}_3\text{O}(\text{BF}_4)$	Hünig's	DCM	0 then r.t.	24	Not observed	

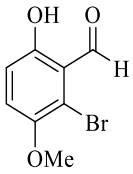
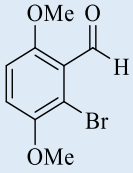
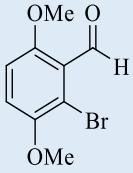
2	MeI	NaH	THF	r.t. and 66	24	Not observed
3	MeI	NaH	DCM	r.t. and 40	24	
4	MeI	Hünig's	DCM	r.t. and 40	18	
5	MeI	K ₂ CO ₃	acetone	r.t. and 56	24	
6	MeI	K ₂ CO ₃	DCM	r.t. and 40	24	
7	MeI	K ₂ CO ₃	DMSO	r.t.	24	
8	MeI	K ₂ CO ₃	DMF	r.t.	24	
9	Me ₃ OBF ₄	Hünig's	DCM	0 to r.t.	36	
10	MeI	NaOMe	MeOH	64	24	 8
11	MeI	K ₂ CO ₃	THF	40	24	 30
12	MeI	K ₂ CO ₃	THF: DMF 10:1	40	24	 37
13	MeI,	K ₂ CO ₃ assisted by TBAB	THF: DMF 10:1	40	24	75

Table 3.3: Examined conditions towards the methylation of 3.20.

We started our investigation towards producing **3.19** by using a trimethyloxonium tetrafluoroborate and Hünig's base (*i*-Pr₂NEt) in DCM at 0 °C. After 36 hours the mono methylated product **3.35** was isolated by column in a moderate yield 45%. We have examined the previous condition using methyl iodide as an alternative methylating agent. However, no product was obtained, the ¹H NMR of crude reaction showed a complex mixture compounds and no product was observed.

Next, we decided to consider the use of methyl iodide as a methylating agent and we continued to screen for a perfect base and solvent system. We examined another condition that includes refluxing methyl iodide and sodium methoxide in methanol. After 24 hours the mono-methylated product **3.35** was isolated by a column chromatography in a low yield 8%.

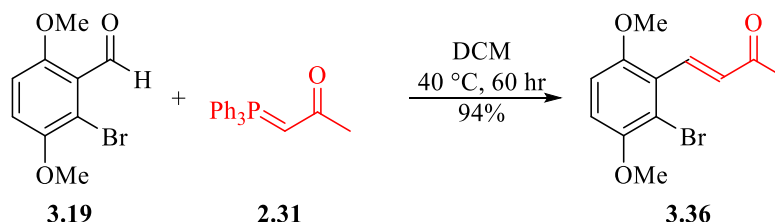
We continued our investigation to produce **3.19** by screening another condition using sodium hydride and methyl iodide in THF at different temperatures. However, the ¹H NMR of crude reaction showed a complex mixture of by-products, and product **3.19** was not observed. Next, we have used DCM as an alternative solvent, unfortunately, product **3.19** also was not seen.

Next, we continued our effort to find the optimum conditions for producing **3.19**, we examined the use of potassium carbonate and methyl iodide by screening range of solvents including acetone, DCM, THF, DMF and DMSO. After extensive investigations, the formation of the dimethylated product **3.19** was successfully achieved by heating methyl iodide and potassium carbonate in THF at 40 °C for 24 hours. The desired product **3.19** was isolated by column in a moderate yield 30%. To improve the yield of **3.19**, the previous reaction was repeated using a mixture of solvents THF:DMF 10:1. It was found that the addition of freshly distilled DMF slightly increases the yield of product **3.19** to be 37%. Interestingly, the yield of **3.19** was significantly improved to 75% by using the phase transfer catalyst tetrabutylammonium bromide (TBAB), potentially through an increase in the solubility of the inorganic base in the organic solvent.

After a successful formation of di-methylated compound **3.19**, we turned our attention into constructing the upper part of our target molecule **1.14** that includes α,β -unsaturated ketone through the formation of **3.36**.

3.3.6. Synthesis of (*E*)-4-(2-Bromo-3,6-dimethoxyphenyl)but-3-en-2-one **3.36**

We therefore planned to synthesize α,β -unsaturated ketone **3.36** by refluxing the methylated compound **3.19** with a previously prepared Wittig ylide **2.31** in THF. After 60 hours, the desired product **3.36** was isolated by column in an excellent yield 94%.

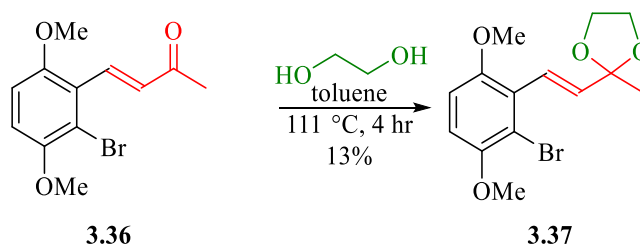


Scheme 3.17: The synthesis of **3.36**.

With **3.36** in hand, we aim to protect the resulting ketone to prevent any unwanted side reactions in subsequent steps.

3.3.7. Protection of (*E*)-4-(2-Bromo-3,6-dimethoxyphenyl)but-3-en-2-one **3.37**

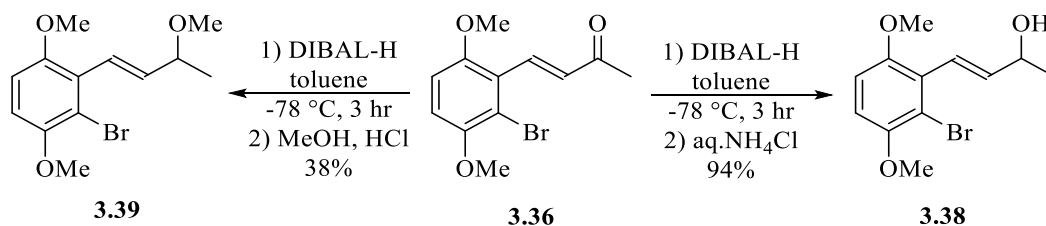
We therefore examined the acetal protection of ketone by refluxing **3.36** with ethylene glycol and *p*-TSA in toluene for 4 hours in a Dean-Stark apparatus. Purification of the crude reaction mixture by column chromatography gave product **3.37** in a low yield 13% and most of the starting material was recovered.



Scheme 3.18: Acetal protection of **3.36**.

Due to the low yielding of **3.37**, we considered an alternative method for protecting **3.36**, via a chemoselective reduction of the ketone using diisobutylaluminum hydride (DIBAL-H) as a reducing agent to produce the corresponding alcohol **3.38**. Thus, we investigated the reaction of **3.36** with DIBAL-H in toluene at -78 °C for 30 min. Quenching the reaction with cold methanol followed by washing the reaction mixture with diluted HCl, lead accidentally to methylate the resulting alcohol and gave **3.39** instead of **3.38**. The isolated yield of compound **3.39** is 38% yield. Therefore, we repeated the previous reaction under the same condition and we quenched the reaction with cold water only following by

aqueous work-up with NH_4Cl . the resulting crude product was purified by column chromatography to give the desired alcohol **3.38** in a high yield 94%.



Scheme 3.19: The synthesis of **3.38** and **3.39**.

Due to time constraint the protection of alcohol **3.38** will be continued in the future.

3.3.8. Biological Assay of the Synthetic Intermediates **2.30** and **3.36**

As the mode of action of our antibacterial agent DEM30355/A **1.14** is unclear, we proposed that **1.14** could be a Michael acceptor as it contains α,β -unsaturated ketone in its structure. Due to the structural similarity between **1.14** and our synthetic intermediates **2.30** and **3.36**, we planned to explore the pharmacophore of **1.14** by investigating the biological activity of **2.30** and **3.36** against the Gram-positive bacterium, *Bacillus subtilis* (Figure 3.5).

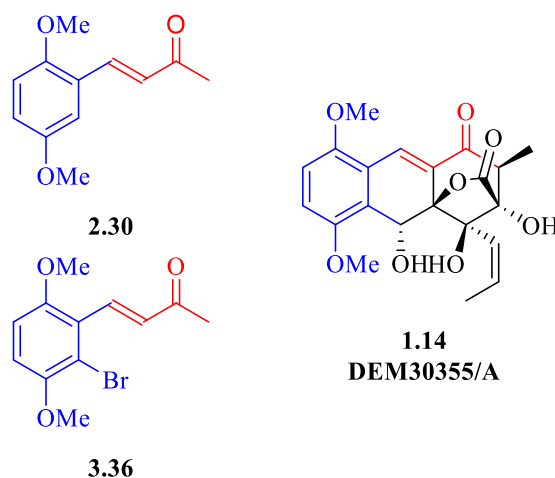


Figure 3.5: Structures of DEM30355/A **1.14**, **2.30** and **3.36**.

However, **2.30** and **3.36** showed no activity against *Bacillus subtilis* strain. Therefore, based on this result we suggest that the DEM30355/A **1.14** is not a Michael acceptor and its potency might originate from a binding event with a key enzyme in the bacteria (Figure 3.6).

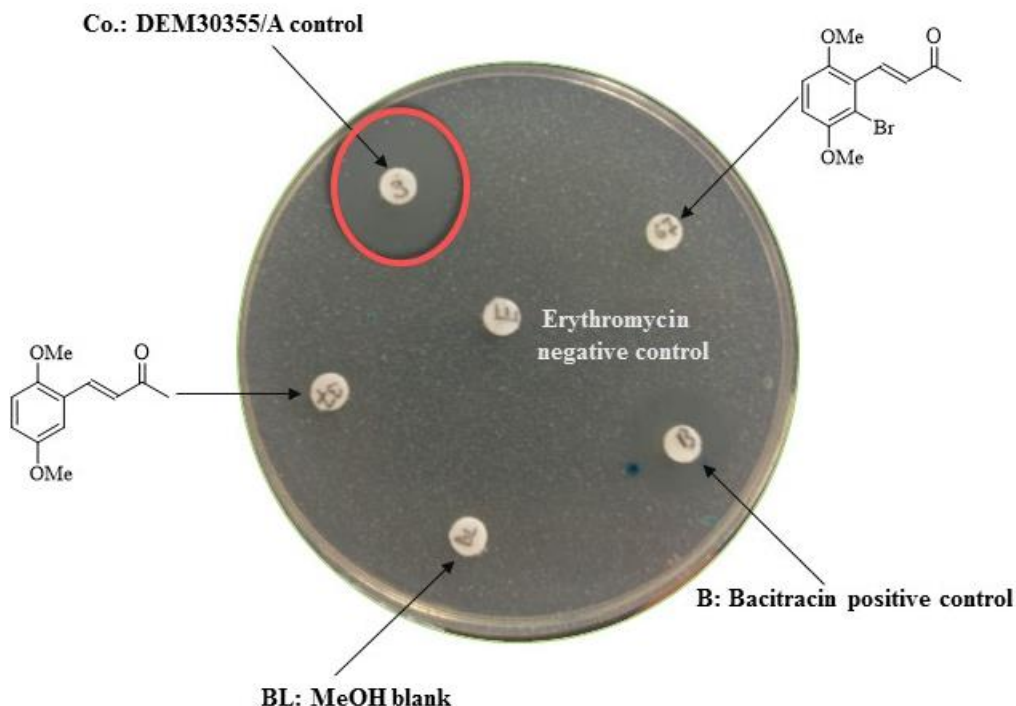


Figure 3.6: Bioassay of 2.30, 3.36 and DEM30355/A 1.14. Red circle highlights halo of inhibition. Bioassay performed by Dr B. Kepplinger.

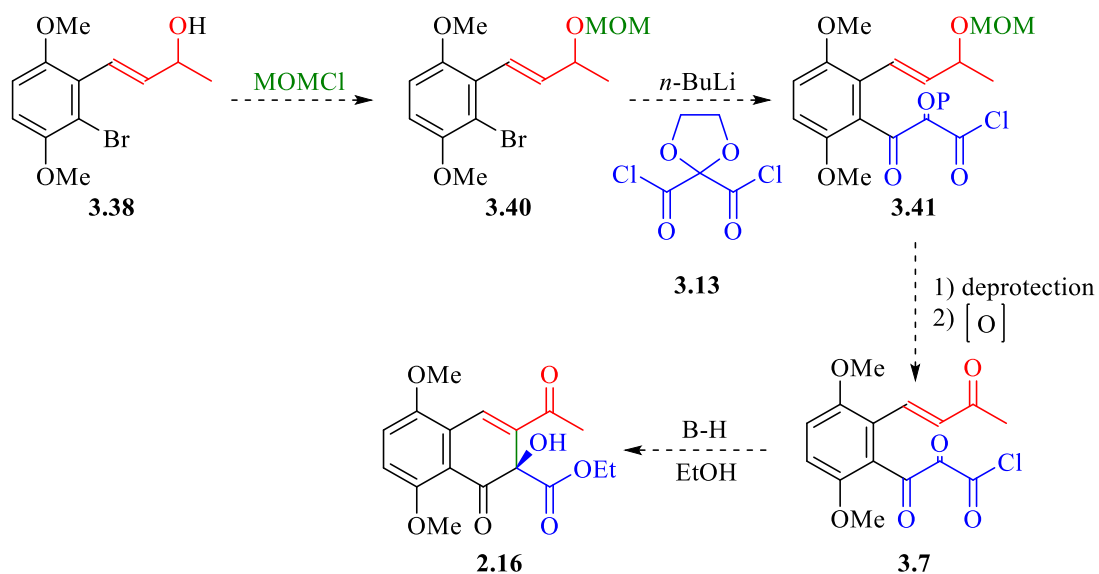
3.4. Conclusion

In this chapter two synthetic routes were examined towards the formation of ring A of **1.14** that includes hydroquinone with 1,2,3,4-substitution pattern. The first route based on the directed *ortho*-lithiation, whereas the second route includes the bromination of 2,5-dihydroxybenzaldehyde **3.21** in a similar nature to Thiele-Winter acetoxylation reaction. Best result was obtained using a bromination approach as compound 2-bromo-3,6-dihydroxybenzaldehyde **3.20** was formed in an excellent yield up to 99%. After considerable investigations we developed a new method for methylating **3.20** to produce **3.19** which is identical to ring A in **1.14**. After that, we have successfully built α,β -unsaturated ketone **3.36** that presents in ring B and C of **1.14** through the reaction of **3.19** with the previously synthesised Wittig reagent **2.31**. The keto group of α,β -unsaturated ketone **3.36** was selectively reduced to give the corresponding alcohol **3.38** in a high yield.

3.5. Future Work

The synthesis of rings A and B in **1.14** could be achieved through the protection of hydroxyl group in **3.18** with MOMCl followed by a halogen-metal exchange reaction using *n*-BuLi, trapping with **3.13** to give the synthetic intermediate **3.41**. After removal of the

protecting groups we would attempt an intramolecular Baylis-Hillman reaction of **3.7** to give the core structure of DEM30355/A **1.14**.



Scheme 3.20: Towards the synthesis of rings A and B of DEM30355/A 1.14.

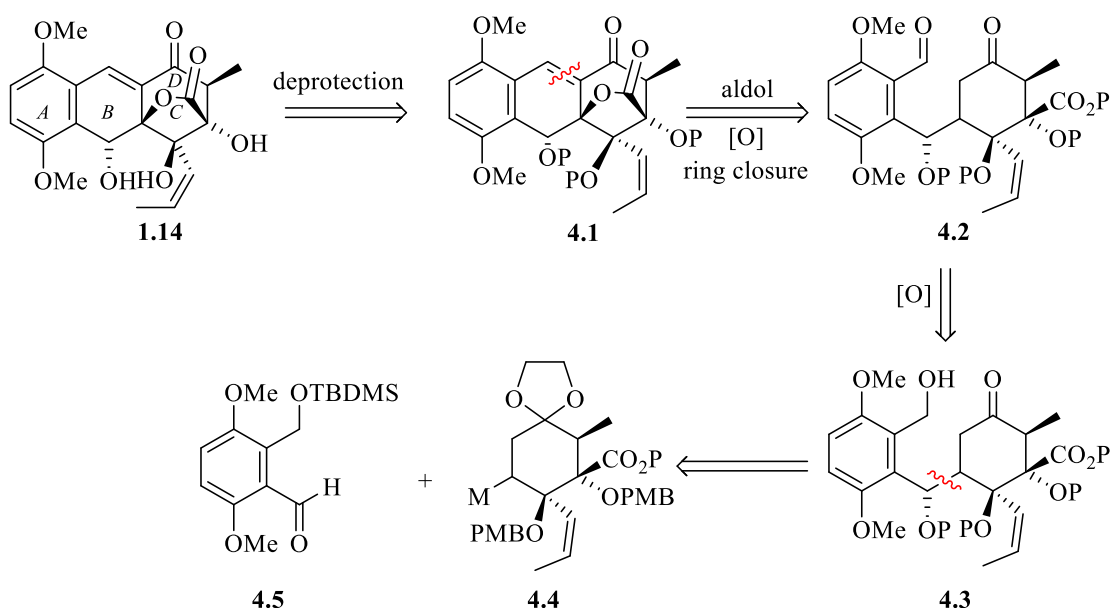
Chapter 4

4. Studies towards the Total Synthesis of DEM30355/A 1.14 via an Intramolecular Aldol Condensation

This chapter describes our efforts towards the formation of DEM30355/A **1.14** following a new strategy based on the synthesis of the aromatic ring A, then building the more complex rings C and D, followed by coupling the fragments via an intramolecular aldol condensation to construct ring B.

4.1. Retrosynthetic Analysis of DEM30355/A 1.14 Based on an Intramolecular Aldol Condensation Approach

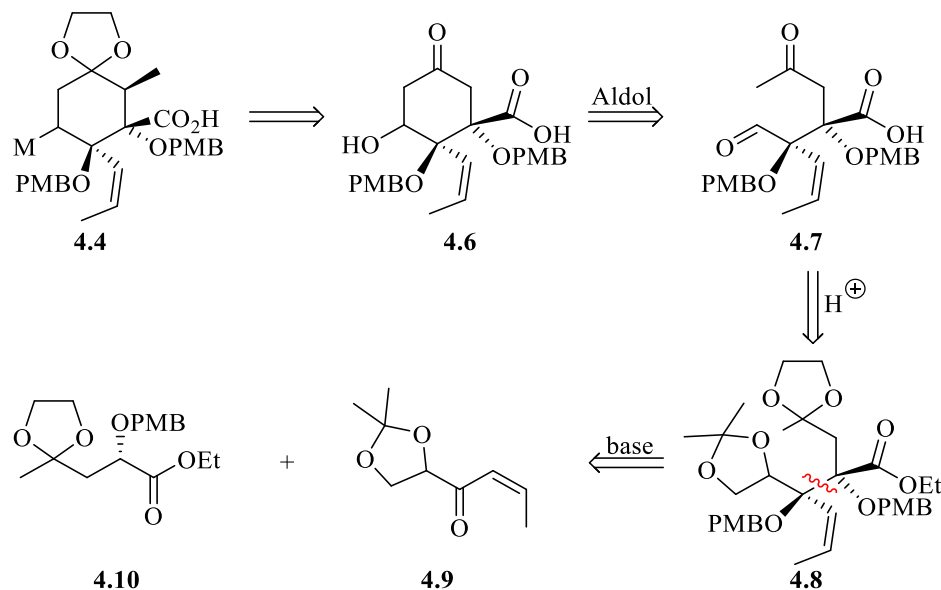
We envisioned that DEM30355/A **1.14** could be generated by the deprotection of compound **4.1**. α,β -Unsaturated ketone **4.1** could be formed through an intramolecular aldol condensation between the aldehyde and ketone in compound **4.2** followed by oxidation of the tertiary carbon and lactone formation. Aldehyde **4.2** could be produced through the oxidation of the primary alcohol **4.3**. Compound **4.3** would be obtained by a nucleophilic addition of an organometallic **4.4** to benzaldehyde **4.5** (Scheme 4.1).



Scheme 4.1: Retrosynthesis of DEM30355/A 1.14 following intramolecular aldol condensation approach.

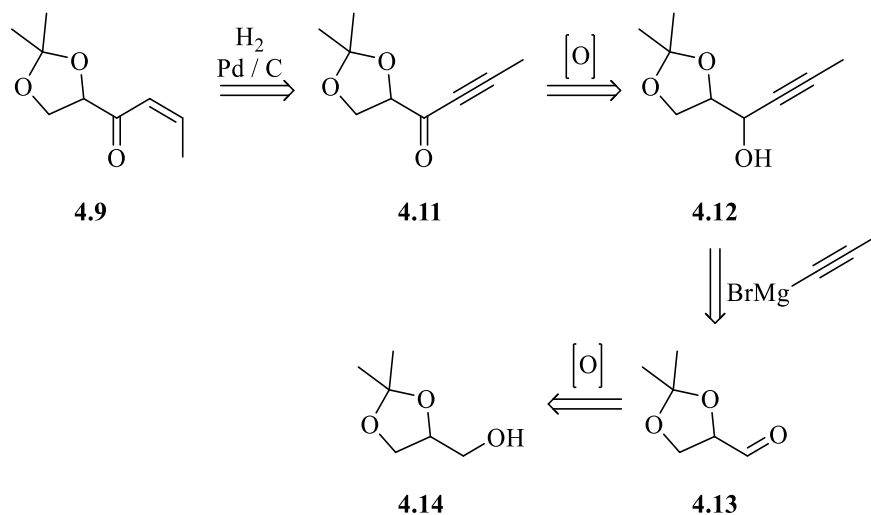
The organometallic compound **4.4** could be formed, via a hydroxyl to halogen conversion and oxidative insertion of a suitable metal, from **4.6**. An intramolecular aldol cyclization between aldehyde and ketone in compound **4.7** could be employed to form **4.6**. The hydrolysis of cyclic acetals and ester group in compound **4.8** would give **4.7**, whilst

the nucleophilic addition of the anion **4.10** to the ketone **4.9** would provide the compound **4.8** which is the carbon skeleton for the C and D (lactone) ring (Scheme 4.2).



Scheme 4.2: Retrosynthesis of ring C and D.

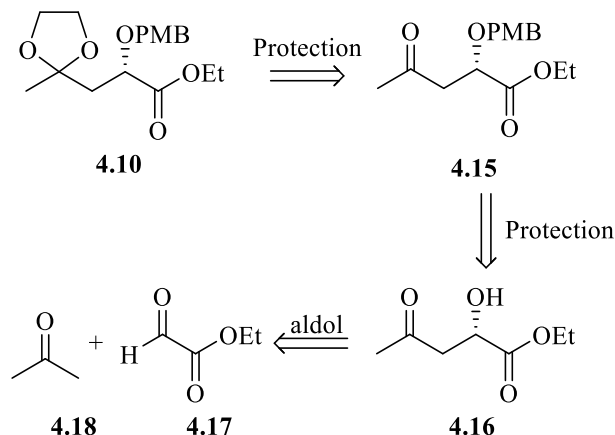
We envisioned that alkene **4.9** could be formed by reducing the alkyne **4.11** under a hydrogen atmosphere. The ketone in compound **4.11** could be prepared through the oxidation of the secondary alcohol **4.12**. The alkyne moiety in **4.12** could be obtained through a nucleophilic addition of a Grignard reagent to aldehyde **4.13**. The oxidation of the commercially available solketal ((2,2-dimethyl-1,3-dioxolan-4-yl)methanol) **4.14** would produce aldehyde **4.13** (Scheme 4.3).



Scheme 4.3: Retrosynthesis of the synthetic intermediate **4.9**.

Next, the synthetic intermediate **4.10** could be obtained through the protection of ketone **4.15**. The secondary alcohol **4.16** could be also protected as a PMB ether to provide

compound **4.15**. Aldol reaction between ethyl glyoxalate **4.17** and acetone **4.18** would generate β -hydroxy carbonyl **4.16** (Scheme 4.4).

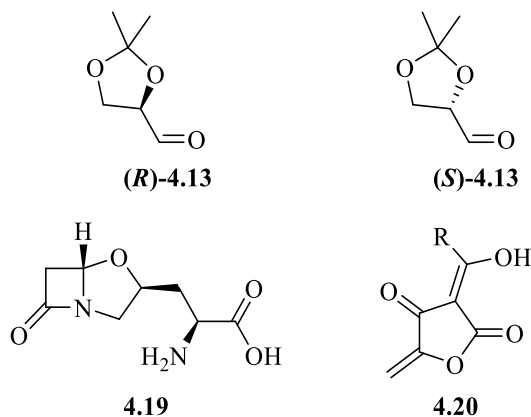


Scheme 4.4: Retrosynthesis of the synthetic intermediate **4.10**.

4.2. Synthesis of Ring C and D of DEM30355/A 1.14 via an Intramolecular Aldol Condensation Approach

4.2.1. Synthesis of 2,2-Dimethyl-1,3-dioxolane-4-carbaldehyde **4.13**

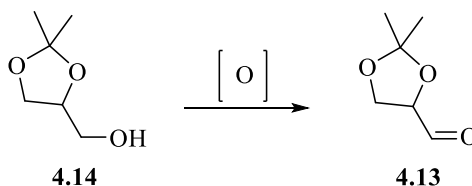
(*R*)- and (*S*)-2,2-dimethyl-1,3-dioxolane-4-carbaldehyde **4.13** are useful and affordable chiral building blocks for constructing chiral centers in the total synthesis of many natural products such as prostaglandins,⁸⁶ clavulanine⁸⁷ **4.19** and agglomerins antibiotics⁸⁸ **4.20** (Figure 4.1).



R = (CH₂)₈Me, (CH₂)₁₀Me
or (CH₂)₃CHCH(CH₂)₅Me

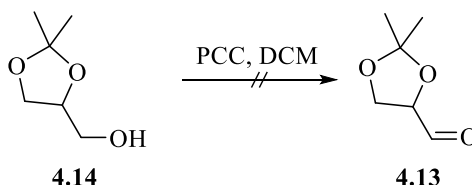
Figure 4.1: Natural products formed from 2,2-dimethyl-1,3-dioxolane-4-carbaldehyde **4.13**.

We have investigated the formation of the synthetic intermediate 2,2-dimethyl-1,3-dioxolane-4-carbaldehyde **4.13** through the oxidation of (2,2-dimethyl-1,3-dioxolan-4-yl)methanol **4.14** by examining different approaches (Scheme 4.5).



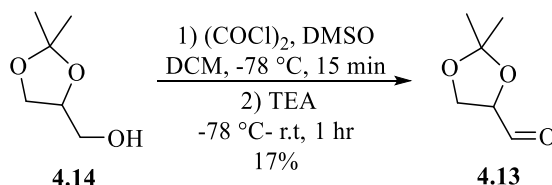
Scheme 4.5: Proposed reaction for the synthesis of **4.13**.

J. Hong *et al* demonstrated that the oxidation of (2,2-dimethyl-1,3-dioxolan-4-yl)methanol **4.14** with pyridinium chlorochromate (PCC) gave the corresponding **4.13**.⁸⁹ based on the Hong procedure, we examined the oxidation of **4.14** with PCC at 0 °C for 6 hours. However, no peak corresponding to the aldehyde was observed in the ¹H NMR of the crude reaction, even after repeating the reaction at room temperature for different lengths of time (6 hours and 12 hours).



Scheme 4.6: Attempted oxidation of **4.13** with PCC.

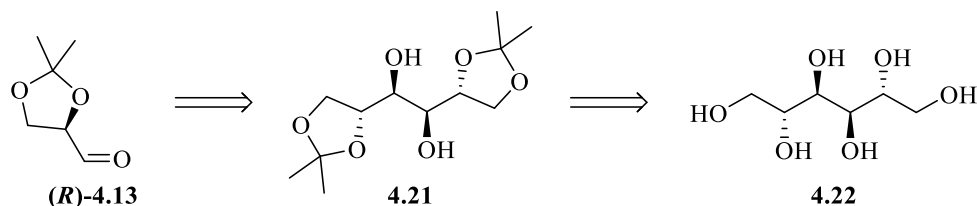
Next, we have examined the synthesis of **4.13** through a Swern oxidation of **4.14**. Based on a literature procedure, we reacted DMSO with oxalyl chloride in DCM at -78 °C to generate the reactive chlorosulfonium intermediate.⁹⁰ After 15 minutes chlorosulfonium intermediate was further reacted with **4.14** in the presence of triethylamine (TEA) base. The reaction crude was purified by column to give aldehyde **4.13** in a low yield 17%.



Scheme 4.7: Oxidation of **4.14** via Swern reaction.

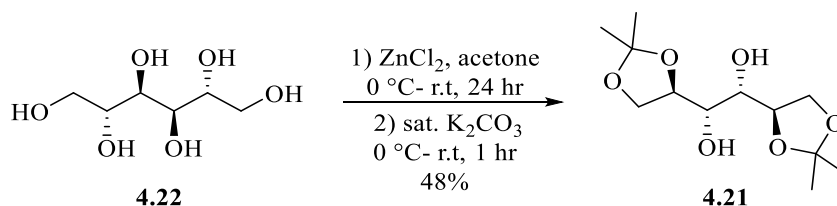
Due to the low yielding product obtained from Swern oxidation of **4.14**, we have examined a third approach that involves in generating (*R*)-2,2-dimethyl-1,3-dioxolane-4-

carbaldehyde (**R**)-**4.13** through the oxidative cleavage of diol **4.21**. Compound **4.21** could be prepared from D-mannitol **4.22** (Scheme 4.8).



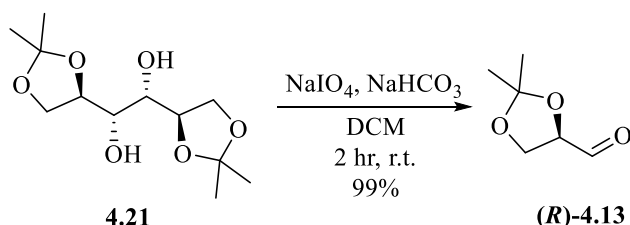
Scheme 4.8: Retrosynthesis of the (*R*)-2,2-dimethyl-1,3-dioxolane-4-carbaldehyde **4.13**.

In the first step we examined the synthesis of **4.21** through the double acetal protection of D-mannitol **4.22** based on Tipson and Cohen method.⁹¹ We started our investigation by reacting D-mannitol **4.22** with ZnCl₂ and acetone for 24 hours. Quenching the reaction with a saturated solution of K₂CO₃ produced the desired product **4.21** in 48% yield after recrystallisation from cyclohexane.



Scheme 4.9: Synthesis of the **4.21**.

With **4.21** in hand, we investigated the formation of compound (**R**)-**4.13** by reacting **4.21** with NaIO₄ and NaHCO₃ in DCM at room temperature based on a literature procedure.⁹² After 2 hours, the reaction was dried with Na₂SO₄ and filtered. The desired product (**R**)-**4.13** was successfully purified by distillation in a high yield 99%.



Scheme 4.10: Synthesis of (*R*)-**4.13** from D-mannitol **4.22**.

Overall, the synthesis of (*R*)-2,2-dimethyl-1,3-dioxolane-4-carbaldehyde (**R**)-**4.13** was successfully achieved from D-mannitol **4.22** under mild conditions in a good yield in comparison to the PCC/Swern oxidation approaches (Table 4.1).

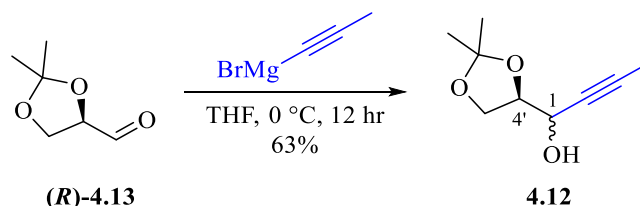
No.	Starting material	Reaction Condition	Product	%Yield
1	 4.14	PCC 0 °C for 6 hours	Starting material was recovered	0
2	 4.14	PCC r.t. for 6 hours	Starting material and minor peak for by-products, no product was observed	0
3	 4.14	PCC r.t. for 12 hours	Starting material and minor peak for by-products, no product was observed -	0
5	 4.14	(COCl) ₂ , DMSO DCM, -78 °C for 15 min then TEA r.t for 1 hour	 4.13	17
6	 4.21	NaIO ₄ , NaHCO ₃ DCM r.t. for 2 hours	 (<i>R</i>)-4.13	99

Table 4.1: Examination of the synthesis of 2,2-dimethyl-1,3-dioxolane-4-carbaldehyde 4.13 under different conditions.

4.2.2. Grignard Addition of 1-Propynylmagnesium Bromide to (*R*)-4.13

After a successful synthesis of (*R*)-4.13, we planned to construct the alkyne chain in compound 4.12 via the nucleophilic addition of the Grignard reagent into the aldehyde (*R*)-4.13. Based on a literature procedure, we examined the reaction of (*R*)-4.13 with 1-propynylmagnesium bromide in THF.⁹³ After 4 hours the ¹H NMR of the crude reaction mixture showed the presence of a distinctive multiplet peak at 4.37 ppm corresponding to the proton at the C4' position of 4.12. Purification by chromatography of the crude reaction mixture gave 4.12 in a moderate yield 28% as a mixture of two diastereoisomers. After

extending the reaction time for 12 hours, the yield of product **4.12** was improved to 63% (Table 4.2).

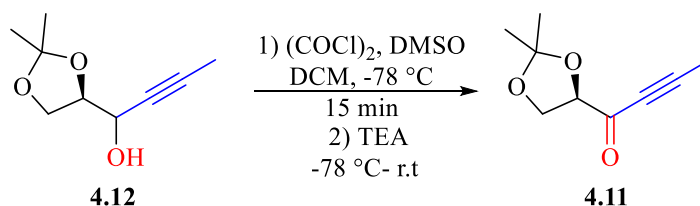


No.	Reaction time (hr)	%Yield
1	4	28
2	12	63

Table 4.2: Examination of Grignard reaction of (R)-4.13 towards 4.12.

4.2.3. Swern Oxidation of 4.12

Next, we turned our attention to the synthesis of **4.11** via a Swern oxidation of **4.12**. We therefore reacted **4.12** under classical Swern conditions. The loss of the stereocenter at the C1 position could be confirmed as the ¹H NMR of the desired product **4.11** was significantly simplified compared to the diastereomeric mixture observed with **4.12**. However, the isolated yield of the product was low 15%. To improve the yield of **4.11** we repeated the Swern reaction but extended the reaction time after the addition of TEA to 90 minutes. After aqueous work up the ¹H NMR of the crude product showed a complete conversion of the starting material giving the product **4.11** in a quantitative yield with no further purification required (Table 4.3).



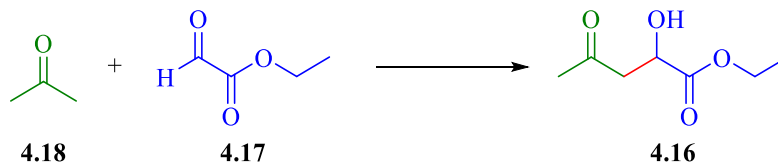
No.	Reaction time following the addition of TEA (min)	%Yield
1	15	15
2	90	100

Table 4.3: Examination of Swern oxidation of 4.12 towards 4.11.

Due to the time constraint the subsequent planned reduction of alkyne **4.11** into the corresponding (Z)-alkene **4.9** will be continued in the future.

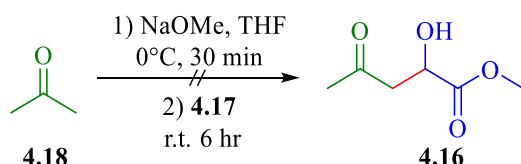
4.2.4. Investigation of the Aldol Reaction of 4.18 and 4.17

Next, we turned our attention to exploring the synthesis of **4.16** through an aldol reaction between ethyl glyoxalate **4.17** and acetone **4.18**



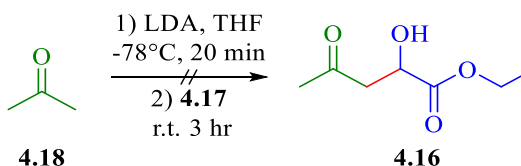
Scheme 4.11 Proposed reaction for the synthesis of **4.16**.

We started our investigation by deprotonating acetone **4.18**, with sodium methoxide in THF, to generate the corresponding enolate, afterward ethyl glyoxalate **4.17** was added to the reaction. After 6 hours none of the desired product was observed by ^1H NMR of the reaction crude, with a complex mixture being formed.



Scheme 4.12: Attempted reaction to produce **4.16** using NaOMe.

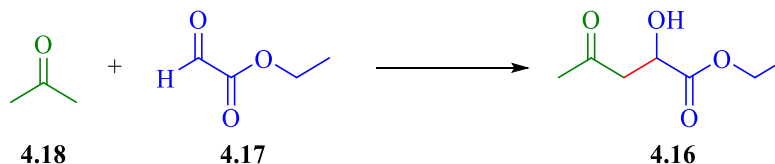
In the second attempt we have used a bulky base lithium diisopropylamide (LDA) to generate the acetone enolate in THF at -78°C , to which was added ethyl glyoxalate **4.17**. After 3 hours the desired product **4.16** was not observed in the ^1H NMR of the crude reaction.



Scheme 4.13: Attempted reaction to produce **4.16** using LDA.

Next, we examined another method that involved using pyrrolidine as an organocatalyst. The reaction of acetone **4.18** and ethyl glyoxalate **4.17** was performed in water at room temperature in the presence of a catalytic amount of pyrrolidine. After 3 hours, the ^1H NMR of the crude reaction mixture showed the presence of two new distinctive double doublet peaks at 2.98 (dd, $J = 17.4, 4.1$ Hz) and 2.89 (dd, $J = 17.4, 6.2$ Hz) corresponding to methylene group of the desired product **4.16**. However the purification of the crude reaction mixture by column chromatography gave the product **4.16**

in a low yield 8%. We then attempted to optimise the reaction conditions by extending the length time of the reaction to 12 hours, which the yield of **4.16** increased to 14% (Table 4.4).



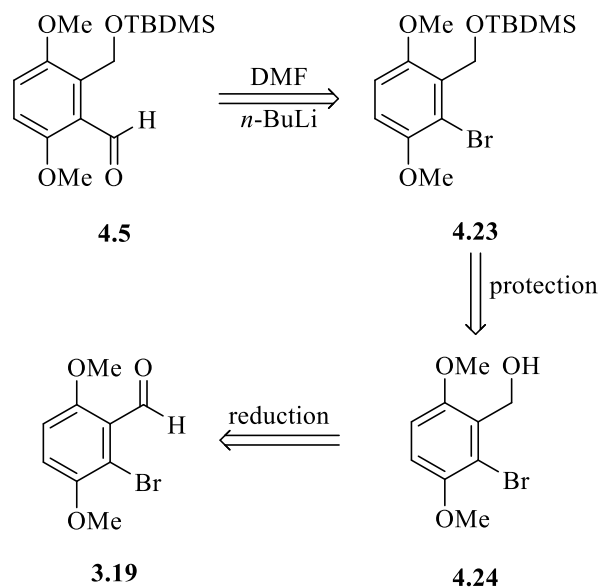
No.	Reaction Condition	%Yield
1	1) 4.18 , NaOMe, THF, 0°C for 30 minutes 2) 4.17 , r.t. 6 hr	Complex mixture of by-product No product was observed
2	1) 4.18 , LDA, THF, -78 °C for 20 minutes 2) 4.17 , r.t. 3 hr	Complex mixture of by-product No product was observed
3	pyrrolidine, H ₂ O	8
4	pyrrolidine, H ₂ O	14

Table 4.4: Examination of aldol reaction between **4.17** and **4.18** under different conditions.

The desired aldol reaction to give **4.16** has been successfully demonstrated, however further optimisation of the reaction will be required in the future.

4.3. Synthesis of the Synthetic Intermediate **4.5** of DEM30355/A 1.14 via an Intramolecular Aldol Condensation Approach

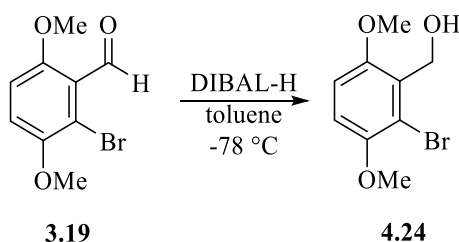
The following section describes the synthesis of **4.5**, which would be a key intermediate in the synthesis of ring A of DEM30355/A **1.14**. We envisioned that compound **4.5** could be prepared through a halogen-metal exchange reaction of arylbromide **4.23** using *n*-BuLi, followed by DMF trapping. The protection of alcohol **4.24** with TBDMSCl would produce compound **4.23**, whilst the primary alcohol **4.24** could be obtained by reducing the previously prepared aldehyde **3.19** (Scheme 4.14).



Scheme 4.14: The retrosynthesis of the key synthetic intermediate 4.5.

4.3.1. Reduction of Aldehyde 3.19 Using DIBAL-H

The first step in this synthesis of **4.5**, includes reducing the previously synthesised aldehyde **3.19** to the corresponding alcohol **4.24** using DIBAL-H. We therefore reacted **3.19** with DIBAL-H in toluene at $-78\text{ }^{\circ}\text{C}$. After 1 hour, the reaction was quenched with NH_4Cl . The appearance of a new singlet peak in the ^1H NMR of the crude reaction, corresponding to two benzylic protons at 4.94 ppm, confirmed the formation of alcohol **4.24**. The purification of the crude reaction mixture by column chromatography gave the desired product **4.24** in a moderate yield 41%. We then optimised the reaction condition by extending the reaction time to 3 hours, the product **4.24** was obtained in an excellent yield 98% (Table 4.5).



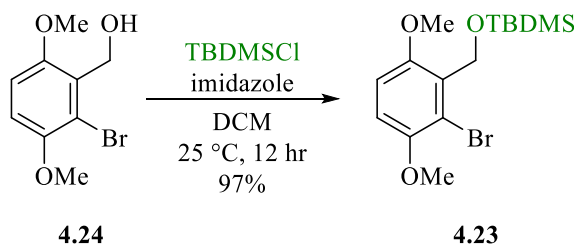
No.	Time (hr)	%Yield
1	1	41
2	3	98

Table 4.5: Examination of the reduction of 3.19 to 4.24 using DIBAL-H.

In the next step, we turned our attention to protect the resulting alcohol **4.24** as a silyl ether.

4.3.2. Silyl Ether Protection of 4.24

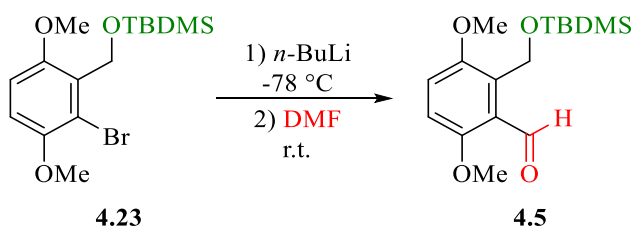
We examined the protection of **4.24** with the silylating agent TBDMSCl in the presence of imidazole in DCM. After 12 hours the product **4.23** was isolated following column chromatography in a high yield 97%.



Scheme 4.15: Protection of the alcohol **4.24** using TBDMSCl.

4.3.3. Halogen-Metal Exchange Reaction of 4.23

With compound **4.23** in hand, we examined the synthesis of **4.5** through a halogen-metal exchange reaction of **4.23** in combination with trapping with DMF. We started our investigation by reacting **4.23** with *n*-BuLi in THF for 30 minutes at -78°C . The resulting aryllithium intermediate was trapped with DMF. We found that quenching the reaction after 30 minutes gave the desired product **4.5** in 42%. Whereas the yield of **4.5** decreased with longer reaction times (Table 4.6).



No.	Reaction time after DMF addition	%Yield
1	30 min	42
2	1 hr	34
3	3 hr	0

Table 4.6: Examination of halogen-metal exchanged reaction trapping with DMF.

The lower yields observed with longer reaction times were due to the formation of an undesired by-product in this reaction. A more in depth discussion of the effect of reaction

time of the yield of **4.5** along with an examination of the by-products formed in this reaction will be discussed in chapter 5.

4.4. Conclusion

In conclusion, this chapter has examined a new synthetic route towards our target natural product antibiotic DEM30355/A **1.14** based on the synthesis of two key intermediates **4.5** and **4.4**. In our work towards **4.4** we have examined a number of approaches for the formation of intermediate **4.11**, with the oxidative cleavage of acetal protected D-mannitol **4.22** followed by addition of 1-propynylmagnesium bromide and a subsequent Swern oxidation providing most successful. The synthesis of key intermediate **4.5** was also examined through a reduction, protection and halogen-metal exchange reaction followed by trapping with DMF.

4.5. Future Work

The further work would primarily focus on the synthesis of the synthetic intermediate **4.6**.

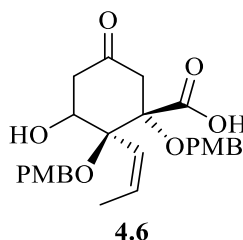
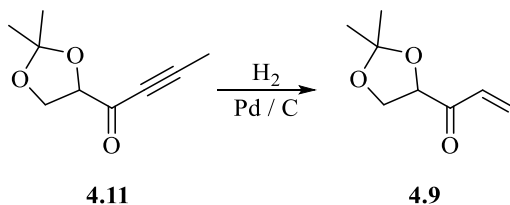


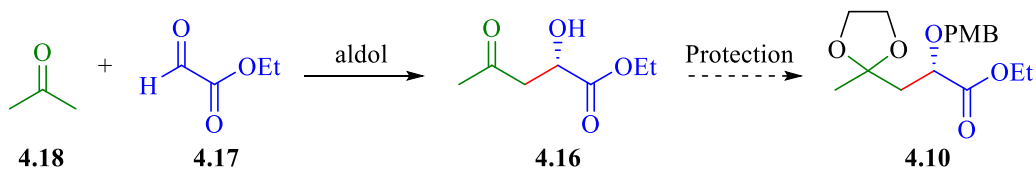
Figure 4.2: Structure of **4.6**.

Therefore, we firstly aim to complete the synthesis of (*Z*)-alkene **4.9** through the hydrogenation of alkyne **4.11**.



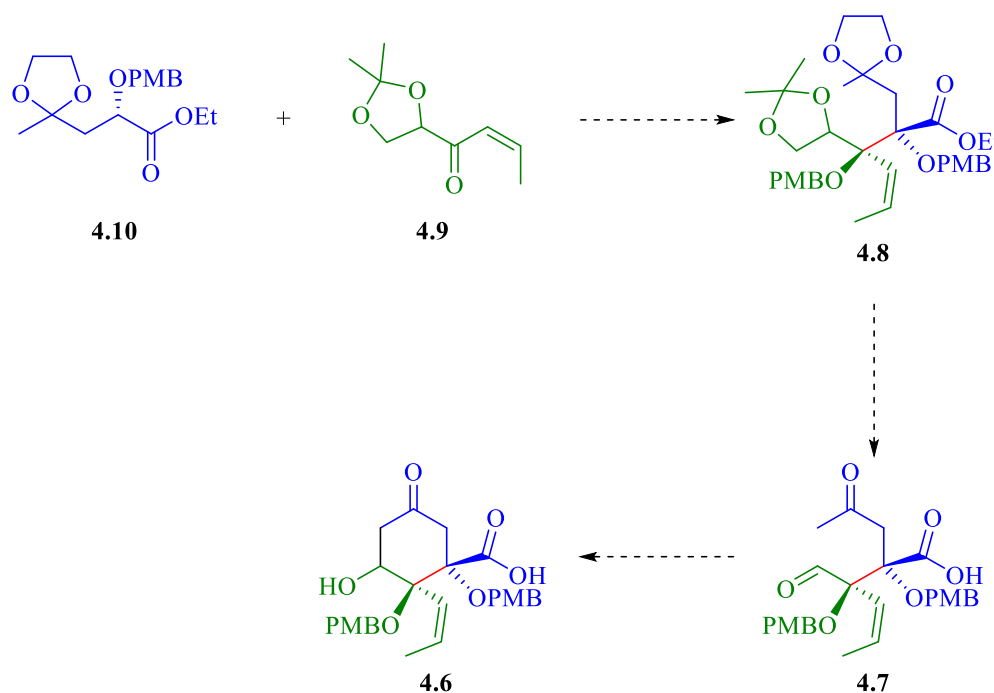
Scheme 4.16: Proposed reaction for the synthesis of **4.9**.

Secondly, we would like to optimise the condition of aldol reaction of **4.18** and **4.17** to improve the yield of **4.16**. The following double protection of **4.16** would provide the synthetic intermediate **4.10**.



Scheme 4.17: Proposed route towards the synthesis of 4.10.

After a successful synthesis of **4.9** and **4.10**, we wish to investigate the nucleophilic addition of anion **4.10** to the prochiral ketone **4.9** to generate **4.8** with a new quaternary stereogenic centre. After a selective protection of acetals in **4.8**, we would explore the synthesis of **4.6**, the core structure of ring C of DEM30355/A **1.14**, via an intramolecular aldol reaction of **4.7** (Scheme 4.18).



Scheme 4.18: Proposed route towards the synthesis of 4.6.

Chapter 5

5. Towards The Total Synthesis of (-)-(3R)-5-Hydroxymellein

5.1. Introduction

Alongside our work on the total synthesis of DEM30355/A **1.14**, we wanted to explore the use of our synthetic approaches to make related bioactive polyketides. We chose a target (-)-(3R)-5-hydroxymellein **5.1** as a simple test system to validate our synthetic approach to the synthetic intermediate **4.6** (Figure 5.1).

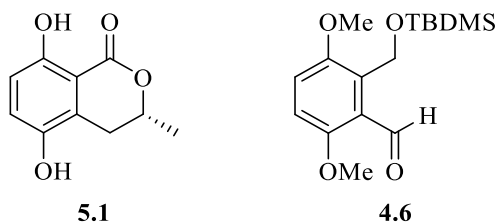
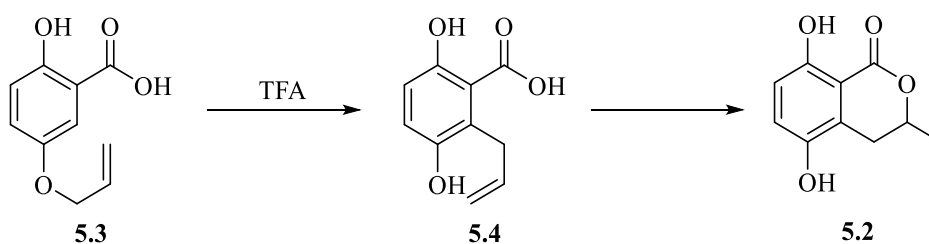


Figure 5.1: The chemical structure of (-)-(3R)-5-hydroxymellein **5.1** and compound **4.6**.

Our chosen target (-)-(3R)-5-hydroxymellein **5.1** was first isolated by M. de Alvarenga *et al.* in 1978 from unidentified fungus⁹⁴ and has since been isolated from other sources including *Septoria (Phaeosphaeria) nodorum* Berk⁹⁵ and *Xylaria* sp. YC-10⁹⁶ fungi. (-)-(3R)-5-Hydroxymellein **5.1** shows antiparasitic activity against the malaria causing protozoan parasite *Plasmodium falciparum* (IC₅₀ = 19 µg/mL) and cytotoxic activity against Vero cells (IC₅₀ = 16 µg/mL).⁹⁷ The total synthesis of racemic 5-hydroxymellein **5.2** has been achieved previously by Harwood in 1982. This synthesis was based around a key Claisen rearrangement of 5-allyloxy-2-hydroxybenzoic acid catalysed by trifluoroacetic acid (TFA), followed by a cyclisation of **5.4** to give **5.2** in 32% yield.⁹⁸



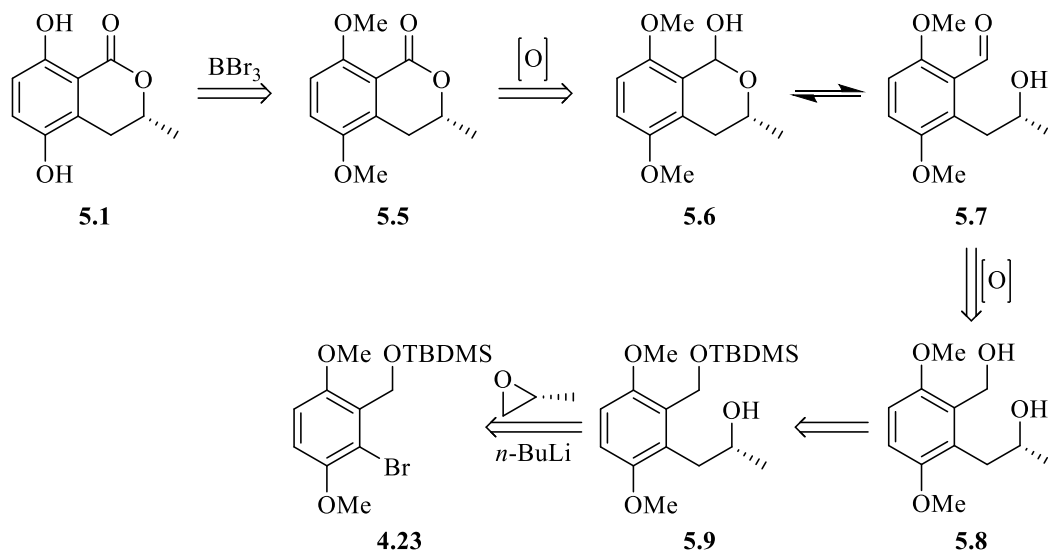
Scheme 5.1: The total synthesis of the racemic 5-hydroxymellein **5.2**.

In our research we aim to synthesise the enantiomerically pure (-)-(3R)-5-hydroxymellein **5.1** as it is found in nature.

5.2. Retrosynthesis of (-)-(3R)-5-Hydroxymellein **5.1**

We envisioned that (3R)-5-hydroxymellein **5.1** could be obtained through the demethylation of lactone **5.5** with BBr₃. The oxidation of lactol **5.6** could produce the corresponding lactone **5.5**. Lactol **5.6** would be in an equilibrium with **5.7**, thus compound

5.7 could be obtained by a selective oxidation of the primary alcohol of 5.8. A protected variant of alcohol of 5.9 could be formed by a halogen-metal exchange reaction of 4.23 with *n*-BuLi, to generate the corresponding aryl lithium, followed by a regioselective attack on (*R*)-(+)-propylene oxide 5.10 (Scheme 5.2).



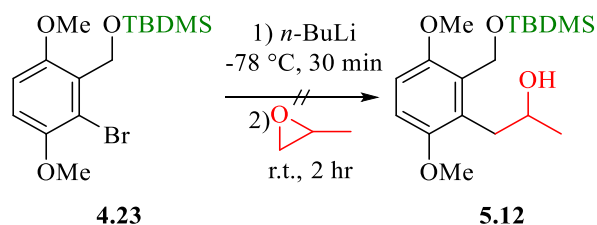
Scheme 5.2: Retrosynthetic analysis of (-)-(3*R*)-5-hydroxymellein 5.1.

Note that (±)-propylene oxide 5.11, rather than (*R*)-(+)-propylene oxide 5.10, was used for experimental optimization throughout the following discussions due to the expense of (*R*)-(+)-propylene oxide. On completion of the synthesis we would plan to repeat these steps with (*R*)-(+)-propylene oxide to make (-)-(3*R*)-5-hydroxymellein 5.1.

5.3. Examination of Routes towards of (-)-(3*R*)-5-Hydroxymellein 5.1

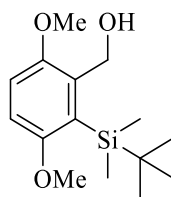
5.3.1. The Halogen-Metal Exchange and Trapping Reactions of 4.23

We therefore began our synthetic approach toward the target (3*R*)-5-hydroxymellein 5.1 through an examination of the halogen-metal exchange reaction of ((2-bromo-3,6-dimethoxybenzyl)oxy)(*tert*-butyl)dimethylsilane 4.23 with *n*-BuLi in combination with trapping with (±)-propylene oxide 5.11 (Scheme 5.3).



Scheme 5.3: Attempted halogen-metal exchange reaction of 4.23 with trapping by propylene oxide 5.11.

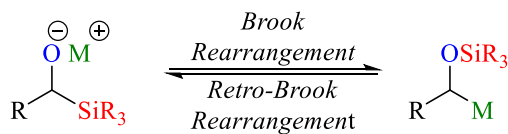
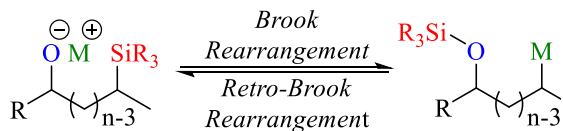
We started our investigation by performing the halogen-metal exchange reaction of **4.23** with *n*-BuLi for 30 minutes at -78 °C, followed by the addition of propylene oxide **5.11** at room temperature. After 2 hours, the ¹H NMR of the crude reaction mixture did not show the expected peaks for the desired product **5.12**. However a new aromatic AB system with peaks at 6.91 and 6.77 ppm (d, *J* = 9.1 Hz) could be observed in the ¹H NMR. In addition the two peaks corresponding to the two methyl groups had shifted apart to give two distinct peaks at 3.71 and 3.87 ppm, and a new broad peak at 2.71 ppm corresponding to an OH group was seen. The analysis of this NMR suggested that this new compound did not appear to be a simple dehalogenation of **4.23** therefore this compound was isolated by column chromatography to give **5.13** in a 99% yield. Further analysis of the purified compound showed the presence of a signal at 3620 cm⁻¹ in the IR spectrum, which confirmed that the molecule contains an OH group. High resolution mass spectrometry of **5.13** gave a signal at of 305.1544 which corresponds to [M+Na]⁺. The isotopic profile that we would expect for the presence of a bromine atom could not be observed, suggesting the bromine had been lost. Based on this analysis we have assigned the structure of **5.13** as shown below (**Figure 5.2**).



5.13

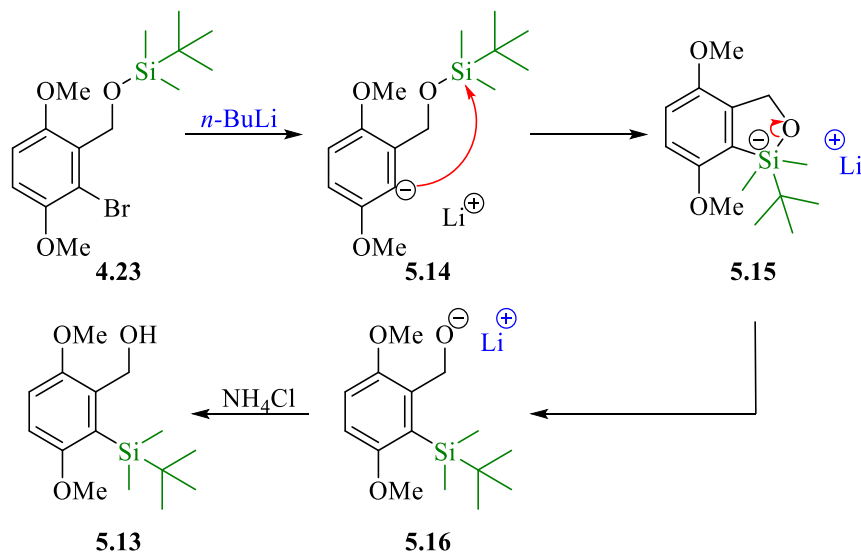
Figure 5.2: The structure of the rearranged compound 5.13.

We postulated that compound **5.13** was produced as a result of an intramolecular [1,4]-silyl migration from the oxygen to the aryl anion, generated by a halogen-metal exchange of **4.23** with *n*-BuLi. This silyl migration is known as a retro-Brook rearrangement. The Brook rearrangement was discovered by A. Brook in the late 1950s, it is defined as an intramolecular [1,*n*]-anionic migration of a silyl group from a carbon to an oxygen atom in the presence of a strong base.⁹⁹ The reverse process in which the silyl group migrated from an oxygen to a carbon atom is called the retro-Brook rearrangement and it was firstly reported by J. Speier at 1952 (**Scheme 5.4**).¹⁰⁰

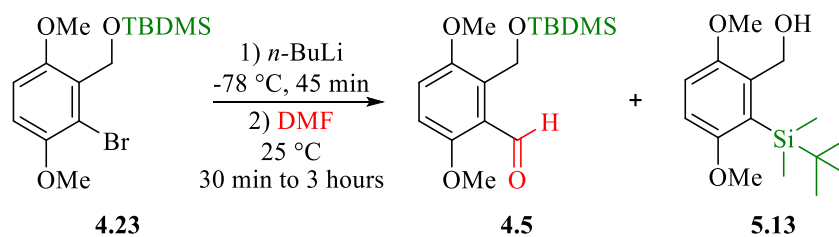
[1,2]-Silyl migration*[1,n]*-Silyl migration

Scheme 5.4: Brook and retro-Brook rearrangement.

Therefore, our proposed mechanism for the formation of **5.13**, via a retro-Brook rearrangement, involves the generation of aryllithium **5.14** via a halogen-metal exchange reaction of **4.23** with *n*-BuLi. Then, the reactive aryllithium **5.14** can attack the silicon to form the pentacoordinate silicon intermediate **5.15**. Intermediate **5.15** can then undergo Si-O bond cleavage to give the more stable anion **5.16** which is then protonated during the work-up with NH₄Cl (Scheme 5.5).

Scheme 5.5: Our proposed mechanism for the formation of **5.13** via a retro-Brook rearrangement.

Interestingly when we re-examined the ¹H NMR spectra for the halogen-metal exchange reaction of **4.23** followed by trapping with DMF, as described in Chapter 4, we also observed the formation of the retro-Brook product **5.13**. This provides an explanation for the relatively poor yield in our earlier DMF trapping experiments (Table 5.1)



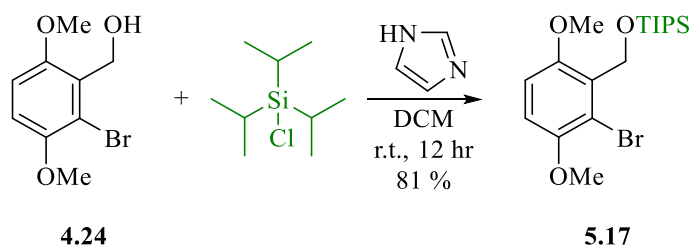
No.	Time	%Yield of 4.5	%Yield of 5.13
1	30 min	42	28
2	1 hr	34	55
3	3 hr	0	99

Table 5.1: The influence of trapping reaction times on the yield of 4.5 and 5.13.

Now that we had a better understanding of the reactivity of **4.23** with BuLi, we attempted to repeat the halogen-metal exchange reaction of **4.23** with BuLi and trap with **5.11** whilst avoiding the competing retro-Brook rearrangement. To do this we examined a reduction in the time allowed for the halogen-metal exchange step from 30 to 10 minutes. Assuming that the halogen-metal exchange is rapid then an earlier addition of the electrophile may help to increase the yield of the desired product **5.12**. However, the ^1H NMR of the crude material still showed only the presence of the rearranged product **5.13**. This suggests that the retro-Brook rearrangement of the corresponding anion of **4.23** occurs faster than the desired intermolecular reaction with propylene oxide **5.11**. Therefore, there is a need for an alternative protecting group that less susceptible to a retro-Brook rearrangement. Thus we chose to protect the alcohol **4.24** with the very bulky triisopropylsilyl group, as the increased bulk should slow the undesired retro-Brook rearrangement by reducing the rate of attack of the anion onto the silicon centre.¹⁰¹

5.3.2. Protection of Alcohol 4.24 with TIPSCl

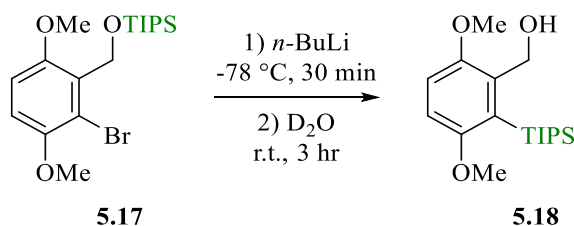
We therefore examined the protection of alcohol **4.24**, through the reaction of **4.24** with TIPSCl and imidazole in DCM at room temperature. After 12 hours, the desired product **5.17** was successfully isolated by column chromatography in a good yield 80%.



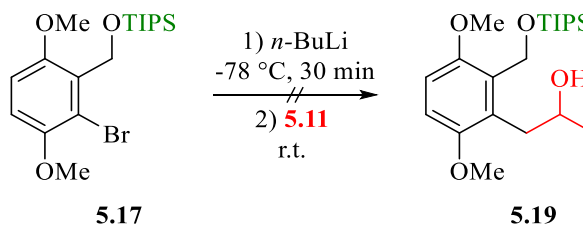
Scheme 5.6: The protection of alcohol 4.24 using TIPSCl.

5.3.3. Halogen-Metal Exchange Reaction of 5.17

After a successful synthesis of TIPS protected **5.17**, we carried out a test reaction to investigate if a retro-Brook rearrangement would occur in this substrate in the presence of *n*-BuLi. To assist in the investigation of this reaction we used D₂O to trap the products. We therefore reacted **5.17** with *n*-BuLi for 30 minutes, then the resulting product was trapped with D₂O and after 3 hours the reaction was quenched. Two compounds were seen in the ¹H NMR of the reaction mixture, unreacted starting material was the major product and a new compound **5.18** was present. The ¹H NMR showed a new AB system (two doublets at 6.87 and 6.72 ppm) accompanied by two new singlet peaks at 3.84 and 3.69 ppm, which indicated two methoxy groups. Comparison of the ¹H NMR of **5.18** with that of the retro-Brook product **5.13** showed considerable similarity, thus we proposed that this reaction has given a 3:1 ratio of unreacted starting material **5.17** to retro-Brook product **5.18**. TBDMS protected alcohol **4.24** was completely consumed after the same reaction time to give the retro-Brook product **5.13** in a 99%, thus this suggests that the TIPS protecting group undergoes a slower retro-Brook rearrangement than TBDMS.

Scheme 5.7: Examination of the halogen-metal exchange reaction of **5.17**.

The previous result prompted us to explore halogen-metal exchange reaction of **5.17** trapping with propylene oxide, anticipating that the slow rearrangement may allow for efficient trapping of the aryllithium.

Scheme 5.8: Attempted halogen-metal exchange of **5.17** followed by trapping with propylene oxide **5.11**.

We therefore examined a halogen-metal exchange reaction of **5.17** with *n*-BuLi for 30 minutes, followed by trapping with propylene oxide **5.11**. The reaction was quenched 12 hours later and analyzed by ¹H NMR. However, no product was observed, peaks

corresponding to starting material could be seen along with those of a second major compound, likely to be the dehalogenated species **5.20** (Figure 5.3). Due to the complex nature of these reaction, we decided to change the silyl protecting group to an acetal, as this would prevent any competing retro-Brook chemistry.

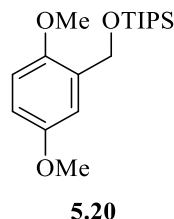
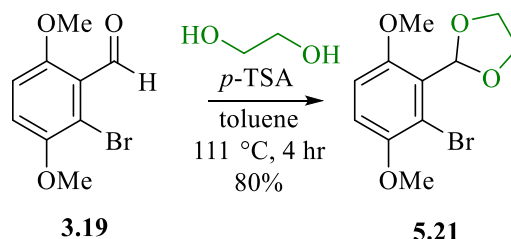


Figure 5.3: The structure of the dehalogenated compound **5.20**.

5.3.4. Protection of Aldehyde **3.19** as a Cyclic Acetal

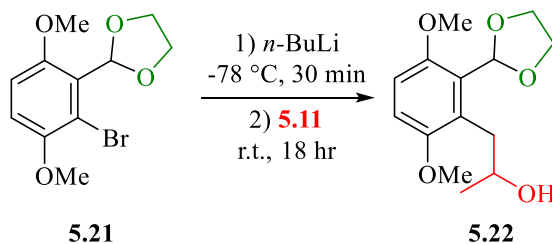
Thus we investigated the protection of aldehyde **3.19** with ethylene glycol, catalysed by *p*-TSA. After refluxing the reaction for 4 hours at Dean-Stark apparatus, the product 2-(2-bromo-3,6-dimethoxyphenyl)-1,3-dioxolane **5.21** was successfully isolated from the crude material by column chromatography in a high 80% yield.



Scheme 5.9: Protection of aldehyde **3.19** as acetal **5.21**.

5.3.5. Halogen-Metal Exchange Reaction of Cyclic Acetal **5.21**

With compound **5.21** in hand, we then investigated the halogen-metal exchange reaction of **5.21** with *n*-BuLi followed by trapping with propylene oxide **5.11**. The halogen-metal exchange step ran for 30 minutes, followed by the addition of **5.11**. After 18 hours the reaction was quenched.

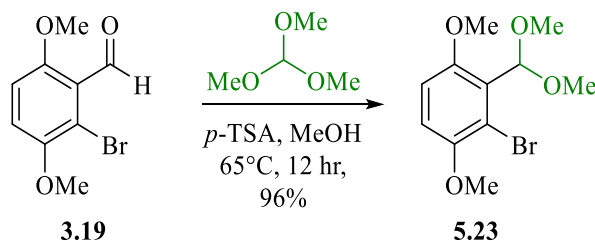


Scheme 5.10: Attempted halogen-metal exchange and trapping reaction towards **5.22**.

The $^1\text{H NMR}$ of the crude reaction showed mainly the corresponding dehalogenated product, with traces of the desired target **5.22**. As the cyclic acetal seemed to be an unsuitable protecting group in this reaction we decided to convert aldehyde **3.19** into acyclic acetal as an alternative protecting group for aldehyde **3.19**.

5.3.6. Protection of Aldehyde **3.19** as an Acyclic Acetal

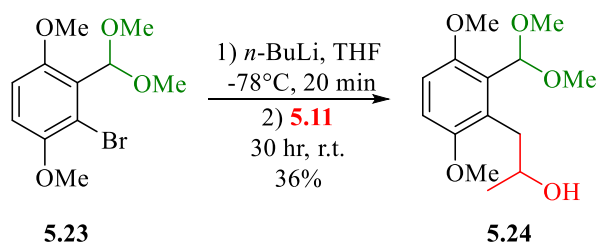
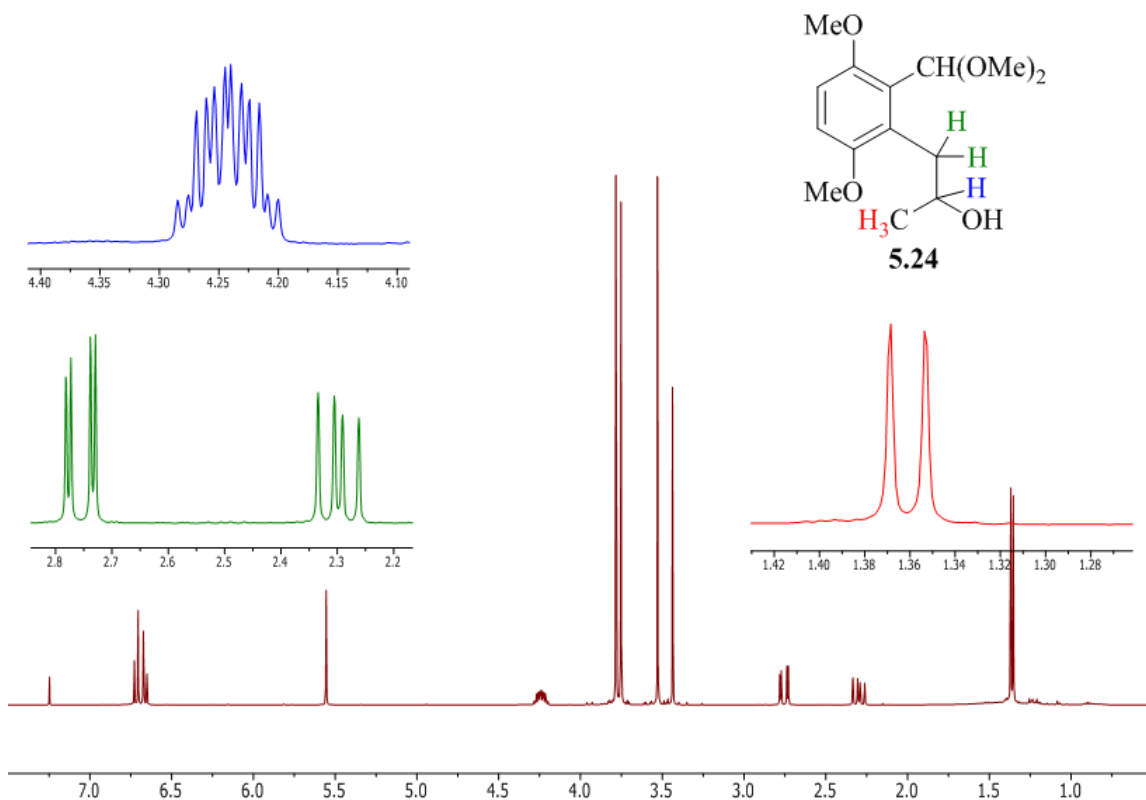
Based on a modified literature procedure, we examined the protection of aldehyde **3.19** with trimethyl orthoformate in methanol, in the presence of catalytic amount of *p*-TSA and molecular sieves 4 Å.¹⁰² The formation of product **5.23** was successfully achieved in an excellent yield 96%, after refluxing the reaction for 12 hours. Due to the purity of the **5.23** formed, no purification was required and the material was used in the subsequent reaction directly.



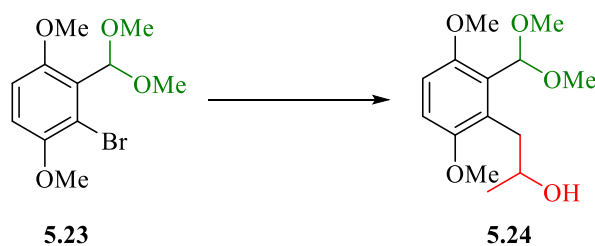
Scheme 5.11: Protection of aldehyde **3.19** with trimethyl orthoformate.

5.3.7. Halogen-Metal Exchange Reaction of Acyclic Acetal **5.23**

After a successful synthesis of **5.23**, we investigated the halogen-metal exchange reaction of **5.23** followed by trapping with **5.11**. Thus we reacted **5.23** with *n*-BuLi at -78 °C. After 30 minutes propylene oxide **5.11** was added and the reaction was warmed to room temperature. After 2 hours the reaction was quenched with NH_4Cl . The $^1\text{H NMR}$ of the crude mixture showed peaks corresponding dehalogenated material and a new set of peaks which including a one proton doublet of doublet of quartets at 4.24 ppm, a three proton doublet at 1.36 ppm, and two double, doublets at 2.76 and 2.30 ppm all of which are consistent with the desired product **5.24** (Figure 5.4). However **5.24** was a minor component of the reaction as the yield of isolated product by column chromatography was poor 12%. We therefore decided to optimise the reaction condition to improve the yield of the product **5.24**. We therefore examined extending the reaction time for the trapping of **5.11**, following the halogen-metal exchange. After 30 hours, the reaction was quenched and the crude material was purified by column chromatography to give the desired product **5.24** in a moderate yield of 36%.

Scheme 5.12: The synthesis of **5.24** via H-M exchange reaction.Figure 5.4: The ¹H NMR spectrum of **5.24**.

We then attempted to further optimise the reaction conditions using Lewis acid additives to accelerate the rate of the ring opening reaction of propylene oxide **5.11**. We therefore repeated the halogen-metal exchange reaction of **5.23** and examined the effects of adding **5.11** and then boron trifluoride diethyl etherate at low temperature. After running this reaction several times under different conditions the desired product **5.24** was not observed in the ¹H NMR of the crude reaction and a complex mixture of by-products was seen. We then investigated the use of other Lewis acids, thus the reaction was repeated as previously with the addition of CeCl₃ during the ring opening step. However, after 2 hours only the dehalogenated product could be observed (**Table 5.2**).



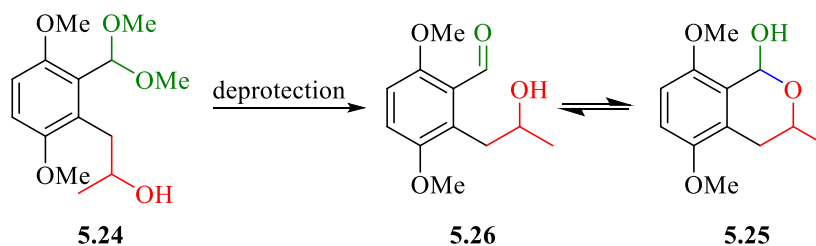
No.	Reaction Condition	Additives	% Yield
1	<i>n</i> -BuLi, THF, -78°C, 20 min then 5.11 , 2 hr, r.t.	-	12
2	<i>n</i> -BuLi, THF, -78°C, 20 min then 5.11 , 30 hr, r.t.	-	36
3	<i>n</i> -BuLi, THF, -78°C, 20 min then 5.11 , 2 hr, r.t..	BF ₃ .O(C ₂ H ₅) ₂	No product, complex mixture of by-products were observed.
4	<i>n</i> -BuLi, THF, -78°C, 20 min then 5.11 , 2 hr, -78 °C.	BF ₃ .O(C ₂ H ₅) ₂	No product, complex mixture of by-products were observed.
5	<i>n</i> -BuLi, THF, -78°C, 10 min then 5.11 , 2 hr, -78 °C.	BF ₃ .O(C ₂ H ₅) ₂	No product, complex mixture of by-products were observed.
6	<i>n</i> -BuLi, THF, -78°C, 20 min then 5.11 , 2 hr, r.t.	CeCl ₃	No product, mainly dehalogenated product observed.

Table 5.2: Examination of the H-M exchange reaction of 5.23 with trapping by propylene oxide 5.11.

Despite screening a number of Lewis acid additives, the best conditions for the formation of **5.24** involved long reaction times for the ring opening of propylene oxide. However, this approach allowed us access to sufficient **5.24** for us to examine the next steps in our planned synthesis.

5.3.8. Deprotection of Acetal **5.24**

The next step involved the planned removal of the acetal protecting group in **5.24** in order to produce the corresponding lactol **5.25**, which could in turn be subsequently oxidised and deprotected to give 5-hydroxymellein.



Scheme 5.13: Proposed acetal hydrolysis with acid.

We examined the hydrolysis of **5.24** using 0.1 M of aqueous HCl in acetonitrile. The reaction was monitored by TLC. After 12 hours only starting material could be observed by TLC and ^1H NMR. We then repeated the reaction using 0.2 M of aqueous HCl in 1,4-dioxane, however again starting material was recovered with no product was observed.

Next, we turned our attention to examining an alternative acidic condition for the cleavage of the acetal **5.24** using trifluoroacetic acid (TFA). We therefore reacted **5.24** with TFA in the presence of H_2O at room temperature. After 30 minutes the starting material was consumed and new two spots were formed in the TLC plate. The ^1H NMR of the crude reaction showed the presence of new peaks corresponding to lactol **5.25** as a minor component along with the related dehalogenated product. Purification of the crude reaction mixture by column chromatography gave the desired lactol **5.25** in 28%.

Next, to improve the yield of this step we examined a method reported by Sun for acetal deprotection under neutral condition using a catalytic amount of molecular iodine in acetone.¹⁰³ We therefore carried out a reaction of **5.24** with iodine in acetone at room temperature. The reaction was quenched with sodium thiosulfate after 45 minutes. After chromatography the ^1H NMR of the isolated product showed the presence of two benzylic peaks at 5.49 and 5.45 ppm (d, $J = 3.5$ Hz, 1H) and two sets of peaks at 3.03 (dd, $J = 14.8, 3.5$ Hz, 1H), 2.89 (dd, $J = 14.8, 10.2$ Hz, 1H) and 2.80 (dd, $J = 17.2, 3.4$ Hz, 1H) 2.34 (dd, $J = 17.2, 10.8$ Hz 1H) corresponding to two benzylic methylene groups both in a 1:1 ratio. This is consistent with the presence of both of the possible diastereomers of lactol **5.25** (Figure 5.5).

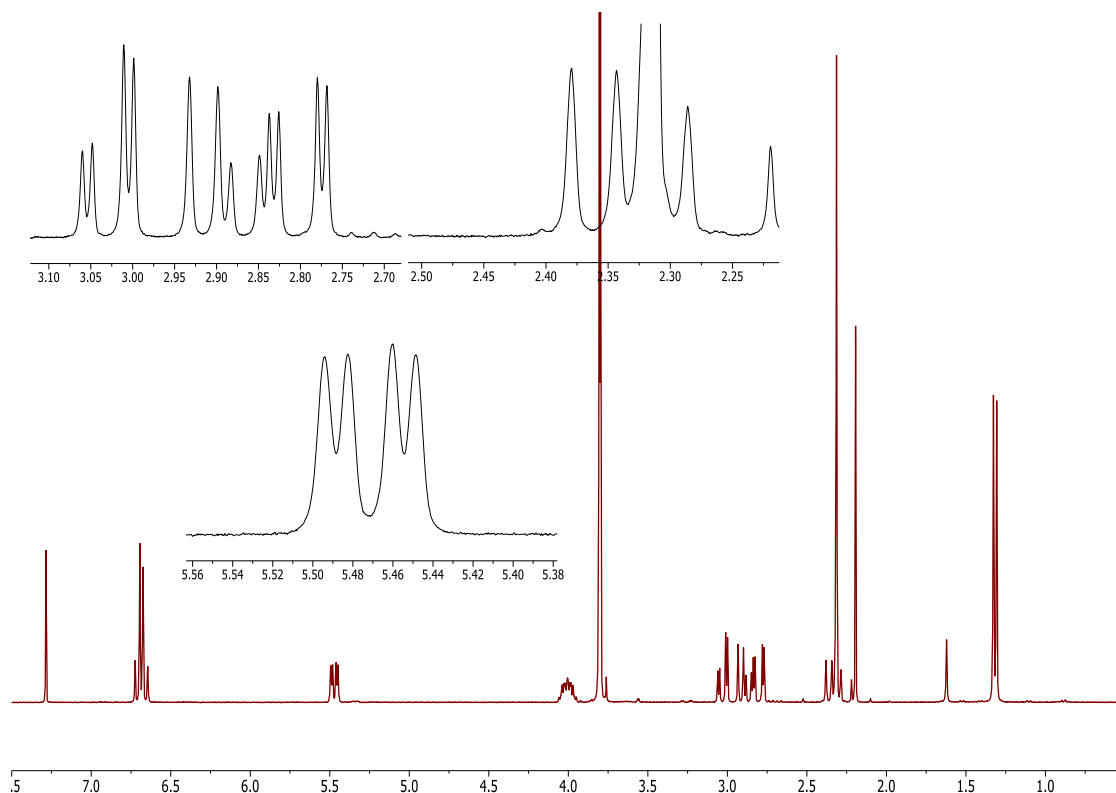


Figure 5.5: The ^1H NMR spectrum of **5.25**.

Further analysis was carried out to confirm the structure of **5.25**. High resolution mass spectroscopy showed a signal at 207.1060 which indicates the presence of the corresponding oxonium arising from loss of water from **5.25** (Figure 5.6)

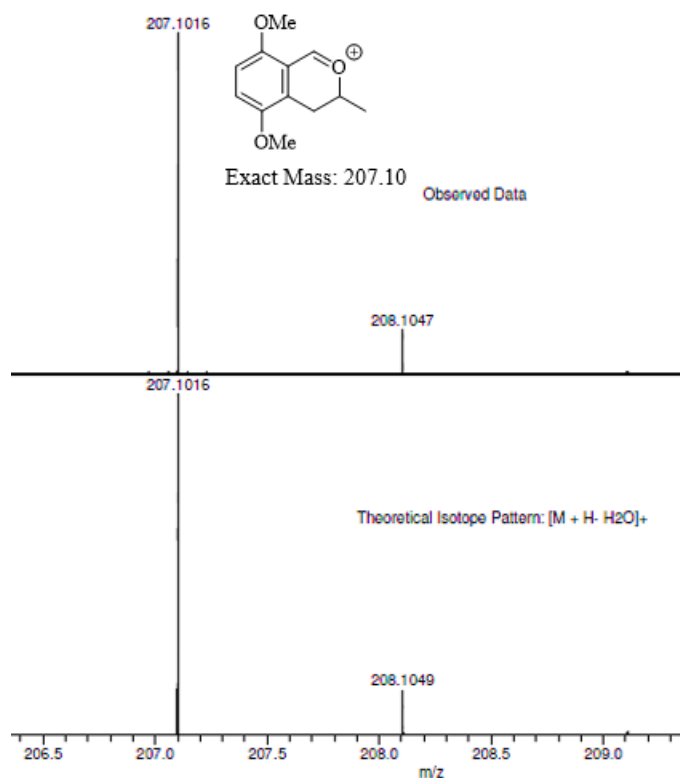


Figure 5.6: The HRMS of lactol **5.25**.

Crystals were then obtained through slow diffusion of petrol into a solution of **5.25** in DCM. Interestingly, the single crystal X-ray analysis of the formed crystals showed the presence of dimeric diacetal **5.27** instead of the expected lactol **5.25** (Figure 5.7).

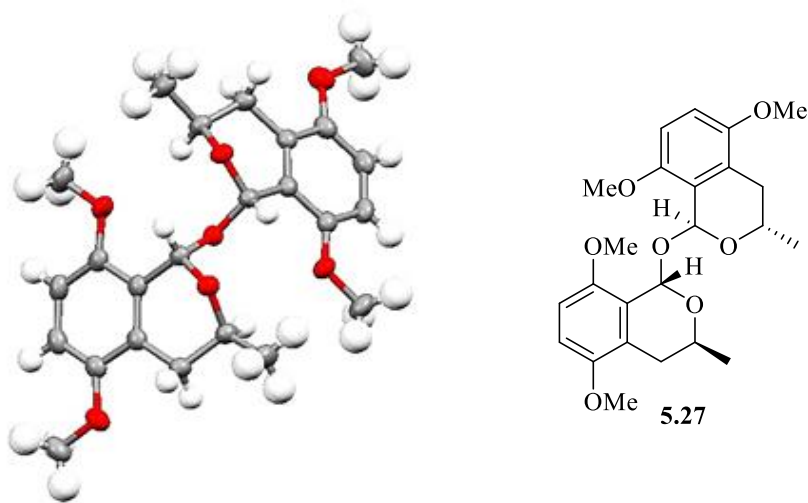


Figure 5.7: Crystal structure of (1*S*,1'*S*,3*S*,3'*S*)-**5.27**.

The crystal contains a racemic 1:1 mixture of the (1*S*,1'*S*,3*S*,3'*S*)-**5.27** and the (1*R*,1'*R*,3*R*,3'*R*)-**5.27** (Figure 5.8).

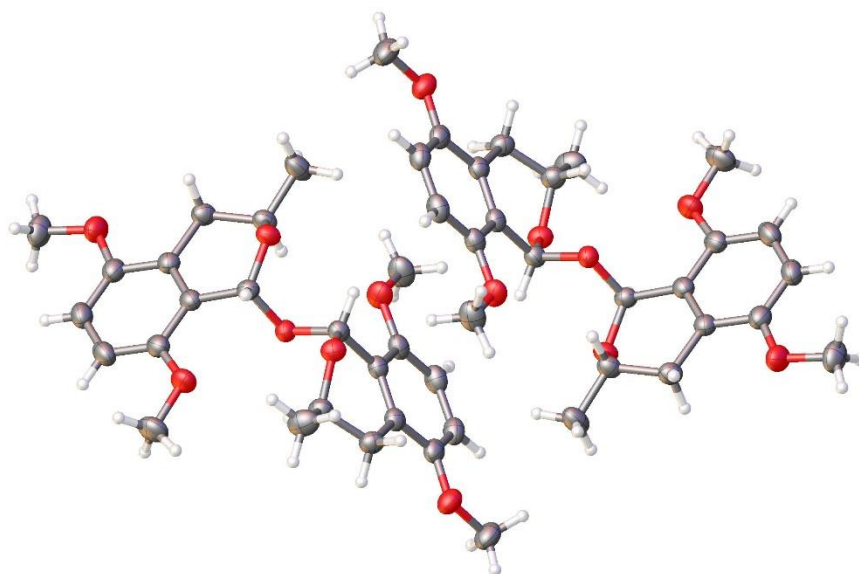


Figure 5.8: Crystal packing diagram showing a pair of enantiomers of **5.27**.

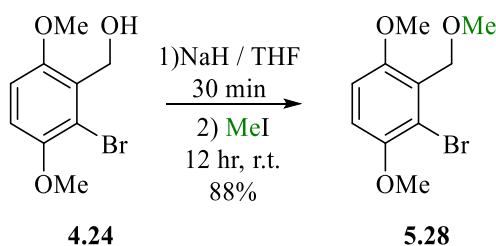
Interestingly despite the presence of both the possible diastereomers in the ^1H NMR of lactol **5.24**, the crystal structure only contains dimers with (1*S*,1'*S*,3*S*,3'*S*) and the (1*R*,1'*R*,3*R*,3'*R*) stereochemistry. The dimer is likely formed through a condensation

reaction between two lactols. The observed stereochemistry in the crystal maybe due to a preferential crystallisation of the (1*S*,1'*S*,3*S*,3'*S*)/(1*R*,1'*R*,3*R*,3'*R*) diastereomer.

Although this approach was promising, due to the low yields in the formation of **5.24** we decided to examine in parallel an alternative protecting group strategy employing a methyl ether.

5.3.9. Protection of Alcohol **4.24** with Methyl Iodide

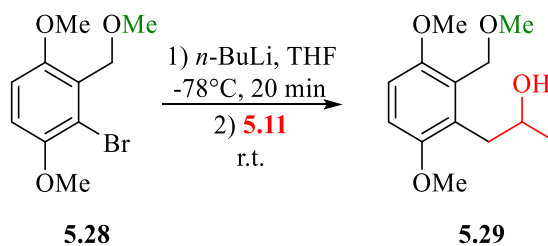
We also investigated the protection of alcohol **4.24** as a methyl ether using methyl iodide and sodium hydride in THF at room temperature. After 12 hours, product **5.28** was successfully isolated by column chromatography in a good yield 88%.



Scheme 5.14: Protection of alcohol **4.24** as a methyl ether.

5.3.10. Halogen-Metal Exchange Reaction of Methyl Ether **5.28**

With **5.28** in hand, we examined the formation of **5.29** via a halogen-metal exchange reaction followed by trapping with **5.11**. We reacted **5.28** with *n*-BuLi at -78 °C prior to the addition of propylene oxide **5.11**. After 2 hours the reaction was quenched and the ¹H NMR of the crude showed the formation of product **5.29**, along with some dehalogenated, with an isolated yield of 31%. We therefore optimised the reaction conditions to improve the yield of **5.29** by extending time for the reaction with propylene oxide **5.11**. The reaction was quenched 4 hours following the addition of **5.11** and the yield of **5.29** had increased significantly to 78% (Table 5.3).



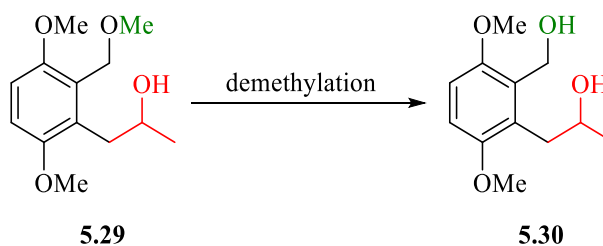
No.	Reaction time following addition of 5.11	%Yield
1	2 hr	31
2	4 hr	78

Table 5.3: Examination of the halogen metal exchange reaction of 5.26 followed by trapping with 5.11.

After the positive outcomes that obtained from this reaction, we aimed to deprotect 5.29 in order to produce the corresponding diol 5.30.

5.3.11. Deprotection of Methyl Ether 5.29

We therefore examined the cleavage of methyl ether 5.29. We firstly looked at the use of demethylating agent BBr_3 in DCM.



Scheme 5.15: Proposed cleavage of methyl ether 5.29.

We started our investigation through the reaction of 5.29 with BBr_3 at -78°C . After 30 minutes the reaction was quenched with cold saturated aqueous solution NaHCO_3 . The appearance of two new diastereomeric benzylic peaks at 4.76 (d, $J = 9.7$ Hz, 1H) and 4.70 (d, $J = 9.7$ Hz, 1H) ppm in the ^1H NMR confirmed the formation of a new compound (Figure 5.9).

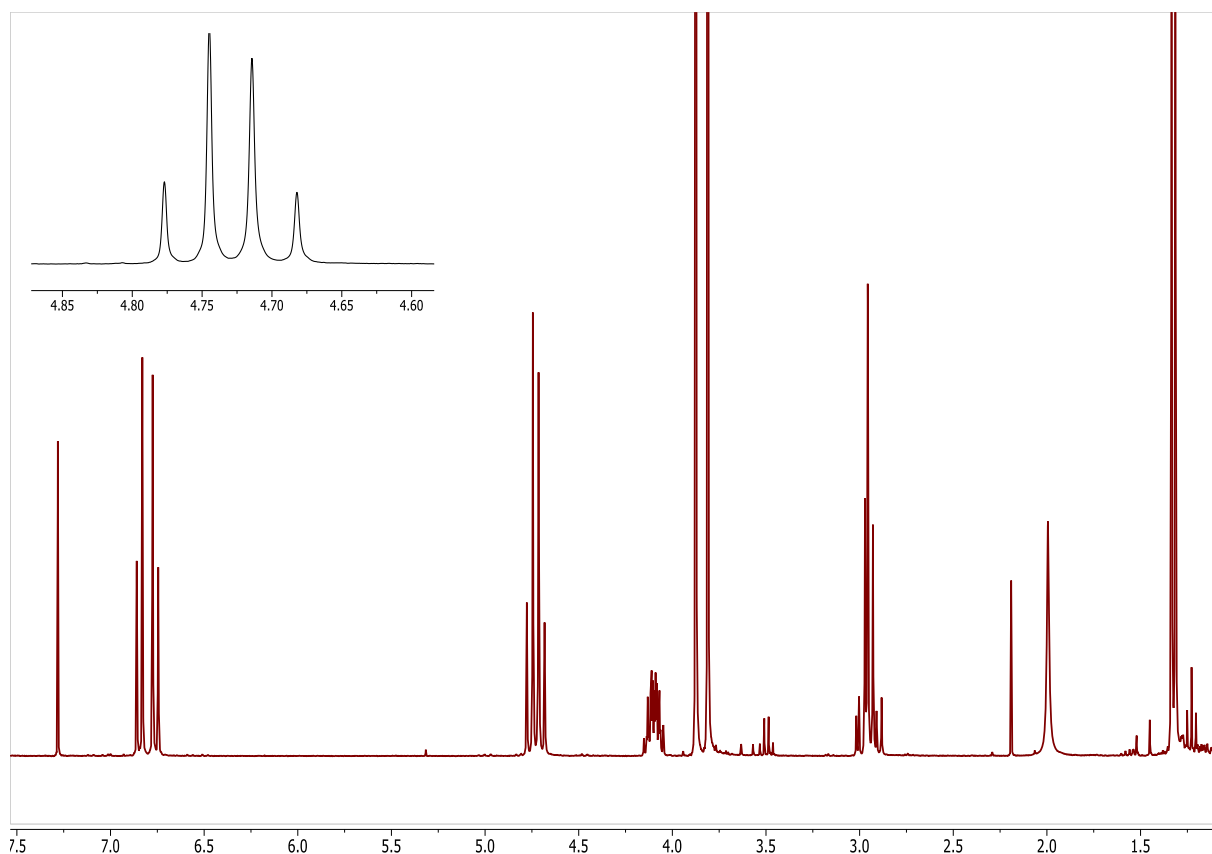


Figure 5.9: The ^1H NMR for the reaction product of **5.29** with BBr_3 .

The IR spectra however showed that no OH groups were present. The high resolution mass spectrometry showed a signal at 209.1172 which corresponds to a molecular formula of $\text{C}_{12}\text{H}_{17}\text{O}_3$ which suggests that the product was not the desired diol **5.30**. Based on the previous analysis, we therefore propose that the reaction of **5.29** with BBr_3 gave compound **5.31** very cleanly in a 99% yield (**Figure 5.10**).

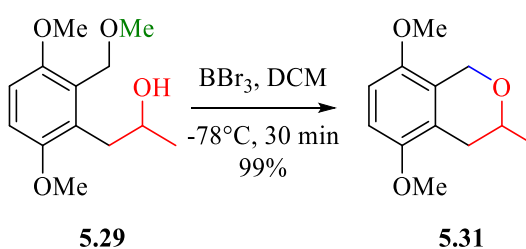
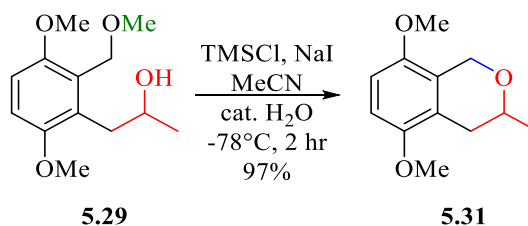


Figure 5.10: Structure of **5.31**.

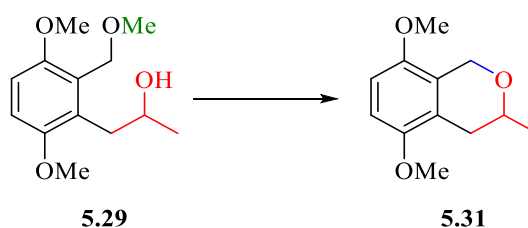
We propose that **5.31** was formed through a Lewis acid activation of the methoxy group followed by an intramolecular substitution by the hydroxyl to form the observed **5.31** ether. In parallel, we also examined another method for the deprotection of methyl ether **5.29** using *in situ* generated trimethylsilyl iodide.¹⁰⁴ Based on a modified literature procedure, we reacted **5.29** with sodium iodide and trimethylsilyl chloride in acetonitrile in the presence of water at 40°C .¹⁰⁵ After 2 hours the crude reaction mixture was purified by

column chromatography. The ^1H NMR spectrum of the isolated product was identical to compound **5.31** suggesting that a very similar reaction had occurred.



Scheme 5.16: Synthesis of 5.31 via the cleavage of 5.29 with TMSI.

Despite failing to make our target molecule **5.30**, we have successfully synthesised compound **5.31** through the demethylation of **5.29** following two different methods using the Lewis acid BBr_3 and TMSI both in high yield (**Table 5.4**).



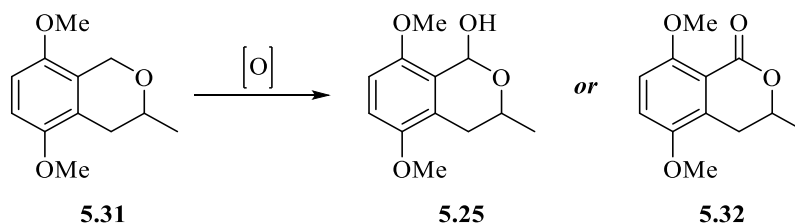
No.	Demethylating Agent	Reaction Time	Product	%Yield
1	BBr_3	30 min	 5.31	99
2	TMSI	2 hr	 5.31	97

Table 5.4: Examination of the cyclisation 5.29 using BBr_3 and TMSI.

5.3.12. Oxidation of the Benzyl Ether **5.31**

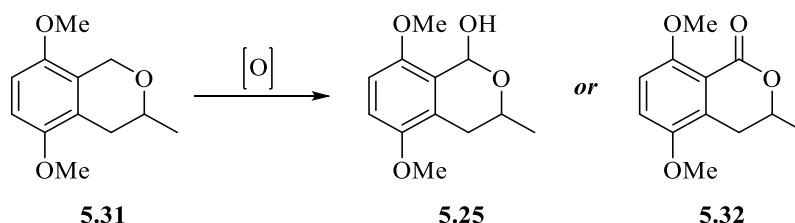
Compound **5.31**, despite being an unexpected product, could still prove useful in the formation of 5-hydroxymellein and its analogues if the benzylic position adjacent to oxygen could be selectively oxidised. Thus, we attempted to oxidise benzyl ether **5.31** to

produce the corresponding lactol **5.25** and/or lactone **5.32**, an analogue of 5-hydroxymellein **5.2**.



Scheme 5.17: Proposed oxidation reaction of benzyl ether 5.31.

We have screened a number of reaction conditions using several different oxidising agents including: 2,3-dichloro-5,6-dicyanobenzoquinone (DDQ), *meta*-chloroperbenzoic acid; (*m*-CPBA), manganese dioxide (MnO₂) and a combination of potassium permanganate and manganese dioxide (KMNO₄/MnO₂) using different solvents under variable temperatures.^{106,107,108,109} However, none of these conditions gave the desired products **5.25** or **5.32** (Table 5.5).



No.	Oxidising Agents	Reaction Condition	Reaction Outcomes	Product
1	DDQ	toluene 4 hr, r.t.	Starting material recovered	-
2	DDQ	toluene 6 hr, reflux	No product, starting material was decomposed	-
3	DDQ	DCM/MeOH 24 hr, r.t.	Starting material recovered	-
4	DDQ	DCM/MeOH 48 hr, r.t.	Ring opening of 5.31 by MeOH reproducing 5.29 with minor unidentified products observed, the yield of isolated 5.29 is 17%	<p style="text-align: center;">5.29</p>

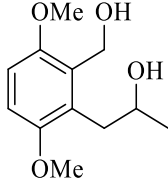
5	<i>m</i> -CPBA	DCM 4 hr, r.t.	No product was observed, starting material was decomposed	-
6	MnO ₂	DCM 12 hr, r.t.	Ring opening of 5.31 by H ₂ O to produce diol 5.30 in 26% yield	 5.30
7	KMNO ₄ /MnO ₂	DCM 6 hr, r.t.	No product was observed, starting material was decomposed	-

Table 5.5: Examined reactions conditions for the oxidation of benzyl ether **5.31.**

Interestingly, we observed in a number of cases the ring opening of the ether **5.31** by MeOH during the oxidation reaction with DDQ to reproduce **5.29**, and by H₂O in the case of using MnO₂ to give the desired diol **5.30**.

Due to the time constraint the investigation on the oxidation of benzyl ether **5.31** will be continued in the future.

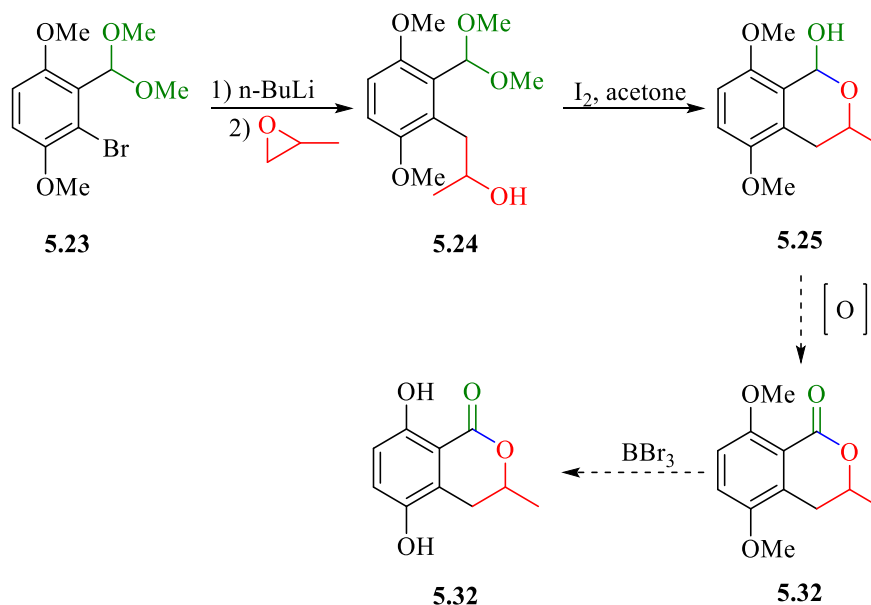
5.4. Conclusion

In conclusion, we investigated several synthetic routes towards the total synthesis of (-)-(3*R*)-5-hydroxymellein **5.1** based on the approach we have previously developed in chapter 4 for producing the aromatic ring of DEM30355/A **1.14**. Using racemic propylene oxide **5.11** as a test reagent, we have successfully proved that the chiral centre can be created through the halogen-metal exchange reaction of arylbromides followed by (\pm)-propylene oxide trapping in the presence of certain protecting groups. In case of using silyl protecting groups, the Brook rearrangement occurred during H-M exchange reaction due to the slow rate of the ring opening reaction of **5.11**. The best substrate for our halogen-metal exchange/trapping strategy was methoxy ether **5.28**. Despite difficulties in deprotecting the methyl ether, due to the unexpected formation of cyclic ethers, in our attempts to oxidise ether **5.31** we have observed ring opening to the desired diol, which has the potential for further oxidation/deprotection to give 5-hydroxymellein.

5.5. Future Work

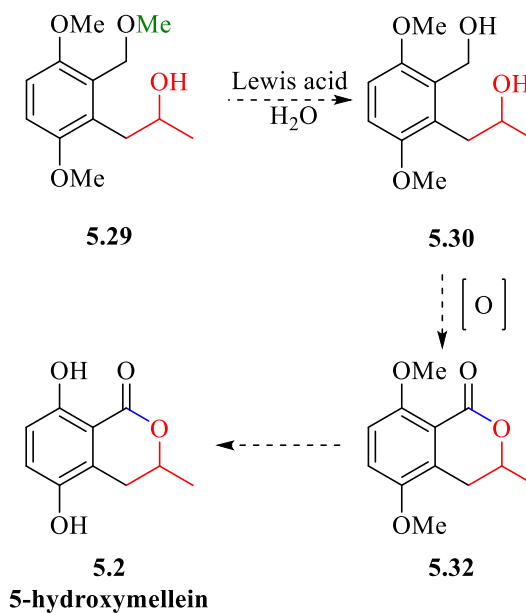
Our aim is to complete the total synthesis of 5-hydroxymellein **5.2** through use of the two efficient synthetic routes we developed using dimethyl acetal and methoxy ether as protecting groups.

Following in our synthetic route whereby dimethyl acetal is used as a protecting group, we plan to improve the yield of **5.24** by optimising the halogen-metal exchange reaction conditions, and thus complete this route towards our target natural product.



Scheme 5.18: Towards the total synthesis of 5-hydroxymellein **5.2** using methoxy ether protecting group.

If the halogen metal exchange and trapping in the first route could not be improved then we would look to continue our alternative approach. Thus in the second synthetic route, based upon the use of methoxy ether as a protecting group, the reaction conditions for the deprotection of methoxy ether **5.29** could be optimised to produce diol **5.30**, through use of a Lewis acid and water. The total synthesis of 5-hydroxymellein would then be completed through the oxidation of diol **5.30** to produce lactone **5.32**, followed by the demethylation of the phenolic hydroxyl groups.



Scheme 5.19: Towards the total synthesis of 5-hydroxymellein **5.2** using dimethyl acetal protecting group.

Next, in order to synthesise an enantiopure (-)-(3*R*)-5-hydroxymellein **5.1**, it would be necessary to repeat the synthesis with (*R*)-(+)-propylene oxide **5.10**. Additionally, in a similar way, the synthesis of (-)-(3*S*)-5-hydroxymellein enantiomer **5.33** could be achieved by using (*S*)-(+)-propylene oxide (**Figure 5.11**).¹¹⁰

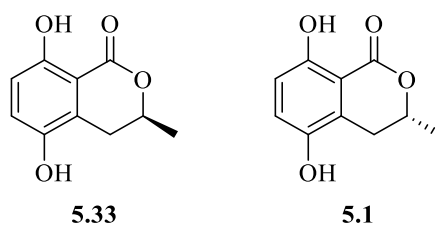


Figure 5.11: Structures of (-)-(3*R*)-5-hydroxymellein **5.1** and (-)-(3*S*)-5-hydroxymellein **5.33**.

With the development of a successful synthetic route to the natural product, a number of 5-hydroxymellein analogues could be generated. Given the activity of 5-hydroxymellein against malaria causing protozoan *Plasmodium falciparum*, we wish to investigate the biological activity these analogues, including the related natural products mellein **5.34**, 4-hydroxymellein **5.35**, 6-hydroxymellein **5.36** and 7-hydroxymellein **5.37** (**Figure 5.12**).

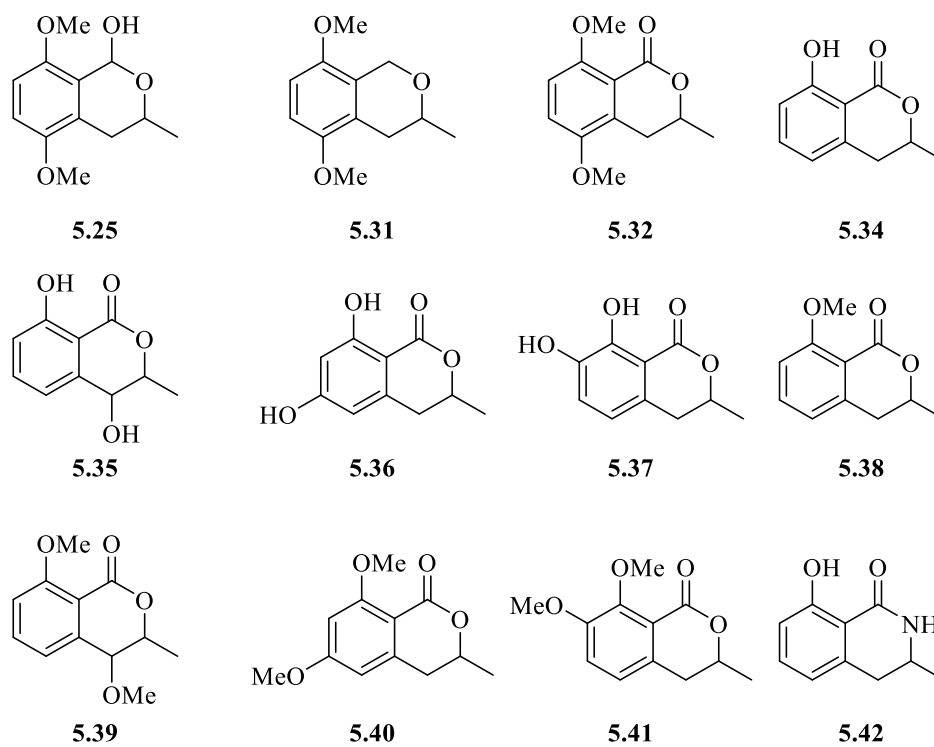
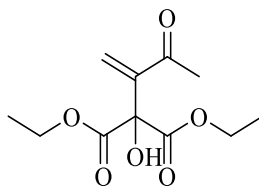


Figure 5.12: Suggested analogues of 5-hydroxymellein.

Chapter 6**6. Experimental Section****6.1. Experimental Information**

Reagents and chemicals were purchased from commercial suppliers (Sigma Aldrich, Alfa Aesar and TCI) and used as received. All air and water sensitive reactions were performed under a nitrogen atmosphere using standard Schlenk line techniques. Solvents were distilled under an atmosphere of nitrogen prior to use. THF, diethyl ether and toluene were distilled from sodium wire in the presence of benzophenone. DCM and toluene were distilled from calcium hydride. Thin layer chromatography (TLC) was visualized with ultraviolet light (UV) ($\lambda = 235$ nm). Melting points were determined in open glass capillary tubes on a Stuart SMP3 melting point apparatus. Infra-red (IR) spectra were obtained as neat samples using a Varian 800 FT-IR Scimitar Series spectrometer scanning from 4000-600 cm^{-1} . Flash column chromatography was used for purification (Merck Kieselgel 60 silica gel). ^1H and ^{13}C NMR spectra were recorded directly with a Jeol ECS-400 MHz spectrometer operating at 399.78 and 100.53 MHz respectively, or Bruker Avance 300 MHz spectrometer operating at 300.13 and 75.47 MHz respectively. Chemical shift are quoted in part per million (ppm) relative to tetramethylsilane (TMS). Mass spectrometry analyses carried out using Micromass LCT Premier Mass Spectrometer in Electron Spray (ES) mode or the EPSRC National Mass Spectrometry Service Centre, Swansea. X-ray diffraction data was obtained on an Oxford Diffraction Gemini.

Diethyl 2-hydroxy-2-(3-oxobut-1-en-2-yl)malonate 2.18

Into a 25 mL round bottom flask, 1,4-diazabicyclo[2.2.2]octane **2.20** (56.08 mg, 0.50 mmol) was dissolved in THF (5 mL) then 3-butene-2-one **2.19** (0.407 mL, 5.00 mmol) and diethyl ketomalonate (0.762 mL, 5.00 mmol) were added respectively. The reaction mixture was stirred for 4 days at room temperature. DCM (25 mL) was added to the reaction mixture, then the organic layer washed with diluted HCl (25 mL, 1M) and sodium bicarbonate (50 mL). Organic layers were combined, dried over anhydrous MgSO₄ and the solvent was evaporated under reduced pressure. The crude material was subjected to silica gel column chromatography (petroleum ether 40/60:diethyl ether 1:1) to give product **2.18** (0.12 g, 0.49 mmol, 98%) as a pale yellow oil.

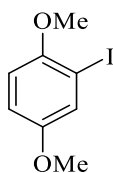
R_f 0.2 (vanillin TLC stain active, petroleum ether 40/60:diethyl ether 1:1).

¹H NMR (300 MHz, CDCl₃) δ_H 6.32 (d, *J* = 1.0 Hz, 1H, C=CH₂), 6.21 (d, *J* = 1.0 Hz, 1H, C=CH₂), 4.42 – 4.21 (q, *J* = 7.1 Hz, 4H, CH₂-CH₃), 2.41 (s, 3H, O=C-CH₃), 1.31 (t, *J* = 7.1 Hz, 6H, CH₂-CH₃).

¹³C NMR (101 MHz, CDCl₃) δ_C 198.06 (H₃C-C=O), 169.02 (O-C=O), 145.42 (C=CH₂), 128.12 (C=CH₂), 79.21 (C-OH), 62.96 (O-CH₂-CH₃), 26.38 (H₃C-C=O), 13.98 (CH₂-CH₃).

MS (ESI) [M+Na]⁺ calculated for C₁₂H₁₈O₆Na: 267.0845, found: 267.0852.

IR (neat): ν_{max}/cm⁻¹ 3445, 2981, 1737, 1633.

2-Iodo-1,4-dimethoxybenzene 2.28

Into a 50 cm³ round bottomed flask, 1,4-dimethoxybenzene **2.29** (0.276 g, 2.00 mmol), (diacetoxyiodo) benzene (0.708 g, 2.20 mmol) and iodine (0.507 g, 2.00 mmol) were dissolved in 5 mL of acetonitrile. The reaction was stirred for 24 hours at room temperature. The reaction mixture was diluted with DCM (10 mL). The organic layer was washed with a saturated solution of sodium thiosulfate (2×15 mL) and brine (15 mL). The combined organic extracts were dried over MgSO₄, filtered and the solvent was removed under reduced pressure. The resulting crude product was purified by silica gel column chromatography (petroleum ether 40/60:diethyl ether 7:3) to give **2.28** (0.410 g, 1.60 mmol, 78%) as a yellow oil.

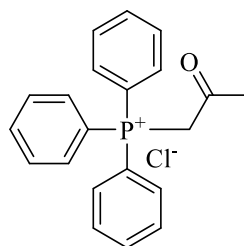
R_f 0.55 (UV active, petroleum ether 40/60:diethyl ether 7:3).

¹H NMR (300 MHz, CDCl₃) δ_H 7.35 (d, *J* = 3.0 Hz, 1H, C³H), 6.87 (dd, *J* = 9.1, 3 Hz, 1H, C⁵H), 6.76 (d, *J* = 9.1 Hz, 1H, C⁶H), 3.83 (s, 3H, O-CH₃), 3.76 (s, 3H, O-CH₃).

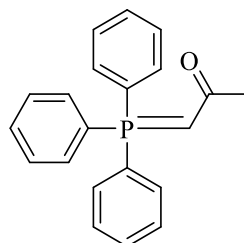
¹³C NMR (101 MHz, CDCl₃) δ_C 154.32 (O-C-CH₃), 152.76 (O-C-CH₃), 124.87 (C-Ar), 114.84 (C-Ar), 111.65 (C-Ar), 86.83 (C-Ar), 57.07(O-CH₃), 56.02 (O-CH₃).

MS (ESI) [M+Na]⁺ calculated for C₈H₉O₂INa: 286.9520, found: 286.9522.

IR (neat): ν_{max}/cm⁻¹ 1607, 1530, 1436.

1-(Triphenylphosphoranylidene)propan-2-one 2.31**(2-Oxopropyl)triphenylphosphonium chloride 2.33**

Into a 250 mL round bottom flask, triphenylphosphine **2.35** (6.55 g, 25.0 mmol) was dissolved in toluene (100 mL). Chloroacetone **2.34** (1.99 mL, 25.0 mmol) was added then the reaction mixture was refluxed for 24 hours. Precipitated phosphonium chloride salt was filtered to give **2.33** (6.88 g, 19.3 mmol, 78%).



Into a 250 mL round bottom flask, phosphonium chloride salt **2.33** (6.88 g, 19.0 mmol) was dissolved in water (100 mL) then DCM (60 mL) was added to the solution. The solution was made alkaline by the dropwise addition of NaOH (25 mL, 1M) then the reaction was stirred for 1 hour. The organic layer was separated and the aqueous layer was washed with DCM (2×25 mL). The organic layers were combined, dried with MgSO₄, filtered and the solvent was removed under reduced pressure to give the desired product **2.31** (6 g, 18.0 mmol, 75%). The product **2.33** (4.86 g, 15.3 mmol, 61%) was recrystallized from toluene (65 mL) as yellow crystals.

mp 210-211°C (lit: 210-211°C).¹¹¹

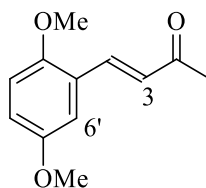
R_f 0.3 (UV active, petroleum ether 40/60:diethyl ether 1:1).

¹H NMR (400 MHz, CDCl₃) δ_H 3.68 (d, 1H, *J*_(P) = 27 Hz), 2.07 (s, 3H), 7.72 – 7.38 (m, 15H).

¹³C NMR (101 MHz, CDCl₃) δ_C 191.00, 133.10, 132.03, 128.95, 127.79, 51.23, 28.66.

MS (ESI) [M+Na]⁺ calculated for C₈H₉O₂INa: 286.9511, found: 286.9514.

IR (neat): ν_{max}/cm⁻¹ 3050, 2989, 1538.

(E)-4-(2,5-Dimethoxyphenyl)but-3-en-2-one 2.30

In a 250 mL round bottom flask, 1-(triphenylphosphoranylidene)propan-2-one **2.31** (1.59 g, 5.00 mmol) was added into a solution of 2,5-dimethoxybenzaldehyde **2.32** (0.83 g, 5.00 mmol) in DCM (50 mL). A drying tube was connected to the condenser then the reaction was refluxed for 48 hours. The reaction mixture was cooled to room temperature then the solvent was removed under reduced pressure. Pre-column (diethyl ether:petroleum ether 40/60 7:3) was used to remove $\text{Ph}_3\text{P}=\text{O}$. Collected fractions was combined then the solvent was removed under reduced pressure. The resulting crude product was purified by silica gel column chromatography (petroleum ether 40/60:diethylether 7:3) to give **2.30** (0.70 g, 3.39 mmol, 68%) as a yellow powder.

mp: 49-50 °C (lit. 48-50 °C).¹¹²

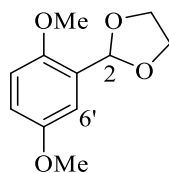
R_f 0.47 (UV active, petroleum ether 40/60 – diethyl ether, 7:3).

¹H NMR (300 MHz, CDCl_3) δ_{H} 7.87 (d, $J = 16.5$ Hz, 1H, C^3H), 7.09 (d, $J = 3.0$ Hz, 1H, C^6H), 6.94 (dd, $J = 9.1, 3.0$ Hz, 1H, C^4H), 6.87 (d, $J = 9.1$ Hz, 1H, C^3H), 6.72 (d, $J = 16.5$ Hz, 1H, C^4H), 3.87 (s, 3H, O- CH_3), 3.80 (s, 3H, O- CH_3), 2.41 (s, 3H, C^1H).

¹³C NMR (101 MHz, CDCl_3) δ_{C} 199.19 (C^2), 153.63 (C^2), 152.83 (C^5), 138.59 (C^3), 127.97 (C^4), 123.92 (C-Ar), 117.69 (C- Ar), 112.59 (C- Ar), 112.49 (C-Ar), 56.16 (O- CH_3), 55.85 (O- CH_3), 27.20 (C^1).

MS (ESI) $[\text{M}+\text{Na}]^+$ calculated for $\text{C}_{12}\text{H}_{14}\text{O}_3\text{Na}$: 229.0801, found: 229.0806.

IR (neat): $\nu_{\text{max}}/\text{cm}^{-1}$ 3004, 2838, 1668.

2-(2,5-Dimethoxyphenyl)-1,3-dioxolane **3.12**

In a 50 cm³ round bottomed flask, 2,5-dimethoxybenzaldehyde **2.32** (0.830 g, 5.00 mmol) and *p*-toluenesulfonic acid monohydrate (50 mg, 0.30 mmol) were dissolved in toluene (15 mL) followed by the addition of ethylene glycol (8.36 mL, 150 mmol). The mixture was refluxed for 4 hours in a Dean-Stark apparatus. The reaction mixture was allowed to cool to room temperature, diluted with ethyl acetate (20 mL). The organic layer was washed with a saturated aqueous solution of Na₂CO₃ (2×10 mL) and brine (20 mL), dried over Na₂SO₄, filtered and the solvents were removed under reduced pressure. The crude material was purified by silica gel column chromatography (petroleum ether 40/60:diethyl ether 7:3) to give product **3.12** (0.901 g, 4.29 mmol, 86%) as a colourless oil.

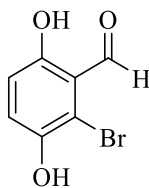
R_f: 0.25 (UV active, petroleum ether 40/60:diethyl ether, 7:3).

¹H NMR (400 MHz, CDCl₃) δ_H 7.11 (d, *J* = 3.0 Hz, 1H, C^{6'}H), 6.86 (dd, *J* = 9.1, 3.0 Hz, 1H, C^{4'}H), 6.82 (d, *J* = 9.1 Hz, 1H, C^{3'}H), 6.12 (s, 1H, C²H), 4.15 – 4.08 (m, 2H, C¹H), 4.08 – 3.99 (m, 2H, C³H), 3.82 (s, 3H, O-CH₃), 3.77 (s, 3H, O-CH₃).

¹³C NMR (101 MHz, CDCl₃) δ_C 153.64 (C^{2'}), 152.02 (C^{5'}), 126.77 (C- Ar), 115.38 (C- Ar), 112.23 (C-Ar), 112.16 (C- Ar), 99.23 (C²), 65.40 (C^{1,3}), 56.38 (O-CH₃), 55.88 (O-CH₃).

MS (ES⁺) calculated for C₁₁H₁₄O₄Na: 210.0936; observed: 233.0942.

IR (neat): ν_{max}/cm⁻¹ 2890, 2998, 2790.

2-Bromo-3,6-dihydroxybenzaldehyde 3.20

In a dark 250 mL round bottom flask, 2,5-dihydroxybenzaldehyde **3.21** (3.453 g, 25.0 mmol) was dissolved in 100 mL of chloroform. Bromine (1.33 mL, 26.0 mmol) was added dropwise over 30 minutes then the reaction was stirred for 2.5 hours at room temperature. The reaction was washed with a saturated solution of Na₂S₂O₃ (8×20 mL) to remove excess bromine. The combined organic layers were separated, dried over Na₂SO₄, filtered then the solvent was removed under reduced pressure to afford product **3.20** (5.403 g, 24.9 mmol, 99%) as a yellow powder.

mp 130-130.5 °C (lit. 123-125 °C).⁷⁹

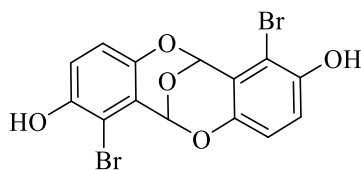
R_f 0.22 (UV active, petroleum ether 40/60 – diethyl ether, 7:3).

¹H NMR (300 MHz, CDCl₃) δ_H 11.67 (s, 1H, O=C-H), 10.29 (s, 1H, OH), 7.26 (d, *J* = 9.1 Hz, 1H, C⁵H), 6.94 (d, *J* = 9.1 Hz, 1H, C⁴H), 5.39 (s, 1H, OH).

¹³C NMR (101 MHz, CDCl₃) δ_C 196.92 (C=O), 158.07 (C⁶), 145.0 (C³), 125.42 (C- Ar), 118.62 (C- Ar), 116.05 (C- Ar), 111.80 (C- Ar).

HRMS (pNSI): calculated for C₇H₅BrO₃: 218.9474; observed: 218.9475.

IR (neat): ν_{max}/cm⁻¹ 3515, 3259, 1633.

1,7-Dibromo-6*H*,12*H*-6,12-epoxydibenzo[*b,f*][1,5]dioxocine-2,8-diol 3.31

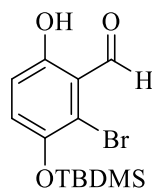
mp 232-233.5 °C.

R_f: 0.2 (UV active, petroleum ether 40/60:diethyl ether 1:1).

¹H NMR (400 MHz, CDCl₃) δ_H 6.98 (d, *J* = 9.1 Hz, 1H), 6.84 (d, *J* = 9.1 Hz, 1H), 6.36 (s, 1H), 5.28 (s, 1H).

¹³C NMR (101 MHz, CDCl₃) δ_C 156.88, 147.38, 131.54, 118.44, 117.23, 108.63, 89.64.

IR (neat): ν_{max}/cm⁻¹ 3407, 1588.

Bromo-3-[[[(1,1-dimethylethyl)dimethylsilyl]oxy]-6-hydroxybenzaldehyde 3.33

Into a 50 mL round bottom flask, 2-bromo-3,5-dihydroxybenzaldehyde **3.20** (1 g, 4.61 mmol) was dissolved in DCM (20 mL). Imidazole (0.470 g, 6.93 mmol) and *tert*-butyldimethylsilyl chloride (0.972 g, 6.54 mmol) were added then the reaction mixture was stirred for 1 hour at room temperature. The reaction mixture was poured into water (20 mL) and the product was extracted with ethyl acetate (2 x 10 mL). Combined organic layers washed with brine (40 mL) dried over MgSO₄ and filtered, then the solvent was removed under reduced pressure. The resulting crude material was purified by silica gel column chromatography (petroleum ether: diethyl ether 25:1) to provide desired product **3.33** (0.626 g, 1.89 mmol, 41%) as a yellow powder.

mp 42-44 °C (lit. 42-45°C).⁷⁹

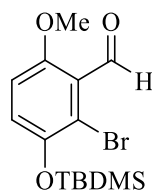
R_f 0.5 (UV active, petroleum ether 40/60 – diethyl ether, 25:1).

¹H NMR (300 MHz, CDCl₃) δ_H 11.73 (s, 1H), 10.39 (s, 1H), 7.09 (d, *J* = 9.1 Hz, 1H), 6.86 (d, *J* = 9.1, 1H), 1.07 (s, 9H), 0.26 (s, 6H).

¹³C NMR (101 MHz, CDCl₃) δ_C 198.39, 176.45, 158.47, 129.23, 118.66, 118.01, 117.64, 25.82, 18.43, -4.09.

MS (ESI) [M+Na]⁺ calculated for C₁₃H₁₉BrO₃SiNa: 331.2801, found: 331.2804.

IR (neat): ν_{max}/cm⁻¹ 3307, 2928, 1651, 1462.

2-Bromo-3-((tert-butyldimethylsilyloxy)-6-methoxybenzaldehyde 3.34

In a Schlenk flask, 2-bromo-3-((*tert*-butyl dimethylsilyloxy)-6-hydroxybenzaldehyde **3.33** (0.331 g, 1.00 mmol) was dissolved in THF (10 mL). Potassium carbonate (2.764 g, 20 mmol) and methyl iodide (0.184 mL, 3.00 mmol) were added then the reaction was heated at 40 °C for 24 hours. The reaction mixture was poured into water (20 mL) and the product was extracted with ethyl acetate (2 x 20 mL). The combined organics extracts were washed with brine (50 mL), dried over anhydrous MgSO₄, filtered and the solvent was removed under reduced pressure. The resulting crude material was purified by silica gel column chromatography (petroleum ether 40/60: diethyl ether 7:3) to give **3.34** (0.201 g, 0.58 mmol, 58%) as a white powder.

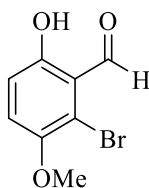
mp 68-69.5 °C (lit. 67-69 °C).⁷⁹

R_f 0.47 (UV active, petroleum ether 40/60:diethyl ether 7:3).

¹H NMR (300 MHz, CDCl₃) δ_H 10.15 (s, 1H), 6.80 (d, *J* = 9.1 Hz, 1H), 6.62 (d, *J* = 9.1 Hz, 1H), 3.63 (s, 3H), 0.81 (s, 9H), 0.01 (s, 6H).

¹³C NMR (101 MHz, CDCl₃) δ_C 191.16, 155.83, 147.11, 124.73, 118.03, 114.81, 111.56, 56.63, 25.85, 18.47, -4.12.

IR (neat): ν_{max}/cm⁻¹ 2945, 2927, 1695.

2-Bromo-6-hydroxy-3-methoxybenzaldehyde 3.35

In a 100 mL round bottom flask, 2-bromo-3,6-dihydroxybenzaldehyde **3.20** (0.217 g, 1.00 mmol) was dissolved in methanol (30 mL). Sodium methoxide (0.118 g, 2.20 mmol) and methyl iodide (0.124 mL, 2.20 mmol) were added then the reaction was refluxed for 24 hours. Methanol was removed under reduced pressure to give black residue. The resulting residue dissolved in ethyl acetate (10 mL), and then the organic layer was washed with water (10 mL). The organic layer dried over anhydrous MgSO_4 , filtered then the solvent was removed under reduced pressure. The crude was purified by silica gel chromatography (petroleum ether 40/60: diethyl ether 4:1) to give **3.35** (18 mg, 0.08 mmol, 8%) as yellow crystals.

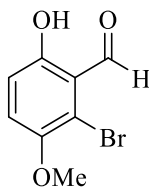
mp 75-76.5 °C.

R_f 0.6 (UV active, petroleum ether 40/60:diethyl ether 4:1).

¹H NMR (300 MHz, CDCl_3) δ_{H} 11.59 (s, 1H), 10.43 (s, 1H), 7.20 (d, $J = 9.1$ Hz, 1H), 6.96 (d, $J = 9.1$, 1H), 3.91 (s, 3H).

¹³C NMR (101 MHz, CDCl_3) δ_{C} 198.5, 157.9, 149.6, 123.4, 117.9, 117.5, 116.4, 57.5.

IR (neat): $\nu_{\text{max}}/\text{cm}^{-1}$ 2840, 1650, 1560, 1467, 1280, 1170.

2-Bromo-6-hydroxy-3-methoxybenzaldehyde 3.35

In a Schlenk flask, 2-bromo-3,6-dihydroxybenzaldehyde **3.30** (0.217 g, 1.00 mmol) and trimethyloxonium tetrafluoroborate (0.477 g, 3.20 mmol) were dissolved in DCM (5 mL). At 0 °C, *N,N*-diisopropylethylamine (0.52 mL, 3.00 mmol) was added. The reaction mixture was allowed to stir for 36 hours at room temperature. The mixture was diluted with DCM (10 mL), washed with saturated solution of sodium bicarbonate (2×15 mL). The combined organic layers were washed with brine (15 mL), dried over MgSO₄, filtered and the solvent was removed under reduced pressure. The resulting crude material was purified by silica gel column chromatography (petroleum ether 40/60:diethyl ether 4:1) to produce **3.35** (0.104 g, 0.38 mmol, 45%) as a yellow powder.

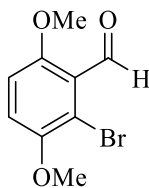
mp 75-76.5 °C.

R_f 0.5 (UV active, petroleum ether 40/60:diethyl ether 1:1).

¹H NMR (300 MHz, CDCl₃) δ_H 11.59 (s, 1H), 10.43 (s, 1H), 7.20 (d, *J* = 9.1 Hz, 1H), 6.96 (d, *J* = 9.1, 1H), 3.91 (s, 3H).

¹³C NMR (101 MHz, CDCl₃) δ_C 198.5, 157.9, 149.6, 123.4, 117.9, 117.5, 116.4, 57.5.

IR (neat): ν_{max}/cm⁻¹ 3352, 1560.

2-Bromo-3,6-dimethoxybenzaldehyde 3.19

In a Schlenk flask, 2-bromo-3,6-dihydroxybenzaldehyde **3.30** (3.255 g, 15.0 mmol), potassium carbonate (41.46 g, 300 mmol) and tetrabutylammonium bromide (0.483 g, 1.50 mmol) were dissolved in THF (150 mL). Methyl iodide (5.58 mL, 90.0 mmol) and DMF (15 mL) were added and the reaction was stirred for 24 hours at 40 °C. The reaction mixture was cooled down and filtered through sintered glass. The filtrate was washed with water (75 mL) and the product was extracted with DCM (2×75 mL). The combined organic layers were dried over Na₂SO₄, filtered and the solvents were removed under reduced pressure. The crude material was subjected to silica gel column chromatography (petroleum ether 40/60:diethyl ether 1:1) to give **3.19** (2.752 g, 11.2 mmol, 75 %) as colourless crystals.

mp 101-102 °C.

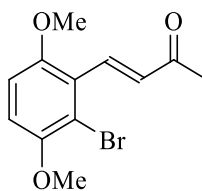
R_f 0.5 (UV active, petroleum ether 40/60:diethyl ether 1:1).

¹H NMR (300 MHz, CDCl₃) δ_H 10.34 (s, 1H), 6.96 (d, *J* = 9.1 Hz, 1H), 6.86 (d, *J* = 9.1 Hz, 1H), 3.82 (s, 3H), 3.81 (s, 3H).

¹³C NMR (101 MHz, CDCl₃) δ_C 191.00, 155.48, 150.47, 124.76, 117.20, 114.71, 111.52, 57.24, 56.66.

HRMS (pNSI): calculated for C₉H₉BrO₃: [M+H]⁺: 246.9787; observed: 246.9786.

IR (neat): ν_{max}/cm⁻¹ 2930, 2837, 1689.

(E)-4-(2-Bromo-3,6-dimethoxyphenyl)but-3-en-2-one 3.36

In a Schlenk flask, 2-bromo-3,6-dimethoxybenzaldehyde **3.19** (1 g, 4.10 mmol) and 1-(triphenylphosphoranylidene)propan-2-one **2.31** (1.439 g, 4.55 mmol) were dissolved in DCM (25 mL). The mixture was refluxed for 60 hours. The resulting reaction mixture was cooled, filtered and the solvent was removed under reduced pressure. The resulting crude material was purified by silica gel (petroleum ether 40/60:diethyl ether 1:1) to give **3.36** (1.123 g, 3.93 mmol, 94 %) as a pale yellow powder.

mp 110-112 °C.

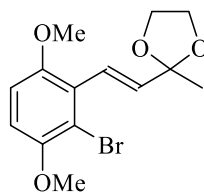
R_f 0.275 (UV active, petroleum ether 40/60:diethyl ether 1:1).

¹H NMR (300 MHz, CDCl₃) δ_H 7.85 (d, *J* = 16.5 Hz, 1H), 7.04 (d, *J* = 16.5 Hz, 1H), 6.91 (d, *J* = 9.1 Hz, 1H), 6.87 (d, *J* = 9.1 Hz, 1H), 3.88 (s, 3H), 3.85 (s, 3H), 2.42 (s, 3H).

¹³C NMR (101 MHz, CDCl₃) δ_C 199.72, 153.62, 150.53, 139.28, 133.70, 124.61, 116.79, 113.12, 110.44, 57.01, 56.13, 27.03.

HRMS (pNSI): calculated for C₁₂H₁₄BrO₃ [M+H]⁺: 286.0155; observed: 286.0154.

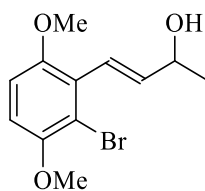
IR (neat): ν_{max}/cm⁻¹ 2998, 2836, 1565, 1253.

(E)-2-(2-Bromo-3,6-dimethoxystyryl)-2-methyl-1,3-dioxolane 3.37

Into a 50 cm³ round bottomed flask, (*E*)-4-(2-bromo-3,6-dimethoxyphenyl)but-3-en-2-one **3.36** (44.7 mg, 0.16 mmol) was dissolved in toluene (5 mL). *p*-Toluenesulfonic acid monohydrate (3.00 mg, 0.01 mmol) and ethylene glycol (0.043 mL, 0.78 mmol) were added then the mixture was refluxed for 4 hours in a Dean-Stark apparatus. The reaction mixture was allowed to cool to room, diluted with DCM (10 mL), washed with a saturated solution of Na₂CO₃ (2×15 mL). The combined organics were washed with brine (15 mL), dried over MgSO₄, filtered and the solvent was removed under reduced pressure. The resulting crude material was purified by silica gel chromatography (petroleum ether 40/60:diethyl ether 7:3) to give **3.37** (5 mg, 0.02 mmol, 13%) as a colourless oil.

R_f 0.4 (UV active, petroleum ether 40/60 : diethyl ether 1:1).

¹H NMR (300 MHz, CDCl₃) δ_H 6.89 (d, *J* = 16.5 Hz, 1H), 6.81 (d, *J* = 7.0 Hz, 2H), 6.36 (d, *J* = 16.5 Hz, 1H), 4.04 (m, *J* = 0.9 Hz, 4H), 3.87 (s, 3H), 3.81 (s, 3H), 1.61 (s, 3H).

(E)-4-(2-Bromo-3,6-dimethoxyphenyl)but-3-en-2-ol 3.38

In a Schlenk flask, (*E*)-4-(2-bromo-3,6-dimethoxyphenyl)but-3-en-2-one **3.36** (0.558 g, 1.94 mmol) was dissolved in toluene (10 mL). At -78 °C, diisobutylaluminum hydride solution (0.42 mL, 1.0 M in toluene, 0.42 mmol) was added dropwise to the solution and then the reaction was allowed to stir for 3 hours. The reaction was poured into a mixture of ice and saturated solution of NH₄Cl (10 mL). The phases were separated, and the aqueous layer was washed with DCM (2×10 mL). The combined organic extracts were washed with brine (25 mL), dried over MgSO₄, filtered and the solvent was removed under reduced pressure. The residue was purified by silica gel column chromatography (petroleum ether 40/60: diethyl ether 1:1) to produce **3.38** (0.526 mg, 1.83 mmol, 94%) as a white crystalline powder.

mp 69.5-71°C.

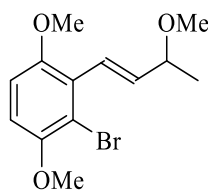
R_f 0.475 (UV active, petroleum ether 40/60:diethyl ether 1:2).

¹H NMR (300 MHz, CDCl₃) δ_H 6.84 (d, *J* = 9.1 Hz, 1H), 6.78 (d, *J* = 9.1 Hz, 1H), 6.72 (d, *J* = 16.1, 1H), 6.52 (dd, *J* = 16.1, 6.3 Hz, 1H), 4.53 (dq, *J* = 6.4, 1.1 Hz, 1H), 3.87 (s, 3H), 3.82 (s, 3H), 1.41 (d, *J* = 1.1 Hz, 3H).

¹³C NMR (101 MHz, CDCl₃) δ_C 152.47, 150.47, 140.83, 127.21, 124.37, 115.08, 110.85, 110.43, 69.65, 56.89, 56.24, 23.26.

HRMS (pNSI): calculated for C₁₂ H₁₅ BrO₃ Na: [M+Na]⁺: 311.0075; observed: 311.0076.

IR (neat): ν_{max}/cm⁻¹ 3382, 2968, 1565.

(E)-4-(2-Bromo-3,6-dimethoxyphenyl)but-3-en-2-ol 3.39

In a Schlenk flask, (*E*)-4-(2-bromo-3,6-dimethoxyphenyl)but-3-en-2-one **3.36** (76.4 mg, 0.18 mmol) was dissolved in toluene (10 mL). At -78 °C, diisobutylaluminum hydride solution (0.032 mL, 1.0 M in toluene, 0.03 mmol) was added dropwise to the solution then the reaction was allowed to stir for 3 hours. The reaction was poured into a mixture of cold methanol (10 mL) and 1.0 M of HCl (10 mL). The phases were separated, and the aqueous layer was washed with DCM (2×10 mL). The combined organic extracts were washed with brine (25 mL), dried over MgSO₄, filtered and the solvent was removed under reduced pressure. The crude reaction material was purified by silica gel column chromatography (petroleum ether 40/60:diethyl ether 1:1) to afford titled compound (30.50 mg, 0.10 mmol, 38%) as colourless crystals.

mp 80.5-82 °C.

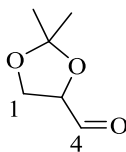
R_f 0.6 (UV active, petroleum ether 40/60:diethyl ether 1:1).

¹H NMR (300 MHz, CDCl₃) δ_H 6.84 (d, *J* = 9.1 Hz, 1H), 6.79 (d, *J* = 9.1 Hz, 1H), 6.72 (d, *J* = 16.1 Hz, 1H), 6.52 (dd, *J* = 16.1, 6.3 Hz, 1H), 4.53 (m, *J* = 6.3, 1.1 Hz, 1H), 3.87 (s, 3H), 3.82 (s, 3H), 1.41 (d, *J* = 1.1 Hz, 3H).

¹³C NMR (101 MHz, CDCl₃) δ_C 152.60, 150.51, 138.77, 127.47, 126.54, 115.01, 110.57, 110.52, 79.03, 56.97, 56.38, 56.24, 21.62.

HRMS (pNSI): calculated for C₁₃ H₁₇ BrO₃ Na [M+Na]⁺: 323.0253; observed: 323.0253.

IR (neat): ν_{max}/cm⁻¹ 2835, 1569, 1474.

(±)-2,2-Dimethyl-1,3-dioxolane-4-carbaldehyde 4.13

In a Schlenk flask, oxalyl chloride (0.5 mL, 5.50 mmol) was dissolved in DCM (3 mL). At -78 °C, a solution of methyl sulfoxide (0.9 mL, 12.0 mmol) in DCM (5 mL) was added. The reaction mixture was allowed to stir for 15 minutes. (±)-(2,2-Dimethyl-1,3-dioxolan-4-yl)methanol **4.14** (0.6 mL, 5.00 mmol) was added then the reaction was stirred for additional 15 minutes at -78 °C. Triethylamine (3.5 mL, 25.0 mmol) was added and the reaction was warmed to room temperature. The reaction was quenched with an aqueous solution of NH₄Cl (10 mL), the phases were separated, and the aqueous layer was extracted with DCM (2×10 mL). The combined organic extracts were washed with brine (20 mL), dried over MgSO₄, filtered and the solvent was removed under reduced pressure. The resulting residue was purified by silica gel column chromatography (petroleum ether 40/60:diethyl ether 2:1) to produce **4.13** (0.110 g, 0.84 mmol, 17%) as a colourless oil.

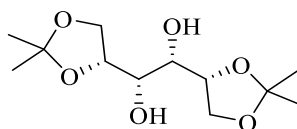
R_f 0.4 (UV active, petroleum ether 40/60: ethyl acetate 3:2).

¹H NMR (300 MHz, CDCl₃) δ_H 9.75 (d, *J* = 1.9 Hz, 1H, C⁴H), 4.41 (ddd, *J* = 7.1, 4.8, 1.9 Hz, 1H, C³H), 4.20 (d, *J* = 8.8, 7.1 Hz, 1H, C¹H), 4.13 (dd, *J* = 8.8, 4.8 Hz, 1H, C¹H), 1.51 (s, 3H, CH₃), 1.44 (s, 3H, CH₃).

¹³C NMR (101 MHz, CDCl₃) δ_C 201.95 (C⁴), 111.36 (C²), 79.92 (C³), 65.66 (C¹), 26.32 (C²-CH₃), 25.21 (C²-CH₃).

HRMS (pNSI): calculated for C₆H₁₀O₃: [M+H]⁺: 131.0703; observed: 131.0702.

IR (neat): ν_{max}/cm⁻¹ 3326, 2980, 1381.

1,2:5,6-Di-*O*-isopropylidene-D-mannitol 4.21

In a Schlenk flask, at 0 °C, D-mannitol **4.22** (1.821 g, 10.0 mmol) was added to a suspension of zinc chloride (2.896 g, 21.3 mmol) in acetone (18 mL), then the reaction was warmed to room temperature. After 24 hours, potassium carbonate (3.109 g, 22.5 mmol) was added then the reaction was vigorously stirred at 0 °C. The resulting suspension was filtered, extracted with ethyl acetate (2×4 mL), and the organic filtrate was washed with water (15 mL). The combined organic layers were washed with saturated solution of NaHCO₃ and brine (25 mL), dried over Na₂SO₄ and the solvents was removed under reduced pressure. The desired product **4.21** was recrystallized from cyclohexane (1.2525 g, 4.78 mmol, 48 %) as white crystals.

mp 120-121.5 °C. (lit.119.5-121 °C).¹¹³

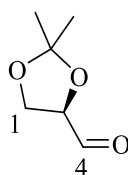
R_f 0.3 (UV active, petroleum ether 40/60:ethyl acetate 2:3).

¹H NMR (300 MHz, CDCl₃) δ_H 4.27 – 4.11 (m, 4H), 3.99 (dd, *J* = 8.4, 5.5 Hz, 2H), 3.77 (t, *J* = 6.2 Hz, 2H), 2.58 (d, *J* = 6.6 Hz, 2H), 1.44 (s, 6H), 1.38 (s, 6H).

¹³C NMR (101 MHz, CDCl₃) δ_C 109.47, 76.37, 71.28, 66.81, 26.80, 25.27.

HRMS (pNSI): calculated for C₁₂H₂₂O₆: [M-H]⁻:261.1344; observed: 261.1340.

IR (neat): ν_{max}/cm⁻¹ 3388, 2980, 1381.

(R)-(-)-2,2-Dimethyl-1,3-dioxolane-4-carbaldehyde (R)-4.13

In a Schlenk flask, 1,2:5,6-Di-*O*-isopropylidene-D-mannitol **4.21** (1.242 g, 4.73 mmol) and sodium periodate (2.026 g, 9.47 mmol) were dissolved in DCM (10 mL). Saturated aqueous solution of sodium bicarbonate (0.51 mL) was added then the reaction was allowed to stir for 2 hours at room temperature. Next, Na₂SO₄ was added then the reaction was stirred for 5 minutes. The reaction mixture was filtered through a sintered glass to a pre-weighted round bottomed flask then the residue was washed with DCM (2×4 mL). The desired product **(R)-4.13** was obtained from DCM using a short bath distillation at 40 °C under atmospheric pressure (1.230 g, 9.45 mmol, 99%) as a colourless oil.

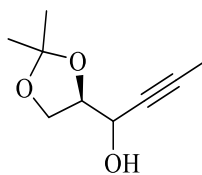
R_f 0.4 (UV active, petroleum ether 40/60: ethyl acetate 3:2).

¹H NMR (300 MHz, CDCl₃) δ_H 9.75 (d, *J* = 1.9 Hz, 1H, C⁴H), 4.41 (ddd, *J* = 7.1, 4.8, 1.9 Hz, 1H, C³H), 4.20 (d, *J* = 8.8, 7.1 Hz, 1H, C¹H), 4.13 (dd, *J* = 8.8, 4.8 Hz, 1H, C¹H), 1.51 (s, 3H, CH₃), 1.44 (s, 3H, CH₃).

¹³C NMR (101 MHz, CDCl₃) δ_C 201.95 (C⁴), 111.36 (C²), 79.92 (C³), 65.66 (C¹), 26.32 (C²-CH₃), 25.21 (C²-CH₃).

HRMS (pNSI): calculated for C₆H₁₀O₃: [M+H]⁺: 131.0703; observed: 131.0702.

IR (neat): ν_{max}/cm⁻¹ 3326, 2980, 1381.

1-(2,2-Dimethyl-1,3-dioxolan-4-yl)but-2-yn-1-ol 4.12

In a Schlenk flask, (*R*)-(-)-2,2-dimethyl-1,3-dioxolane-4-carbaldehyde (**R**)-**4.13** (1.224 g, 9.40 mmol) was dissolved in THF (30 mL). 1-Propynylmagnesium bromide solution 0.5 M in THF (37.6 mL, 18.81 mmol) was added at 0 °C then the reaction was warmed to room temperature. After 12 hours, the reaction was quenched with a saturated solution of NH₄Cl (30 mL) and diluted with DCM (30 mL). The organic layer was separated, then the aqueous layer was washed with DCM (30 mL). The combined organics were washed with brine (60 mL), dried over Na₂SO₄, filtered and the solvent was removed under reduced pressure. The crude material was purified by silica gel column chromatography (3:2 petroleum ether 40/60:diethyl ether) to give **4.12** (1 g, 5.87 mmol, 63%) as a brown oil.

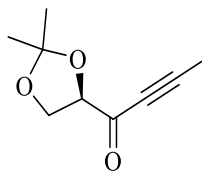
R_f 0.25 (UV active, petroleum ether 40/60:diethyl ether 3:2).

¹H NMR (300 MHz, CDCl₃) ¹H NMR (300 MHz), δ_H 4.40-3.34 (m, 1H), 4.23 – 3.94 (m, 4H), 1.79 (d, *J* = 2.1 Hz, 3H), 1.40 (s, 3H), 1.31 (s, 3H).

¹³C NMR (101 MHz, CDCl₃) δ_C 110.30, 82.42, 82.25, 76.98, 66.22, 64.31, 26.67, 26.32, 3.59.

HRMS (pNSI): calculated for C₉H₁₄O₃: [M+H]⁺: 171.1016; observed: 171.1013.

IR (neat): ν_{max}/cm⁻¹ 3388.

1-(2,2-Dimethyl-1,3-dioxolan-4-yl)but-2-yn-1-one 4.11

In a Schlenk flask, oxalyl chloride (0.095 mL, 1.09 mmol) was dissolved in DCM (5 mL). DMSO (0.07 mL, 1.00 mmol) was added to the solution at $-78\text{ }^{\circ}\text{C}$ then the reaction was stirred for 10 minutes. 1-(2,2-Dimethyl-1,3-dioxolan-4-yl)but-2-yn-1-ol **4.12** (0.155 g, 0.91 mmol) was dissolved in DCM (5 mL) and transferred with a cannula to the reaction mixture. After 15 minutes, triethylamine (0.63 mL, 4.55 mmol) was added and the reaction was stirred for 1.5 hours at room temperature. The reaction was quenched with ammonium chloride solution (10 mL). The organic layer was separated and the aqueous layer was washed with DCM (10 mL). Combined organic layers were washed with brine (20 mL), dried over Na_2SO_4 and the solvent was removed under reduced pressure to give **4.11** (0.153 g, 1.0 mmol, 100%) as a colourless oil.

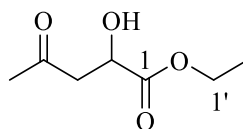
R_f 0.3 (UV active, petroleum ether 40/60:diethyl ether 3:2).

¹H NMR (300 MHz, CDCl_3) δ_{H} 4.47 (dd, $J = 7.4, 5.0$ Hz, 1H), 4.18 (dd, $J = 8.8, 7.4$ Hz, 1H), 4.09 (dd, $J = 8.8, 5.0$ Hz, 1H), 2.02 (s, 3H), 1.45 (d, $J = 0.8$ Hz, 3H), 1.35 (s, 3H).

¹³C NMR (101 MHz, CDCl_3) δ_{C} 186.75, 111.78, 95.42, 80.99, 78.34, 66.78, 26.11, 25.49, 4.47.

HRMS (pNSI): calculated for $\text{C}_9\text{H}_{12}\text{O}_3$: $[\text{M}+\text{H}]^+$: 169.0859 ; observed: 169.0856.

IR (neat): $\nu_{\text{max}}/\text{cm}^{-1}$ 2989, 1671.

Ethyl 2-hydroxy-4-oxopentanoate 4.16

Acetone **4.18** (2 mL, 43.5 mmol), Ethyl glyoxalate solution ~50% in toluene **4.17** (0.86 mL, 8.70 mmol) and water (0.2 mL) were added in a round bottomed flask 50 cm³. Pyrrolidine (0.2 mL, 2.64 mmol) was added then the reaction was stirred for 12 hours at room temperature. The reaction mixture was diluted with DCM (10 mL). The separated organic layer was washed with water (2×10 mL) and brine (10 mL), dried over Na₂SO₄ and the solvent was removed under reduced pressure. The resulting crude material was purified by silica gel column chromatography (ethyl acetate: petroleum ether 40/60 2:1) to give **4.16** (0.195 g, 1.21 mmol, 14%) as a colourless oil.

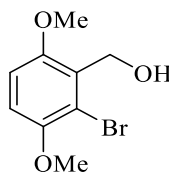
R_f 0.3 (UV active, petroleum ether 40/60:ethyl acetate 1:2).

¹H NMR (300 MHz, CDCl₃) δ_H 4.52 – 4.41 (m, 1H, C²H), 4.24 (q, *J* = 7.1 Hz, 2H, C¹H), 2.98 (dd, *J* = 17.4, 4.1 Hz, 1H, C³H), 2.89 (dd, *J* = 17.4, 6.3 Hz, 1H, C³H), 2.20 (s, 3H, C⁵H), 1.28 (t, *J* = 7.1 Hz, 2H, C²H).

¹³C NMR (101 MHz, CDCl₃) δ_C 206.32 (C⁴), 173.72 (C¹), 66.98 (C²), 61.95 (C¹'), 46.87 (C³), 30.58 (C⁵), 14.17 (C²').

HRMS (pNSI): calculated for C₇H₁₂O₄: [M+H]⁺: 161.0808 ; observed: 161.0804.

IR (neat): ν_{max}/cm⁻¹ 3433, 1715.

(2-Bromo-3,6-dimethoxyphenyl)methanol 4.24

In a Schlenk flask, 2-bromo-3,6-dimethoxybenzaldehyde **3.19** (0.550 g, 2.26 mmol) was dissolved in toluene (20 mL). At -78 °C, diisobutylaluminum hydride solution (3.40 mL, 1.0 M in toluene, 3.40 mmol) was added dropwise to the solution and the reaction was allowed to stir for 3 hours. The reaction was poured into a mixture of ice and a saturated solution of ammonium chloride (20 mL). The phases were separated, and the aqueous layer was washed with DCM (2×20 mL). The combined organic extracts were washed with brine (40 mL), dried over MgSO₄, filtered and the solvent was removed under reduced pressure to provide **4.24** (0.54 g, 2.18 mmol, 97%) as a white crystalline powder.

mp 124-125.5 °C (lit. 127-128°C).¹¹⁴

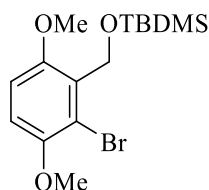
R_f 0.25 (UV active, petroleum ether 40/60:diethyl ether 1:1).

¹H NMR (300 MHz, CDCl₃) δ_H 6.85 (s, 2H), 4.94 (s, 2H), 3.88 (s, 3H), 3.86 (s, 3H).

¹³C NMR (101 MHz, CDCl₃) δ_C 152.72, 150.44, 130.05, 115.21, 111.71, 110.12, 60.66, 56.98, 56.36.

HRMS (pNSI): calculated for C₉H₁₀ BrO₂: [M-OH]⁺: 230.9838; observed: 230.9837.

IR (neat): ν_{max}/cm⁻¹ 3272.

((2-Bromo-3,6-dimethoxybenzyl)oxy)(*tert*-butyl)dimethylsilane 4.23

In a Schlenk flask, imidazole (0.983 g, 14.5 mmol) and *tert*-butyldimethylsilyl chloride (2.179 g, 14.4 mmol) were dissolved in DCM (25 mL) then (2-bromo-3,6-dimethoxyphenyl)methanol **4.24** (1.19 g, 4.82 mmol) was added. The reaction was stirred for 12 hours at room temperature. The reaction mixture was washed with water (25 mL) and extracted with DCM (25 mL). Combined organic extracts washed with brine (30 mL), dried over MgSO₄ and the solvent was removed under reduced pressure. The resulting crude material was purified with silica gel column chromatography (petroleum ether 40/60:diethyl ether 1:2) to give **4.23** (0.404 g, 1.10 mmol, 98%) as a white powder.

mp 73-75°C.

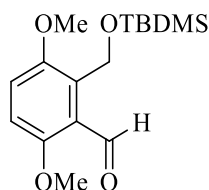
R_f 0.4 (UV active, petroleum ether 40/60:diethyl ether 1:2).

¹H NMR (400 MHz, CDCl₃) δ_H 6.80 (s, 2H), 4.87 (s, 2H), 3.83 (s, 3H), 3.79 (s, 3H), 0.90 (s, 9H), 0.09 (s, 6H).

¹³C NMR (101 MHz, CDCl₃) δ_C 152.93, 150.55, 130.42, 116.56, 111.75, 110.84, 59.87, 56.93, 56.75, 26.10, 18.69, -5.09.

HRMS (pNSI): calculated for C₁₅H₂₅BrO₃Si: [M+Na]⁺: 384.0674; observed: 384.0683.

IR (neat): ν_{max}/cm⁻¹ 2971, 1255.

2-(((*tert*-butyldimethylsilyl)oxy)methyl)-3,6-dimethoxybenzaldehyde **4.5**

In a Schlenk flask, ((2-bromo-3,6-dimethoxybenzyl)oxy)(*tert*-butyl)dimethylsilane **4.23** (0.824 g, 2.28 mmol) was dissolved in THF (20 mL). At $-78\text{ }^{\circ}\text{C}$ *n*-butyllithium 2.5 M in hexane (1.36 mL, 3.42 mmol) was added dropwise and the reaction was stirred for 30 minutes. *N,N*-dimethylformamide (0.9 mL, 11.4 mmol) was added then the reaction was stirred for additional 30 minutes at room temperature. The reaction was quenched with cold water (20 mL). The aqueous layer was washed with DCM (2×20 mL). The combined organic extracts were washed with brine (40 mL), dried over MgSO_4 and the solvent was removed under reduced pressure. The resulting crude material was purified by silica gel column chromatography (petroleum ether 40/60:diethyl ether 7:3) to give **4.5** (0.29 g, 0.96 mmol, 42%) as colourless crystals.

mp 58.5-61 $^{\circ}\text{C}$.

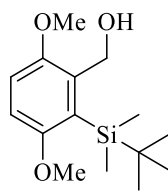
R_f 0.425 (UV active, petroleum ether 40/60:diethyl ether 7:3).

¹H NMR (400 MHz, CDCl_3) δ_{H} 10.51 (s, 1H), 7.01 (d, $J = 9.1$ Hz, 1H), 6.87 (d, $J = 9.1$ Hz, 1H), 4.98 (s, 2H), 3.83 (s, 3H), 3.80 (s, 3H), 0.87 (s, 9H), 0.06 (s, 6H).

¹³C NMR (101 MHz, CDCl_3) δ_{C} 192.86, 155.04, 151.43, 131.34, 125.60, 116.90, 111.74, 56.84, 56.37, 55.40, 26.03, 18.57, -5.27.

HRMS (pNSI): calculated for $\text{C}_{16}\text{H}_{26}\text{O}_4$: $[\text{M}+\text{H}]^+$: 283.1724; observed: 283.1727.

IR (neat): $\nu_{\text{max}}/\text{cm}^{-1}$ 2928, 1651, 1462.

(2-(*tert*-butyldimethylsilyl)-3,6-dimethoxyphenyl)methanol 5.13

In a Schlenk flask, ((2-bromo-3,6-dimethoxybenzyl)oxy)(*tert*-butyl)dimethylsilane **4.23** (0.120 g, 0.33 mmol) was dissolved in THF (10 mL). At $-78\text{ }^{\circ}\text{C}$, *n*-butyllithium 2.5 M in hexane (0.14 mL, 0.34 mmol) was added dropwise and the reaction was stirred for 25 minutes. Propylene oxide (0.04 mL, 0.50 mmol) was then added and the reaction was stirred for 2 hours at room temperature. The reaction was quenched with cold water (15 mL) and the product was extracted with DCM ($2\times 15\text{ mL}$). Combined organic extracts were washed with brine (30 mL), dried over MgSO_4 and the solvent was removed under reduced pressure. The resulting crude was purified by silica gel column chromatography (petroleum ether 40/60:diethyl ether 3:2) to give **5.13** (92.4 mg, 0.33 mmol, 99%) as a white powder.

mp 63.5-65 $^{\circ}\text{C}$.

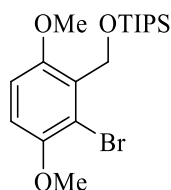
R_f 0.3 (UV active, petroleum ether 40/60:diethyl ether 3:2).

$^1\text{H NMR}$ (300 MHz, CDCl_3) δ_{H} 6.91 (d, $J = 9.1\text{ Hz}$, 1H), 6.77 (d, $J = 9.1\text{ Hz}$, 1H), 4.70 (s, 2H), 3.87 (s, 3H), 3.71 (s, 3H), 0.94 (s, 9H), 0.40 (s, 6H).

$^{13}\text{C NMR}$ (101 MHz, CDCl_3) δ_{C} 158.96, 152.77, 136.39, 127.09, 112.12, 109.77, 61.37, 55.80, 55.25, 27.24, 18.29, 0.09.

HRMS (pNSI): calculated for $\text{C}_{16}\text{H}_{26}\text{O}_4$: $[\text{M}+\text{Na}]^+$: 305.1543; observed: 305.1544.

IR (neat): $\nu_{\text{max}}/\text{cm}^{-1}$ 3591.

((2-Bromo-3,6-dimethoxybenzyl)oxy)triisopropylsilane 5.17

In a Schlenk flask, imidazole (0.408 g, 6 mmol), triisopropylsilyl chloride (1.27 mL, 6 mmol) and (2-bromo-3,6-dimethoxyphenyl)methanol **4.24** (0.494 g, 2 mmol) were dissolved in DCM (15 mL). The reaction was stirred for 18 hours at room temperature. The reaction mixture was washed with water (15 mL) and the product was extracted with DCM (2×15 mL). Combined organic extracts were washed with brine (30 mL), dried over MgSO₄ and the solvent was removed under reduced pressure. The resulting crude product was purified by silica gel column chromatography (petroleum ether 40/60:diethyl ether 10:1) to give **5.17** (0.650 g, 1.61 mmol, 81%) as colourless crystals.

mp 87-88°C.

R_f 0.3 (UV active, petroleum ether 40/60:diethyl ether 10:1).

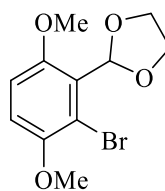
¹H NMR (400 MHz, CDCl₃) δ_H 6.80 (s, 2H), 4.95 (s, 2H), 3.84 (s, 3H), 3.78 (s, 3H), 1.19-1.11 (m, 3H), 1.09 (s, 18H).

¹³C NMR (101 MHz, CDCl₃) δ_C 152.86, 150.44, 130.52, 116.68, 111.61, 110.35, 59.93, 56.92, 56.34, 18.10, 12.27.

HRMS (pNSI): calculated for C₁₈H₃₁BrO₃Si: [M+H]⁺: 403.1299; observed: 403.1300.

IR (neat): ν_{max}/cm⁻¹ 2938, 2864, 1460.

2-(2-Bromo-3,6-dimethoxyphenyl)-1,3-dioxolane 5.21



In a 50 cm³ round bottomed flask, 2-bromo-3,6-dimethoxybenzaldehyde (0.192 g, 0.78 mmol) **3.19**, ethylene glycol (1.30 mL, 23.5 mmol) and *p*-toluenesulfonic acid monohydrate (29.7 mg, 0.16 mmol) were dissolved in toluene (10 mL). The reaction was refluxed for 4 hours. The reaction mixture was washed with water (10 mL) and the organic layer was extracted with DCM (2×10 mL). Combined organic layers washed with brine (20 mL), dried over Mg₂SO₄ and the solvent was removed under reduced pressure. The resulting crude material was purified by silica gel column chromatography (petroleum ether 40/60:diethyl ether: 1:2) to give **5.21** (0.180 g, 0.62 mmol, 80%) as a pale yellow oil.

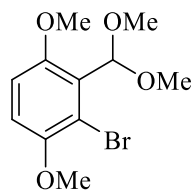
R_f 0.3 (UV active, petroleum ether 40/60:diethyl ether 2:1).

¹H NMR (300 MHz, CDCl₃) δ_H 6.91 (d, *J* = 9.1 Hz, 1H), 6.87 (d, *J* = 9.1 Hz, 1H), 6.53 (s, 1H), 4.35 – 4.22 (m, 2H), 4.10 – 4.03 (m, 2H), 3.85 (s, 3H), 3.82 (s, 3H).

¹³C NMR (101 MHz, CDCl₃) δ_C 153.90, 150.68, 125.36, 117.20, 113.53, 111.77, 101.99, 66.12, 57.18, 56.94.

HRMS (pNSI): calculated for C₁₁H₁₃BrO₄: [M+H]⁺: 290.0104; observed: 290.0101.

IR (neat): ν_{max}/cm⁻¹ 2868, 2837, 1481.

2-Bromo-3-(dimethoxymethyl)-1,4-dimethoxybenzene 5.23

In a 50 cm³ round bottomed flask, 2-bromo-3,6-dimethoxybenzaldehyde **3.19** (0.267 g, 1.09 mmol) and *p*-toluenesulfonic acid monohydrate (36 mg, 0.108 mmol) were dissolved in methanol (10 mL). Trimethyl orthoformate (1.19 mL, 10.89 mmol) was added then the reaction was allowed to stir for 12 hours at room temperature. The reaction mixture was washed with water (20 mL), and the aqueous layer was washed with DCM (2×20 mL). The combined organic extracts were washed with brine (40 mL), dried over MgSO₄, filtered and the solvent was removed to give **5.23** (0.315 g, 1.01 mmol, 99%) as a white crystalline powder.

mp 75-77.5 °C.

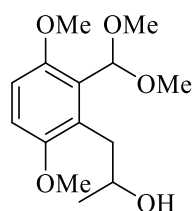
R_f 0.25 (UV active, petroleum ether 40/60:diethyl ether 1:1).

¹H NMR (400 MHz, CDCl₃) δ_H 6.85 (d, *J* = 9.1 Hz, 1H, C⁶-H), 6.84 (d, *J* = 9.1 Hz, 1H, C⁵-H), 5.85 (s, 1H, O-CH-O), 3.83 (s, 3H, Ar-OCH₃), 3.81 (s, 3H, Ar-OCH₃), 3.47 (s, 3H, CH-OCH₃), 3.46 (s, 3H, CH-OCH₃).

¹³C NMR (101 MHz, CDCl₃) δ_C 153.09 (C¹), 150.58 (C⁴), 127.15 (C-Ar), 114.08 (C-Ar), 112.59 (C-Ar), 111.98 (C-Ar), 105.08 (O-CH-O), 57.19 (Ar-OCH₃), 57.10 (Ar-OCH₃), 56.20 (CH-OCH₃), 53.52 (CH-OCH₃).

HRMS (pNSI): calculated for C₁₁H₁₅ BrO₄: [M-OH]⁺: 230.9838; observed: 230.9837.

IR (neat): ν_{max}/cm⁻¹ 2931, 2837, 1687.

1-(2-(Dimethoxymethyl)-3,6-dimethoxyphenyl)propan-2-ol 5.24

In a Schlenk flask, 2-bromo-3-(dimethoxymethyl)-1,4-dimethoxybenzene **5.23** (0.501 g, 1.75 mmol) was dissolved in THF (20 mL). *n*-Butyllithium (0.84 mL, 2.11 mmol) was added dropwise and the reaction was stirred at -78 °C for 20 minutes. Propylene oxide (1.2 mL, 17.5 mmol) was added and the reaction was stirred for 30 hours. The reaction was quenched with saturated solution of NH₄Cl (20 mL) and the product was extracted with DCM (2×20 mL). Combined organic extracts were washed with brine (40 mL), dried over Na₂SO₄ and the solvent was removed under reduced pressure. The resulting crude material was purified by silica gel column chromatography (0.138 g, 0.61 mmol, 36%) as a white powder.

mp 83-85 °C.

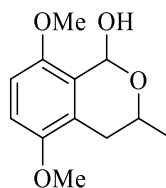
R_f 0.5 (UV active, petroleum ether 40:60 /ether, 1:1).

¹H NMR (300 MHz, CDCl₃) δ_H 6.83 (d, *J* = 9.1 Hz, 1H), 6.75 (d, *J* = 9.1 Hz, 1H), 4.24 (ddq, 9.6, 6.1, 2.8 Hz, 1H), 3.79 (s, 6H), 3.55 (s, 3H), 3.39 (s, 3H), 3.21 (dd, *J* = 13.8, 9.6 Hz, 1H), 3.04 (dd, *J* = 13.8, 2.8 Hz, 1H), 1.31 (d, *J* = 6.1 Hz, 3H).

¹³C NMR (101 MHz, CDCl₃) δ_C 150.95, 150.61, 124.78, 123.79, 109.82, 108.35, 95.37, 62.04, 56.20, 55.78, 55.29, 50.86, 29.99, 21.48.

HRMS (pNSI): calculated for C₁₄H₂₂O₅: [M+Na]⁺: 293.1359; observed: 293.1358.

IR (neat): ν_{max}/cm⁻¹ 3354, 2904.

5,8-Dimethoxy-3-methylisochroman-1-ol 5.25

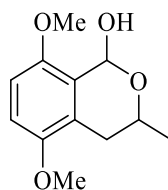
In a round bottomed flask 50 cm³, 1-(2-(dimethoxymethyl)-3,6-dimethoxyphenyl)propan-2-ol **5.24** (170 mg, 0.63 mmol) was dissolved in DCM (5 mL) followed by the addition of water (0.12 mL, 6.28 mmol). Trifluoroacetic acid (0.2 mL, 1.66 mmol) was added then the reaction was stirred for 30 minutes at room temperature. The reaction was washed with an aqueous solution of NaHCO₃ (2×10 mL). Combined organic layers were washed with brine (20 mL), dried over Na₂SO₄ and the solvent was removed under reduced pressure. The resulting crude material was purified by silica gel column chromatography (UV active, petroleum ether 40/60: diethyl ether 1:1) to give **5.25** (39 mg, 0.18 mmol, 28%) as a mixture of colourless oil and crystals.

R_f 0.275 (UV active, petroleum ether 40/60:diethyl ether 1:1).

¹H NMR (300 MHz, CDCl₃) δ_H 6.83 (d, *J* = 9.1 Hz, 1H), 6.75 (d, *J* = 9.1 Hz, 1H), 5.88 (s, 1H), 4.02 (ddq, *J* = 9.6, 6.1, 2.8 Hz, 1H), 3.79 (s, 6H), 3.55 (s, 3H), 3.39 (s, 3H), 3.21 (dd, *J* = 13.8, 9.6 Hz, 1H), 3.04 (dd, *J* = 13.8, 2.8 Hz, 1H), 1.30 (d, *J* = 6.1 Hz, 3H).

¹³C NMR (75 MHz, CDCl₃) δ_C 150.89, 149.09, 126.40, 123.88, 108.05, 107.21, 69.01, 63.05, 55.62, 47.59, 29.78, 21.74.

IR (neat): ν_{max}/cm⁻¹ 3421.

5,8-Dimethoxy-3-methylisochroman-1-ol 5.25

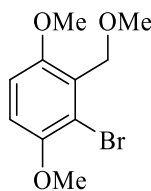
In a round bottomed flask 50 cm³, 1-(2-(dimethoxymethyl)-3,6-dimethoxyphenyl)propan-2-ol **5.24** (60 mg, 0.22 mmol) was dissolved in acetone (5 mL). Iodine was added (5.63 mg, 0.02 mmol) and the reaction was stirred for 45 minutes at room temperature. The reaction was quenched with an aqueous solution of Na₂S₂O₃ (10 mL) and the product was extracted with DCM (2×10 mL). Combined organic extracts were washed with brine (20 mL), dried over Na₂SO₄ and the solvent was removed under reduced pressure. The resulting crude material was purified by silica gel column chromatography (UV active, petroleum ether 40/60:diethyl ether 1:1) to give **5.25** (85 mg, 0.19 mmol, 89%) as a mixture of colourless oil and crystals.

R_f 0.275 (UV active, petroleum ether 40/60:diethyl ether 1:1).

¹H NMR (300 MHz, CDCl₃) δ_H 6.83 (d, *J* = 9.1 Hz, 1H), 6.75 (d, *J* = 9.1 Hz, 1H), 5.88 (s, 1H), 4.02 (ddq, *J* = 9.6, 6.1, 2.8 Hz, 1H), 3.79 (s, 6H), 3.55 (s, 3H), 3.39 (s, 3H), 3.21 (dd, *J* = 13.8, 9.6 Hz, 1H), 3.04 (dd, *J* = 13.8, 2.8 Hz, 1H), 1.30 (d, *J* = 6.1 Hz, 3H).

¹³C NMR (75 MHz, CDCl₃) δ_C 150.89, 149.09, 126.40, 123.88, 108.05, 107.21, 69.01, 63.05, 55.62, 47.59, 29.78, 21.74.

IR (neat): ν_{max}/cm⁻¹ 3419.

2-Bromo-1,4-dimethoxy-3-(methoxymethyl)benzene 5.28

In a Schlenk flask, (2-bromo-3,6-dimethoxyphenyl)methanol **4.24** (0.121 g, 0.49 mmol) and NaH 60% in mineral oil (39.16 mg, 0.98 mmol) were dissolved in THF (10 mL). Methyl iodide (0.60 mL, 0.98 mmol) was added and the reaction was stirred for 12 hours at room temperature. The reaction was quenched with water (15 mL) and the product was extracted with DCM (2×15 mL). Combined organic extracts were washed with brine (25 mL), dried over Na₂SO₄, filtered and the solvent was removed under reduced pressure. The resulting crude product was purified by silica gel column chromatography (petroleum ether 40/60:diethyl ether 1:2) to give **5.28** (0.112 g, 0.43 mmol, 88%) as a white crystalline powder.

mp 61-62.5 °C.

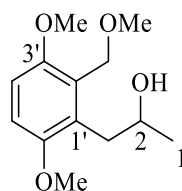
R_f 0.5 (UV active, petroleum ether 40:60 /ether, 1:1).

¹H NMR (300 MHz, CDCl₃) δ_H 6.79 (d, *J* = 9.1 Hz, 1H), 6.74 (d, *J* = 9.1 Hz, 1H), 4.62 (s, 2H), 3.77 (s, 3H), 3.74 (s, 3H), 3.35 (s, 3H).

¹³C NMR (101 MHz, CDCl₃) δ_C 153.32, 150.46, 127.45, 117.12, 112.40, 110.37, 68.20, 58.50, 57.02, 56.64.

HRMS (pNSI): calculated for C₁₄H₂₂O₅: [M+NH₄]⁺: 278.0386; observed: 278.0383.

IR (neat): ν_{max}/cm⁻¹ 2970, 2837, 1065.

1-(3,6-Dimethoxy-2-(methoxymethyl)phenyl)propan-2-ol **5.29**

In a Schlenk flask, 2-bromo-1,4-dimethoxy-3-(methoxymethyl)benzene **5.28** (0.466g, 1.78 mmol) was dissolved in THF (20 mL). *n*-Butyllithium (1.1 mL, 2.67 mmol) was added dropwise at -78 °C then the reaction was stirred for 20 minutes. Propylene oxide (0.6 mL, 8.92 mmol) was added then the reaction was warmed to room temperature. After 4 hours, the reaction was quenched with a saturated solution of NH₄Cl (20 mL). The aqueous layer was washed with DCM (2×20 mL) and the combined organic extracts were washed with brine (20 mL), dried over MgSO₄ and solvent was removed under reduced pressure. The crude reaction mixture was purified by silica gel column chromatography (petroleum ether 40/60:diethyl ether 1:2) to give **5.29** (0.335 g, 1.39 mmol, 78%) as colourless crystals.

mp 58.5-61 °C.

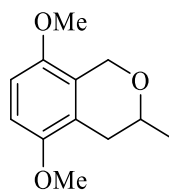
R_f 0.3 (UV active, petroleum ether 40/60:diethyl ether 1:2).

¹H NMR (400 MHz, CDCl₃) δ_H 6.80 (d, *J* = 9.1 Hz, 1H, C⁴H), 6.74 (d, *J* = 9.1 Hz, 1H, C⁵H), 4.72 (d, *J* = 10.2 Hz, 1H, H₂C-OCH₃), 4.39 (d, *J* = 10.2 Hz, 1H, H₂C-OCH₃), 3.97 (ddq, *J* = 9.6, 6.1, 2.8 Hz, 1H, C²H), 3.78 (s, 3H, Ar-OCH₃), 3.77 (s, 3H, Ar-OCH₃), 3.41 (s, 3H, CH₂-OCH₃), 3.02 (dd, *J* = 13.8, 2.8 Hz, 1H, C³H), 2.63 (dd, *J* = 13.8, 9.6 Hz, 1H, C³H), 1.28 (d, *J* = 6.1 Hz, 3H, C¹H).

¹³C NMR (101 MHz, CDCl₃) δ_C 152.24 (C^{3'}), 152.17 (C^{6'}), 129.99 (C-Ar), 125.96 (C-Ar), 110.98 (C-Ar), 109.28 (C-Ar), 67.38 (H₂C-OCH₃), 64.90 (C²), 58.21 (Ar-OCH₃), 56.33 (Ar-OCH₃), 55.85 (H₂C-OCH₃), 36.54 (C³), 24.58 (C¹).

HRMS (pNSI): calculated for C₁₃H₂₁O₄: [M+H]⁺: 241.1434; observed: 241.1428.

IR (neat): ν_{max}/cm⁻¹ 3422, 2932.

5,8-Dimethoxy-3-methylisochromane 5.31

In a Schlenk flask, 1-(3,6-dimethoxy-2-(methoxymethyl)phenyl)propan-2-ol **5.29** (50 mg, 0.21 mmol) was dissolved in DCM (5 mL). Boron tribromide solution 1.0 M in hexane (0.2 mL, 0.23 mmol) was added at -78 °C. After 30 minutes the reaction was quenched into a mixture of ice and water (10 mL). The product was extracted with DCM (2×10 mL) and the combined organic extracts were washed with brine (25 mL), dried over MgSO₄ and the solvent was removed under reduced pressure to give **5.31** (43 mg, 0.206 mmol, 99%) as a dark red oil.

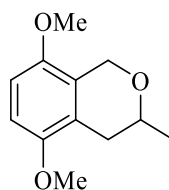
R_f 0.35 (UV, petroleum ether 40/60:diethyl ether 1:1).

¹H NMR (300 MHz, CDCl₃) δ_H 6.85 (d, *J* = 9.1 Hz, 1H), 6.76 (d, *J* = 9.1 Hz, 1H), 4.76 (d, *J* = 9.7 Hz, 1H), 4.70 (d, *J* = 9.7 Hz, 1H), 4.10 (dq, *J* = 9.6, 6.2, 2.8 Hz, 1H), 3.87 (s, 3H), 3.81 (s, 3H), 2.99 (dd, *J* = 13.9, 2.8 Hz, 1H), 2.91 (dd, *J* = 13.9, 9.6 Hz, 1H), 1.32 (d, *J* = 6.2 Hz, 3H).

¹³C NMR (101 MHz, CDCl₃) δ_C 152.14, 151.95, 128.30, 126.61, 111.47, 109.52, 68.34, 56.25, 55.98, 35.83, 26.32, 23.89.

HRMS (pNSI): calculated for C₁₂H₁₆O₃: [M+H]⁺: 209.1172; observed: 209.1172.

IR (neat): ν_{max}/cm⁻¹ 2931.

5,8-Dimethoxy-3-methylisochromane 5.31

In a Schlenk flask, NaI (124.7 mg, 0.83 mmol) was dissolved in acetonitrile (5 mL) and water (0.187 mL, 0.01 mmol), and the reaction was stirred for 30 minutes at 40 °C. Chlorotrimethylsilane (0.1 mL, 0.832 mmol) was added and the reaction was stirred for 30 minutes. A solution of 1-(3,6-dimethoxy-2-(methoxymethyl)phenyl)propan-2-ol (50 mg, 0.21 mmol) **5.29** in acetonitrile (1 mL) was transferred by a cannula to the reaction mixture. After 2 hours, the reaction was cooled down to room temperature, washed with a saturated solution of Na₂S₂O₃ (10 mL) and the product was extracted with DCM (2×10 mL). The combined organic extracts were washed with brine (20 mL), dried over MgSO₄ and the solvent was removed under reduced pressure to give **5.31** (40.4 mg, 0.20 mmol, 97%) as a dark red oil.

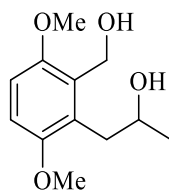
R_f 0.35 (UV, petroleum ether 40/60:diethyl ether 1:1).

¹H NMR (300 MHz, CDCl₃) δ_H 6.85 (d, *J* = 9.1 Hz, 1H), 6.76 (d, *J* = 9.1 Hz, 1H), 4.76 (d, *J* = 9.7 Hz, 1H), 4.70 (d, *J* = 9.7 Hz, 1H), 4.10 (dq, *J* = 9.6, 6.2, 2.8 Hz, 1H), 3.87 (s, 3H), 3.81 (s, 3H), 2.99 (dd, *J* = 13.9, 2.8 Hz, 1H), 2.91 (dd, *J* = 13.9, 9.6 Hz, 1H), 1.32 (d, *J* = 6.2 Hz, 3H).

¹³C NMR (101 MHz, CDCl₃) δ_C 152.14, 151.95, 128.30, 126.61, 111.47, 109.52, 68.34, 56.25, 55.98, 35.83, 26.32, 23.89.

HRMS (pNSI): calculated for C₁₂H₁₆O₃: [M+H]⁺: 209.1172; observed: 209.1172.

IR (neat): ν_{max}/cm⁻¹ 2935.

1-(2-(Hydroxymethyl)-3,6-dimethoxyphenyl)propan-2-ol **5.30**

In a Schelenk flask, 5,8-dimethoxy-3-methylisochromane **5.31** (43.5 mg, 0.21 mmol) and manganese dioxide (0.544 g, 5.26 mmol) were dissolved in DCM (10 mL). The reaction mixture was stirred for 12 hours at room temperature. Then, the reaction was filtered and the residual solid material was washed with DCM (10 mL) then the solvent was removed under reduced pressure. The resulting crude material was purified by silica gel column chromatography to give **5.30** (16.3 mg, 0.07 mmol, 34%) as a pale yellow oil.

R_f 0.5 (UV, petroleum ether 40/60:diethyl ether 1:1).

$^1\text{H NMR}$ (400 MHz, CDCl_3) δ_{H} 6.64 (d, $J = 9.1$ Hz, 1H), 6.60 (d, $J = 9.1$ Hz, 1H), 4.91 (d, $J = 15.9$ Hz, 1H), 4.60 (d, $J = 15.9$ Hz, 1H), 3.77 (s, 3H), 3.75 (s, 3H), 3.70 (ddq, $J = 12.2, 6.1, 3.0$ Hz, 1H), 2.76 (dd, $J = 17.0, 3.0$ Hz, 1H), 2.37 (dd, $J = 17.0, 12.2$ Hz, 1H), 1.35 (d, $J = 6.1$ Hz, 3H).

$^{13}\text{C NMR}$ (101 MHz, CDCl_3) δ_{C} 150.95, 149.53, 124.78, 124.05, 107.50, 106.84, 70.15, 64.66, 30.39, 21.78.

IR (neat): $\nu_{\text{max}}/\text{cm}^{-1}$ 3424, 3320.

References

- 1 M. Butler and A. Buss, *Biochem. Pharmacol.*, 2006, **71**, 919–929.
- 2 S. E. Cosgrove, *Clin. Infect. Dis.*, 2006, **42 Suppl 2**, S82–89.
- 3 T. Frieden, *Antibiotic Resistance Threats in the United States, 2013.*, Centers for disease Control and Prevention, Atlanta, 2013.
- 4 S. C. Davies, *Infections and the Rise of Antimicrobial Resistance. Annual Report of the Chief Medical Officer, Volume 2*, London, 2011.
- 5 World Health Organization, <http://www.who.int/mediacentre/factsheets/fs194/en/>, (accessed June 2015).
- 6 K. Schwab, *Global Risks 2014*, World Economic Forum, Geneva, 2014.
- 7 European Centre for Disease Prevention and Control, *The Bacterial Challenge: Time to React*, ECDC/EMEA Joint Techniacl Report, Stockholm, 2009.
- 8 A. Morse, *Reducing Healthcare Associated Infection in Hospitals in England*, National Audit Office, London, 2009.
- 9 B. Griffiths and I. D. Anderson, *Surg.*, 2009, **27**, 446–449.
- 10 M. E. Hibbing, C. Fuqua, M. R. Parsek and S. B. Peterson, *Nat. Rev. Microbiol.*, 2010, **8**, 15–25.
- 11 G. Tortora, B. Funke and C. Case, *Microbiology: An Introduction*, Pearson, San Francisco, 8th edn., 2004.
- 12 C. Walsh, *Antibiotics: Actions, Origins, Resistance*, American Society for Microbiology, Washington, 2003.
- 13 J. Clardy, M. A. Fischbach and C. T. Walsh, *Nat. Biotechnol.*, 2006, **24**, 1541–1550.
- 14 R. Subramani and W. Aalbersberg, *Microbiol. Res.*, 2012, **167**, 571–80.
- 15 M. A. Kohanski, D. J. Dwyer and J. J. Collins, *Nat. Rev. Microbiol.*, 2010, **8**, 423–435.
- 16 D. J. Newman and G. M. Cragg, *J. Nat. Prod.*, 2012, **75**, 311–35.
- 17 B. Wilson, A. Salyers, D. Whitt and M. Winkler, *Bacterial Pathogenesis: A Molecular Approach*, American Society for Microbiology, Washington, 3rd edn., 2010.
- 18 D. J. Newman, G. M. Cragg and K. M. Snader, *Nat. Prod. Rep*, 2000, **17**, 215–234.
- 19 K. B. Raper, D. F. Alexander and R. D. Coghill, *J. Bacteriol.*, 1944, **48**, 639–659.
- 20 I. Chopra and M. Roberts, *Microbiol. Mol. Biol. Rev.*, 2001, **65** (2) 232–260.

- 21 C. Hu and Y. Zou, *Mini Rev. Med. Chem.*, 2009, **9**, 1397–1406.
- 22 M. S. Butler, M. A. Blaskovich and M. A. Cooper, *J. Antibiot. (Tokyo)*, 2013, **66**, 571–591.
- 23 C. T. Walsh and T. A. Wencewicz, *J. Antibiot. (Tokyo)*, 2014, **67**, 7–22.
- 24 L. L. Ling, T. Schneider, A. J. Peoples, A. L. Spoering, I. Engels, B. P. Conlon, A. Mueller, T. F. Schäberle, D. E. Hughes, S. Epstein, M. Jones, L. Lazarides, V. A. Steadman, D. R. Cohen, C. R. Felix, K. A. Fetterman, W. P. Millett, A. G. Nitti, A. M. Zullo, C. Chen and K. Lewis, *Nature*, 2015, **517**, 455–459.
- 25 S. B. Levy, *Sci. Am.*, 1998, **278**, 46–53.
- 26 J. M. A. Blair, M. A. Webber, A. J. Baylay, D. O. Ogbolu and L. J. V. Piddock, *Nat. Rev. Microbiol.*, 2014, **13**, 42–51.
- 27 H. Nikaido, *Annu Rev Biochem.*, 2010, 119–146.
- 28 A. J. Alanis, *Arch. Med. Res.*, 2005, **36**, 697–705.
- 29 J. G. Lawrence, *Curr. Opin. Microbiol.*, 1999, **2**, 519–523.
- 30 S. B. Levy and B. Marshall, *Nat. Med.*, 2004, **10**, S122–S129.
- 31 G. D. Wright, *BMC Biol.*, 2010, **8**, 123.
- 32 S. B. Levy, *Antimicrob. Agents Chemother.*, 1992, **36**, 695–703.
- 33 G. D. Wright, *Chem. Commun.*, 2011, **47**, 4055–4061.
- 34 P. F. McDermott, R. D. Walker and D. G. White, *Int. J. Toxicol.*, **22**, 135–143.
- 35 B. H. Normark and S. Normark, *J. Intern. Med.*, 2002, **252**, 91–106.
- 36 Davies, J., & Davies, D., *Microbiol. Mol. Biol. Rev.*, 2010, **74**, 417–433.
- 37 L. B. Rice, *J. Infect. Dis.*, 2008, **197**, 1079–1081.
- 38 World Health Organization, <http://www.who.int/mediacentre/factsheets/fs104/en/>, (accessed June 2015).
- 39 World Health Organization Europe, <http://www.euro.who.int/en/health-topics/communicable-diseases/tuberculosis/tuberculosis>, (accessed June 2015).
- 40 A. Zumla, P. Nahid and S. T. Cole, *Nat. Rev. Drug Discov.*, 2013, **12**, 388–404.
- 41 World Health Organization, http://www.who.int/tb/challenges/mdr/mdr_tb_factsheet.pdf, (accessed June 2015).
- 42 M. Li, X. Du, A. E. Villaruz, B. A. Diep, D. Wang, Y. Song, Y. Tian, J. Hu, F. Yu, Y. Lu and M. Otto, *Nat. Med.*, 2012, **18**, 816–819.
- 43 P. C. Appelbaum, *Clin. Microbiol. Infect.*, 2006, **12 Suppl 1**, 16–23.
- 44 G. Morales, J. J. Picazo, E. Baos, F. J. Candel, A. Arribi, B. Peláez, R. Andrade, M.-A. de la Torre, J. Fereres and M. Sánchez-García, *Clin. Infect. Dis.*, 2010, **50**,

- 821–825.
- 45 J. O'Neill, *Rev. Antimicrob. Resist.*, 2014, 1–16.
- 46 A. M. Rimando (ed.) and S. R. Bareson (ed.), *Polyketides: Biosynthesis, Biological Activity, and Genetic Engineering*, American Chemical Society, San Diego, 2007.
- 47 K. J. Weissman and P. F. Leadlay, *Nat. Rev. Microbiol.*, 2005, **3**, 925–936.
- 48 J. Staunton and K. J. Weissman, *Nat. Prod. Rep.*, 2001, **18**, 380–416.
- 49 C. Hertweck, *Angew. Chem. Int. Ed. Engl.*, 2009, **48**, 4688–4716.
- 50 H. Iwaki, Y. Nakayama, M. Takahashi, S. Uetsuki, M. Kido and Y. Fukuyama, *J. Antibiot. (Tokyo)*, 1984, **37**, 1091–1093.
- 51 X. Yan, K. Probst, A. Linnenbrink, M. Arnold, T. Paululat, A. Zeeck and A. Bechthold, *Chem. Bio. Chem.*, 2012, **13**, 224–230.
- 52 D. Komagata, R. Sawa, N. Kinoshita, C. Imada, T. Sawa, H. Naganawa, M. Hamada, Y. Okami and T. Takeuchi, *J. Antibiot. (Tokyo)*, 1992; **45** (10), 1681–1683
- 53 X. Yan, PhD thesis, The Albert Ludwig University of Freiburg, 2012.
- 54 J. G. Allen and S. J. Danishefsky, *J. Am. Chem. Soc.*, 2001, **123**, 351–352.
- 55 K. Yamamoto, M. F. Hentemann, J. G. Allen and S. J. Danishefsky, *Chem. Eur. J.*, 2003, **9**, 3242–3252.
- 56 L. H. Mejorado and T. R. R. Pettus, *J. Am. Chem. Soc.*, 2006, **128**, 15625–15631.
- 57 D. Basavaiah, P. Dharma Rao and R. S. Hyma, *Tetrahedron*, 1996, **52**, 8001–8062.
- 58 D. Basavaiah, A. J. Rao and T. Satyanarayana, *Chem. Rev.*, 2003, **103**, 811–892.
- 59 K. Morita, Z. Suzuki and H. Hirose, *Bull. Chem. Soc. Jpn.*, 1968, **41**, 2815–2815.
- 60 L. R. Reddy, P. Saravanan and E. J. Corey, *J. Am. Chem. Soc.*, 2004, **126**, 6230–6231.
- 61 D. Basavaiah and V. V. L. Gownswari, *Synth. Commun.*, 1989, **19**, 2461–2465.
- 62 R. F. Heck, *J. Am. Chem. Soc.*, 1968, **90**, 5538–5542.
- 63 A. de Meijere and F. E. Meyer, *Angew. Chemie Int. Ed. English*, 1995, **33**, 2379–2411.
- 64 T. G. Crisp, *Chem. Soc. Rev.*, 1998, **27**, 427–436.
- 65 N. J. Whitcombe, K. K. Hii and S. E. Gibson, *Tetrahedron*, 2001, **57**, 7449–7476.
- 66 I. P. Beletskaya and A. V. Cheprakov, *Chem. Rev.*, 2000, **100**, 3009–3066.
- 67 M. R. Netherton and G. C. Fu, *Org. Lett.*, 2001, **3**, 4295–4298.
- 68 M. C. Carreño, J. García Ruano, G. Sanz, M. A. Toledo and A. Urbano, *Tetrahedron Lett.*, 1996, **37**, 4081–4084.
- 69 T. Yamamoto, K. Toyota and N. Morita, *Tetrahedron Lett.*, 2010, **51**, 1364–1366.

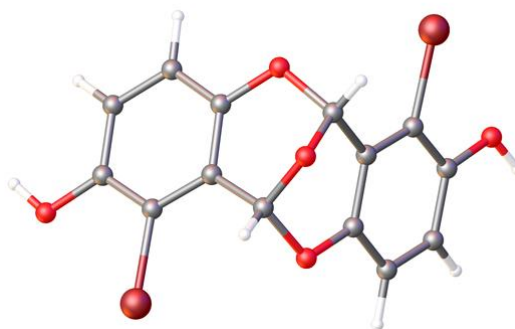
- 70 R. Akue-Gedu, E. Debiton, Y. Ferandin, L. Meijer, M. Prudhomme, F. Anizon and P. Moreau, *Bioorganic Med. Chem.*, 2009, **17**, 4420–4424.
- 71 N. N. Karade, G. B. Tiwari, D. B. Huple and T. a. J. Siddiqui, *J. Chem. Res.*, 2006, **2006**, 366–368.
- 72 G. Sartori, Giovanni; Bigi, Franca; Goffredi, Gino; Maggi, Raimondo; Portioli, Roberto; Casnati, *J. Chem. Res. Miniprint*, 1993, **8**, 2061–2079.
- 73 M. Lautens, K. Fagnou and D. Yang, *J. Am. Chem. Soc.*, 2003, **125**, 14884–14892.
- 74 B. H. Lipshutz, *Chem. Rev.*, 1986, **86**, 795–819.
- 75 V. Snieckus, *Chem. Rev.*, 1990, **90**, 879–933.
- 76 K. Sato, N. Asao and Y. Yamamoto, *J. Org. Chem.*, 2005, **70**, 8977–8981.
- 77 J. Blatchly and J. McOmie, *Org. React.*, 1972, **19**, 199.
- 78 W. P. Almeida and C. R. D. Correia, *Tetrahedron Lett.*, 1994, **35**, 1367–1370.
- 79 C. Li, R. P. Johnson and J. A. Porco, *J. Am. Chem. Soc.*, 2003, **125**, 5095–5106.
- 80 X. Lei and J. A. Porco, *J. Am. Chem. Soc.*, 2006, **128**, 14790–14791.
- 81 Y. Hu, C. Li, B. A. Kulkarni, G. Strobel, E. Lobkovsky, R. M. Torczynski and J. A. Porco, *Org. Lett.*, 2001, **3**, 1649–1652.
- 82 K. Takao, R. Nanamiya, Y. Fukushima, A. Namba, K. Yoshida and K. Tadano, *Org. Lett.*, 2013, **15**, 5582–5585.
- 83 K. B. Borisenko, K. Zauer and I. Hargittai, *J. Phys. Chem.*, 1996, **100**, 19303–19309.
- 84 U. S. Hiremath, *Tetrahedron Lett.*, 2013, **54**, 3419–3423.
- 85 J. Li, *Name Reactions: A Collection of Detailed Mechanisms and Synthetic Applications Fifth Edition*, Springer Science & Business Media, Cham, 2014.
- 86 G. Stork and T. Takahashi, *J. Am. Chem. Soc.*, 1977, **99**, 1275–1276.
- 87 S. De Bernardo, J. P. Teng, G. J. Sasso and M. Weigele, *J. Org. Chem.*, 1985, **50**, 3457–3462.
- 88 R. Schobert and C. Jagusch, *J. Org. Chem.*, 2005, **70**, 6129–6132.
- 89 J. H. Hong, C.-H. Oh and J.-H. Cho, *Tetrahedron*, 2003, **59**, 6103–6108.
- 90 D. R. Borchering, S. Narayanan, M. Hasobe, J. G. McKee, B. T. Keller and R. T. Borchardt, *J. Med. Chem.*, 1988, **31**, 1729–1738.
- 91 R. S. Tipson and A. Cohen, *Carbohydr. Res.*, 1968, **7**, 232–243.
- 92 A. E. Leyes and C. D. Poulter, *Org. Lett.*, 1999, **1**, 1067–1070.
- 93 J. Mulzer and G. Funk, *Synthesis-Stuttgart.*, 1995, **1995**, 101–112.
- 94 M. A. de Alvarenga, R. B. Fo, O. R. Gottlieb, J. P. de P. Dias, A. F. Magalhães, E.

- G. Magalhães, G. C. de Magalhães, M. T. Magalhães, J. G. S. Maia and R. Marques, *Phytochemistry*, 1978, **17**, 511–516.
- 95 M. Devys, M. Barbier, J.-F. Bousquet and A. Kollmann, *Phytochemistry*, 1994, **35**, 825–826.
- 96 S.-H. Wu, Y.-W. Chen and C.-P. Miao, *Chem. Nat. Compd.*, 2011, **47**, 858–861.
- 97 C. Jiménez-Romero, E. Ortega-Barría, A. E. Arnold and L. Cubilla-Rios, *Pharm. Biol.*, 2009, **46**, 700–703.
- 98 L. M. Harwood, *J. Chem. Soc. Chem. Commun.*, 1982, 1120.
- 99 W. H. Moser, *Tetrahedron*, 2001, **57**, 2065–2084.
- 100 J. L. Speier, *J. Am. Chem. Soc.*, 1952, **74**, 1003–1010.
- 101 P. G. M. Wuts and T. W. Greene, *Greene's Protective Groups in Organic Synthesis*, John Wiley & Sons, Hoboken, 2006.
- 102 D. L. J. Clive and M. Yu, *Chem. Commun.*, 2002, 2380–2381.
- 103 J. Sun, Y. Dong, L. Cao, X. Wang, S. Wang and Y. Hu, *J. Org. Chem.*, 2004, **69**, 8932–8934.
- 104 G. A. Olah, A. Husain, B. G. B. Gupta and S. C. Narang, *Angew. Chemie Int. Ed. English*, 1981, **20**, 690–691.
- 105 U. Zutter, H. Iding, P. Spurr and B. Wirz, *J. Org. Chem.*, 2008, **73**, 4895–902.
- 106 E. Lee-Ruff and F. J. Ablenas, *Can. J. Chem.*, 1989, **67**, 699–702.
- 107 G. Kerti, T. Kurtán, T.-Z. Illyés, K. E. Kövér, S. Sólyom, G. Pescitelli, N. Fujioka, N. Berova and S. Antus, *European J. Org. Chem.*, 2007, **2007**, 296–305.
- 108 D. Ma, C. Xia and H. Tian, *Tetrahedron Lett.*, 1999, **40**, 8915–8917.
- 109 A. Shaabani, P. Mirzaei, S. Naderi and D. G. Lee, *Tetrahedron*, 2004, **60**, 11415–11420.
- 110 M. J. Cheng, M. Der Wu, G. F. Yuan, Y. L. Chen, Y. S. Su, M. T. Hsieh and I. S. Chen, *Phytochem. Lett.*, 2012, **5**, 219–223.
- 111 P. F. Schuda, C. B. Ebner and S. J. Potlock, *Synthesis-Stuttgart.*, 1987, **1987**, 1055–1057.
- 112 A. Rosowsky, C. E. Mota, J. E. Wright, J. H. Freisheim, J. J. Heusner, J. J. McCormack and S. F. Queener, *J. Med. Chem.*, 1993, **36**, 3103–3112.
- 113 H. Yokoyama, K. Otaya, H. Kobayashi, M. Miyazawa, S. Yamaguchi and Y. Hirai, *Org. Lett.*, 2000, **2**, 2427–2429.
- 114 D. L. J. Clive, M. Sannigrahi and S. Hisaindee, *J. Org. Chem.*, 2001, **66**, 954–961.

Appendix

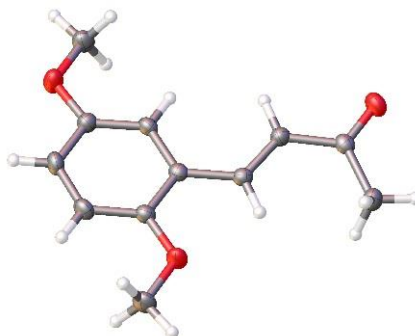
X-ray Crystallography Data

1,7-dibromo-6H,12H-6,12-epoxydibenzo[b,f][1,5]dioxocine-2,8-diol 3.31



Identification code	MJH12	
Chemical formula (moiety)	$C_{14}H_8Br_2O_5$	
Chemical formula (total)	$C_{14}H_8Br_2O_5$	
Formula weight	416.02	
Temperature	150(2) K	
Radiation, wavelength	MoK α , 0.71073 Å	
Crystal system, space group	orthorhombic, Fdd2	
Unit cell parameters	$a = 21.2980(13)$ Å	$\alpha = 90^\circ$
	$b = 25.0474(15)$ Å	$\beta = 90^\circ$
	$c = 4.8731(4)$ Å	$\gamma = 90^\circ$
Cell volume	$2599.6(3)$ Å ³	
Z	8	
Calculated density	2.126 g/cm ³	
Absorption coefficient μ	6.256 mm ⁻¹	
F(000)	1616	
Crystal colour and size	colourless, $0.30 \times 0.10 \times 0.10$ mm ³	
Reflections for cell refinement	1052 (θ range 3.2 to 28.4°)	
Data collection method	Xcalibur, Atlas, Gemini ultra thick-slice ω scans	
θ range for data collection	3.2 to 28.5°	
Index ranges	$h -22$ to 26, $k -33$ to 30, $l -5$ to 6	
Completeness to $\theta = 25.0^\circ$	99.8%	
Reflections collected	2301	

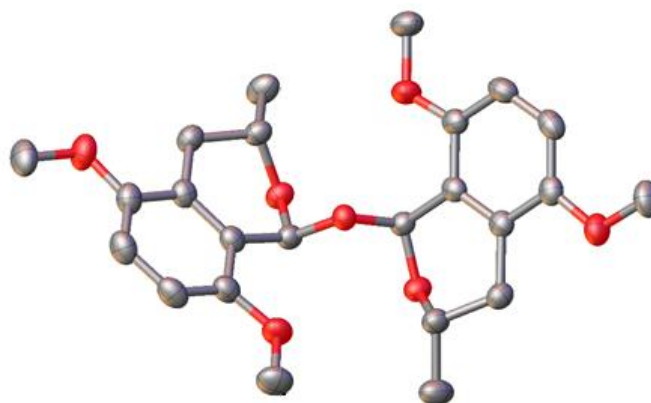
Independent reflections	1086 ($R_{\text{int}} = 0.0318$)
Reflections with $F^2 > 2\sigma$	1029
Absorption correction	semi-empirical from equivalents
Min. and max. transmission	0.2555 and 0.5735
Structure solution	direct methods
Refinement method	Full-matrix least-squares on F^2
Weighting parameters a, b	0.0484, 18.9318
Data / restraints / parameters	1086 / 1 / 113
Final R indices [$F^2 > 2\sigma$]	$R1 = 0.0367$, $wR2 = 0.0908$
R indices (all data)	$R1 = 0.0397$, $wR2 = 0.0929$
Goodness-of-fit on F^2	1.099
Absolute structure parameter	-0.01(2)
Extinction coefficient	0.00040(13)
Largest and mean shift/su	0.000 and 0.000
Largest diff. peak and hole	0.75 and -0.53 e \AA^{-3}

(E)-4-(2,5-dimethoxyphenyl)but-3-en-2-one 2.30

Identification code	mjh120006	
Chemical formula (moiety)	C ₁₂ H ₁₄ O ₃	
Chemical formula (total)	C ₁₂ H ₁₄ O ₃	
Formula weight	206.23	
Temperature	150(2) K	
Radiation, wavelength	MoK α , 0.71073 Å	
Crystal system, space group	monoclinic, P12 ₁ /c1	
Unit cell parameters	a = 10.9406(9) Å	$\alpha = 90^\circ$
	b = 26.6373(16) Å	$\beta = 110.058(9)^\circ$
	c = 7.6565(6) Å	$\gamma = 90^\circ$
Cell volume	2096.0(3) Å ³	
Z	8	
Calculated density	1.307 g/cm ³	
Absorption coefficient μ	0.093 mm ⁻¹	
F(000)	880	
Crystal colour and size	colourless, 0.42 × 0.40 × 0.05 mm ³	
Reflections for cell refinement	3166 (θ range 2.8 to 28.5°)	
Data collection method	Xcalibur, Atlas, Gemini ultra thick-slice ω scans	
θ range for data collection	2.9 to 28.6°	
Index ranges	h -14 to 11, k -32 to 34, l -10 to 10	
Completeness to $\theta = 25.0^\circ$	99.8%	

Identification code	mjh120006	
Chemical formula (moiety)	C ₁₂ H ₁₄ O ₃	
Chemical formula (total)	C ₁₂ H ₁₄ O ₃	
Formula weight	206.23	
Temperature	150(2) K	
Radiation, wavelength	MoK α , 0.71073 Å	
Crystal system, space group	monoclinic, P12 ₁ /c1	
Unit cell parameters	a = 10.9406(9) Å	$\alpha = 90^\circ$
	b = 26.6373(16) Å	$\beta = 110.058(9)^\circ$
	c = 7.6565(6) Å	$\gamma = 90^\circ$
Cell volume	2096.0(3) Å ³	
Z	8	
Calculated density	1.307 g/cm ³	
Absorption coefficient μ	0.093 mm ⁻¹	
F(000)	880	
Crystal colour and size	colourless, 0.42 × 0.40 × 0.05 mm ³	
Reflections for cell refinement	3166 (θ range 2.8 to 28.5°)	
Data collection method	Xcalibur, Atlas, Gemini ultra thick-slice ω scans	
θ range for data collection	2.9 to 28.6°	
Index ranges	h -14 to 11, k -32 to 34, l -10 to 10	
Completeness to $\theta = 25.0^\circ$	99.8%	
Reflections collected	12369	
Independent reflections	4473 ($R_{\text{int}} = 0.0261$)	
Reflections with $F^2 > 2\sigma$	3373	
Absorption correction	semi-empirical from equivalents	
Min. and max. transmission	0.9619 and 0.9954	
Structure solution	direct methods	
Refinement method	Full-matrix least-squares on F^2	
Weighting parameters a, b	0.0516, 0.8280	
Data / restraints / parameters	4473 / 0 / 277	
Final R indices [$F^2 > 2\sigma$]	R1 = 0.0460, wR2 = 0.1064	
R indices (all data)	R1 = 0.0672, wR2 = 0.1208	

Goodness-of-fit on F^2	1.019
Extinction coefficient	0.0020(7)
Largest and mean shift/su	0.001 and 0.000
Largest diff. peak and hole	0.27 and $-0.22 \text{ e } \text{\AA}^{-3}$

1,1'-oxybis(5,8-dimethoxy-3-methylisochromane) 5.27

Identification code	mjh140024_fa
Empirical formula	C ₂₄ H ₃₀ O ₇
Formula weight	430.48
Temperature/K	150.01(10)
Crystal system	monoclinic
Space group	I2/a
a/Å	15.5333(3)
b/Å	10.87020(17)
c/Å	26.3068(4)
α/°	90
β/°	90.8950(14)
γ/°	90
Volume/Å ³	4441.36(12)
Z	8
ρ _{calc} /cm ³	1.288
μ/mm ⁻¹	0.775
F(000)	1840.0
Crystal size/mm ³	0.23 × 0.17 × 0.1
Radiation	CuKα (λ = 1.54184)
2θ range for data collection/°	6.72 to 133.01
Index ranges	-18 ≤ h ≤ 18, -12 ≤ k ≤ 12, -31 ≤ l ≤ 31
Reflections collected	58089
Independent reflections	3905 [R _{int} = 0.0703, R _{sigma} = 0.0212]

Data/restraints/parameters 3905/249/286
Goodness-of-fit on F^2 1.025
Final R indexes [$I \geq 2\sigma(I)$] $R_1 = 0.0359$, $wR_2 = 0.0874$
Final R indexes [all data] $R_1 = 0.0475$, $wR_2 = 0.0955$
Largest diff. peak/hole / $e \text{ \AA}^{-3}$ 0.17/-0.19